

Impact of single strand annealing on double strand break repair and chromosomal stability in mammalian cells

A component of the repair network

Dissertation

zur Erlangung des Doktorgrades der Naturwissenschaften
an der Fakultät für Mathematik, Informatik und Naturwissenschaften
der Universität Hamburg

vorgelegt von

Wael Yassin Mansour (M.Sc.)

aus Kairo

Hamburg 2009



Universität Hamburg

Der experimentelle Teil der vorliegenden Arbeit wurde von Oktober 2004 bis Oktober 2008 im Universitäts-Klinikum Hamburg Eppendorf (UKE), Onkologisches Zentrum, Klinik und Poliklinik für Strahlentherapie und Radioonkologie, im Labor für Strahlenbiologie und Experimentelle Radioonkologie (Leiter: Prof. Dr. Ekkehard Dikomey) durchgeführt.

Gutachter:

Herr Prof. Dr. Christian Betzel

Herr Prof. Dr. Ekkehard Dikomey

Tag der Disputation: 08.05.2009

Summary

Mammalian cells have evolved powerful network of double strand break (DSB) repair pathways to encounter the deleterious effect of these lesions. These repair pathways are nonhomologous end-joining (NHEJ), gene conversion (GC) and single strand annealing (SSA). The repair pathways are mechanistically distinct and differ in the fidelity of the repair. Whereas GC mostly ensures accurate repair, neither NHEJ nor SSA does. The misrepair of DSBs by these repair pathways may induce many types of genetic alterations with consequences such as cell death or cancer. In mammalian cells, these pathways are regulated by a complex signalling, which determines whether a DSB is repaired or misrepaired.

The main aim of this Ph.D. is to understand the regulation of the aforementioned repair pathways. Three main questions were addressed: (1) How can these pathways be regulated to avoid any misrepair? (2) Is there any hierarchy between these repair pathways? (3) Can one pathway be replaced by another?

The most appropriate strategy to address this aim is to assess these repair pathways in relation to each other using specific repair constructs. In this Ph.D., for each repair pathway a specific repair construct was used. In addition, for the first time a new repair construct was developed in order to detect the relation between NHEJ and SSA. These experiments were performed in wild-type cells (CHOK1) and their NHEJ-deficient derivatives (*xrs5*) that have defect in Ku80 gene.

The following points have been reported:

- The use of both GC and SSA was increased 6- and 8-fold in *xrs5* cells, suggesting that NHEJ is dominant over the other two repair pathways. However, *xrs5* cells still repair DSBs by an efficient but slower end-joining pathway compared to their wild type CHOK1 cells. This alternative pathway is non-conservative that leads to increasing deletion length and it is PARP1-dependent. This indicates that Ku-protein may regulate the genomic integrity in mammalian cells by controlling; on the one hand repair fidelity of NHEJ via protecting the DSB ends against nucleolytic activity. On the other hand, Ku-protein suppresses the non-conservative PARP1-dependent end-joining as well as both GC and SSA.
- NHEJ was not affected, if GC is impaired by Rad51-knockdown. Interestingly, when SSA was available, Rad51-knockdown promotes SSA frequency at the

Summary

expense of NHEJ efficiency. This implies that Rad51 may indirectly promote NHEJ by limiting SSA.

- The data presented here propose a model for a functional hierarchy for DSB repair network in mammalian cells. According to this hierarchy, NHEJ dominates and suppresses the other two repair pathways. GC also dominates over and suppresses the most deleterious SSA repair pathway. If one of central repair proteins is missing or the damage signalling is disturbed, these repair pathways crosstalk with each other in order to maintain the survival even at the expense of repair fidelity. As the DNA damage signalling is impaired in most of tumours, assessing the crosstalk and the hierarchy between repair pathways in tumour cells would be of most important in the future. Preliminary results in our laboratory have revealed a switch to misrepairing of the DSBs in tumour cells. This switch may enable the tumour cells not only to survive but also to accumulate genetic alterations.

Table of contents

| | |
|---|-----------|
| 1. INTRODUCTION..... | 1 |
| 1.1. DNA repair mechanisms | 1 |
| 1.2. DNA double strand break (DSBs) | 3 |
| 1.2.1. DSB signalling | 4 |
| 1.2.2. DSB repair pathways | 6 |
| 1.3. DSB repair pathways and cancer..... | 14 |
| 1.4. Regulation of DSB repair pathways..... | 19 |
| 2. MATERIALS AND METHODS..... | 21 |
| 2.1. Materials | 21 |
| 2.1.1. Laboratory equipments | 21 |
| 2.1.2. Plasmids | 22 |
| 2.1.3. Software..... | 23 |
| 2.1.4. Chemicals, reagents and kits..... | 23 |
| 2.1.5. Molecular weight markers..... | 26 |
| 2.1.6. Buffers and solutions | 26 |
| 2.1.7. Oligonucleotides sequence..... | 28 |
| 2.1.8. Cell lines | 29 |
| 2.1.9. Antibodies | 30 |
| 2.1.10. Transfection | 30 |
| 2.1.11. Reagents and media for cell culture | 30 |
| 2.2. Methods..... | 31 |
| 2.2.1. Cell manipulation | 31 |
| 2.2.2. G418 toxicity test | 32 |
| 2.2.3. Colony formation assay | 32 |
| 2.2.4. Immunofluorescence | 32 |
| 2.2.5. Repair substrates..... | 33 |
| 2.2.6. Transfection Techniques | 35 |
| 2.2.7. Transfection efficiency | 36 |
| 2.2.8. Analysis of the repair | 36 |
| 2.2.9. Western Blot | 39 |
| 3. RESULTS | 41 |
| 3.1. pEJSSA cloning..... | 41 |
| 3.1.1. Insertion of SSA1 and SSA2..... | 41 |
| 3.1.2. Functional assay for pEJSSA | 43 |

Table of contents

| | | |
|-------------|--|-----------|
| 3.1.3. | Integration of pEJSSA in Hamster cells | 44 |
| 3.1.4. | Testing for intact stable integration | 44 |
| 3.2. | Repair efficiency | 46 |
| 3.2.1. | NHEJ efficiency for cohesive and non-cohesive ends | 46 |
| 3.2.2. | NHEJ repair kinetics in both CHOK1 and xrs5 cells | 46 |
| 3.2.3. | NHEJ repair fidelity in both CHOK1 and xrs5 cells | 48 |
| 3.2.4. | The role of PARP1 for DSB repair in Ku80-deficient cells | 49 |
| 3.2.5. | SSA as an alternative pathway for NHEJ | 56 |
| 3.2.6. | NHEJ repair junctions in pEJSSA | 58 |
| 3.2.7. | Impact of Ku80 on GC | 58 |
| 3.2.8. | Interplay between GC and NHEJ | 62 |
| 3.2.9. | Interplay between NHEJ, GC and SSA | 62 |
| 3.2.10. | Effect of Rad51-knockdown on NHEJ fidelity | 65 |
| 4. | DISCUSSION | 66 |
| 4.1. | Molecular mechanisms for end-joining in Ku80-deficient and proficient cells...66 | |
| 4.2. | Switch to PARP1-dependent end-joining in Ku80-deficient cells | 69 |
| 4.3. | Gene conversion can replace Nonhomologous end-joining for repairing the DSB but the reverse is not an option | 71 |
| 4.4. | Switch to single strand annealing | 72 |
| 4.5. | A hierarchy for DSB repair | 74 |
| 4.6. | Clinical relevance and perspectives | 76 |
| 4.7. | Features of the chromosomal repair substrates | 77 |
| 5. | REFERENCES | 79 |

List of Figures

| | |
|---|-----------|
| Figure 1. Signalling of double strand breaks (DSBs)..... | 5 |
| Figure 2. Model of key steps of nonhomologous end-joining (NHEJ). | 9 |
| Figure 3. Schematic illustration of DNA double strand break (DSB) repair by gene conversion(GC)..... | 12 |
| Figure 4. Schematic illustration of DNA double strand break (DSB) repair by single strand annealing (SSA)..... | 15 |
| Figure 5. Reporter constructs..... | 34 |
| Figure 6. Transfection efficiency in CHOK1 and xrs5 cells. | 37 |
| Figure7. Sequencing analysis of pEJSSA. | 42 |
| Figure 8. Functional assay for pEJSSA..... | 43 |
| Figure 9. Intact integration of pEJSSA. | 45 |
| Figure 10. Effect of Ku80-deficiency on NHEJ efficiency. | 47 |
| Figure 11. Sequences of NHEJ repair junctions obtained from CHOK1, xrs5 cells harbouring either pEJ or pEJ2..... | 50 |
| Figure 12. Effect of Ku80-deficiency on NHEJ fidelity. | 52 |
| Figure 13. Inhibition of PARP1. | 54 |
| Figure 14. Role of PARP1 on NHEJ..... | 55 |
| Figure 15. Impact of Ku80-deficiency on NHEJ and SSA. | 57 |
| Figure 16. Loss of Ku80 increases inaccurate end-joining..... | 59 |
| Figure 17. RAD51 knockdown using siRNA. | 60 |
| Figure 18. Impact of Ku80 deficiency on GC..... | 61 |
| Figure 19. Impact of Rad51-knockdown on NHEJ. | 62 |
| Figure 20. Interaction between NHEJ, SSA and GC..... | 63 |
| Figure 21. Impact of Rad51-knockdown on NHEJ fidelity. | 64 |
| Figure 22. Prevalent molecular mechanisms for ‘‘accurate’’ NHEJ. | 68 |
| Figure 23. Presumptive fate for repairing of I-SceI-induced DSB..... | 75 |

List of abbreviations

| | |
|-------------------------|--|
| °C | Degree Celsius |
| μ | Micro (10 ⁻⁶) |
| A | Adenine |
| AP- | apurinic or apyrimidinic- |
| APRT | adenine phosphoribosyltransferase |
| ATM | ataxia telangiectasia mutated |
| ATP | Adenosine- 5'- triphosphate |
| ATR | Ataxia telangiectasia and Rad3 related |
| BARD1 | BRCA1 associated RING domain 1 |
| BASC | BRCA1 associated genome surveillance complex |
| BER | base excision repair |
| bp | base pairs |
| Brca1 | breast cancer 1 |
| Brca2 | Breast cancer 2 |
| BRCT | BRCA1- carboxyl-terminal |
| BSA | Bovine serum albumin |
| C | Cytosine |
| CDK1 | cyclin-dependent kinase 1 |
| CDK2 | cyclin-dependent kinase 2 |
| Chk1 | checkpoint kinase 1 |
| Chk2 | checkpoint kinase 2 |
| CO | Crossing over |
| CPD | Cyclobutane pyrimidine dimers |
| CSR | class switch recombination |
| CtIP | C-terminal binding protein interacting protein |
| DAPI | 4',6-Diamidino-2-phenylindole |
| ddH₂O | Double distilled water |
| DDR | DNA-damage-response |
| D-loop | displacement loop |
| DMSO | Dimethyl sulfoxide |
| DNA | Deoxyribonucleic acid |
| DNA LigIV | DNA ligase IV |
| DNA-PK | DNA-dependent protein kinase |
| DSBR | double strand break repair |
| dsDNA | Double stranded DNA |
| DTT | Dithiothreitol |

List of abbreviations

| | |
|--------------------------|--|
| ECL | Electro chemical luminescence |
| EDTA | Ethylene diamine tetra acetic acid |
| EGTA | Ethylenglycol-bis-(2-aminoethylether)-N, N, N', N'-tetra acetic acid |
| Exo1 | exonucleases like exonuclease 1 |
| G | Guanine |
| GC | gene conversion |
| HDR | homology-directed repair |
| HJ | Holliday junction |
| IgH | Ig heavy chain |
| IR | ionizing radiation |
| kDa | Kilodalton(s) |
| l | Liter |
| LB | Luria-bertani |
| LOH | loss of heterozygosity |
| m | Milli (10^{-3}) |
| M | Molar (mol/l) |
| MEM | Minimal essential medium |
| MGMT | methyl guanine methyltransferase |
| MMR | mismatch repair |
| MRN | Mre11/Rad50/Nbs1 |
| mRNA | Messenger ribonucleic acid |
| n | Nano (10^{-9}) |
| NBS1 | Nijmegen breakage syndrome 1 |
| NER | nucleotide excision repair |
| NHEJ | nonhomologous end-joining |
| nt | nucleotides |
| O⁶-meG | O ⁶ -methyl guanine |
| ORF | Open reading frame |
| p | Pico (10^{-12}) |
| PAGE | Polyacrylamide gel electrophoresis |
| PARP1 | poly(ADP-ribose) polymerase 1 |
| PBS | Phosphate buffered saline |
| PCNA | proliferating cell nuclear antigen |
| PCR | Polymerase chain reaction |
| PCR | Polymerase chain reaction |
| PMSF | Phenyl methyl sulfonyl fluoride |

List of abbreviations

| | |
|-----------------------|---|
| PVDF | Poly vinylidene difluoride |
| RNA | Ribonucleic acid |
| ROS | reactive oxygen species |
| RPA | replication protein A |
| rpm | Rotations per minute |
| RT | Room temperature |
| SDS | Sodium dodecyl sulphate |
| SDSA | synthesis dependent strand annealing |
| siRNA | Small interfering RNA |
| siRNA | Small interference RNA |
| SSA | single-strand annealing |
| SSB | Single strand break |
| SSBR | single strand break repair |
| ssDNA | Single stranded DNA |
| T | Thymine |
| t_{ph} | Terminal microhomology |
| Tcr | T-cell receptor |
| TLS | Translesions synthesis |
| Tris Tris- | (Hydroxymethyl)-aminomethane |
| Tween 20 | Polyoxyethylen-sorbitanmonolaurate 20 |
| UV | Ultraviolet |
| V | Volts |
| V(D)J | variable (V), diversity (D) and joining (J) |
| v/v | Volume per volume |
| w/v | Weight per volume |
| XLF | XRCC4-like-factor |
| XRCC | X-ray cross complementation gene |

1. INTRODUCTION

Cellular DNA is permanently exposed to a variety of insults that cause its damage. Both intrinsic activities such as oxidative metabolism with its highly reactive by-products (reactive oxygen species, ROS), and environmental factors such as UV light and ionizing radiation (IR) can cause a plethora of DNA lesions (Lodish, Berk et al. 2004). There are five main types of damage to DNA: (1) each of the four bases in DNA (A, T, C, or G) can be covalently modified at various positions. For example, depurination in which hydrolysis of a purine base (Adenine or Guanine) from the deoxyribose-phosphate backbone occurs. After a depurination, the sugar phosphate backbone remains intact and the sugar ring carries a hydroxyl (-OH) group in the place of the Adenine or Guanine. Another typical example is a spontaneous deamination of a C which results in an U giving then rise to a C:G to A:T transition. (2) Mismatches of the normal bases due to replication errors. These mismatches can either result from misincorporation of noncomplementary nucleotides during strand synthesis. For example, a C could be inserted opposite to an A. Alternatively; these mismatches can be formed by slippage of the polymerase on the DNA strand resulting in deletion or insertion of extra bases. (3) Crosslinks: covalent linkages formed between bases on the same DNA strand ("intrastrand") or between both strands ("interstrand"). (4) Cyclobutane pyrimidine dimers (CPD) are pairs of thymine and cytosine bases in DNA that arise via photochemical reactions. For example ultraviolet light (UV) may result in an abnormal covalent bond between adjacent thymidine bases forming thymine dimers (Whitmore, Potten et al. 2001). (4) Breaks in the backbone which can be limited to one of the two strands (a single-strand break, SSB) or occur on both strands (a double-strand break, DSB). Ionizing radiation is a frequent cause for such breaks, but some chemicals produce DSBs as well.

1.1. DNA repair mechanisms

DNA repair refers to the process of restoring DNA integrity after damage. Depending on the type of damage inflicted, a variety of repair strategies have evolved to restore lost information. If possible, cells use the unmodified complementary strand of the DNA or sister chromatid as a template to recover the original information. However, without access to a template, cells can use error-prone repair mechanisms for restitution of the continuity of the DNA molecule. When the cells fail to exactly restore the genetic information after DNA damage, a permanent change called mutation is formed which may lead to cancer (Lodish, Berk et al. 2004).

Introduction

DNA damage is repaired via six different mechanisms: (1) direct reversal, (2) base excision repair (BER), (3) single strand break repair (SSBR), (4) nucleotide excision repair (NER), (5) mismatch repair (MMR), and (6) double strand break repair (DSBR).

Direct reversal refers to chemical elimination of the alterations to bases without removing the modified residue. The main component of the direct reversal mechanism in mammalian cells is the alkyltransferase which transfers alkyl groups from the DNA to its cysteine residues. Since the alkyl cysteine is very stable, once the alkyl group has been transferred to the protein, the protein is permanently inactivated. The alkyl groups which can be handled by this protein range in size from methyl to benzyl. An example of direct damage reversal is the repair of O⁶-methyl guanine (O⁶-meG) by the protein methyl guanine methyltransferase (MGMT). If not repaired, these O⁶-meG adducts may mispair with thymine during replication leading to G:C to A:T transitions.

Both BER and SSBR are partly overlapping. BER is a multi-step process to repair any base loss or modification such as oxidation, methylation, and deamination. It recognizes and removes the damaged base leaving an abasic site. These sites are then recognized by specified apurinic or apyrimidinic- (AP-) endonucleases which incise the sugar phosphate bond at the 3' or 5' side of the AP-site. At this point a single break is formed and from here on SSBR and BER share in the next steps. The proper base is replaced by a repair polymerase, and a ligase then returns the DNA to its original state.

NER is a repair mechanism which can act on a variety of DNA lesions which have the common property to severely distort the structure of the DNA double helix (bulky lesions) (Hess, Schwitter et al. 1997). Common examples of these lesions are pyrimidine-pyrimidine dimers, bulky chemical adducts, and DNA-DNA cross-links. In this pathway, a large multi-enzyme complex scans the DNA for a distortion in the double helix. Once a bulky lesion has been found, the double helix is unwound in the vicinity of the lesion. The phosphodiester backbone of the abnormal strand is cleaved on both sides of the lesion leading to excision of a 30 nucleotides (nt) fragment of DNA including the lesion. The large gap produced in the DNA helix is then repaired by a DNA polymerase and ligase.

MMR plays an essential role in the correction of replication errors such as base-base mismatches and deletions that result from DNA polymerase misincorporation of nucleotides and template slippage, respectively. The principle of the entire MMR is similar to the process of BER and NER, in that the DNA lesion is recognized, a patch containing the lesion is excised, and the strand is corrected by repair synthesis and ligation (Marti, Kunz et al. 2002).

Furthermore, the cells have evolved a specified DNA damage tolerance process called translesion synthesis (TLS) that allows the DNA replication machinery to replicate past

DNA lesions such as thymine dimers or AP sites. It involves switching out regular DNA polymerases for specialized translesion polymerases (e.g. DNA polymerase η and ξ), often with larger active sites that can facilitate the insertion of bases opposite to damaged nucleotides. The polymerase switching is thought to be mediated by a post-translational modification of the proliferating cell nuclear antigen (PCNA).

DSBR is the main topic of this Ph.D. and it will be discussed in more details in the next sections.

1.2. DNA double strand breaks (DSBs)

The double helical structure of DNA is ideally suited for repair because it carries two separate copies of all genetic information, one in each of its two strands. Lesions affecting only one of the DNA strands can be repaired accurately using the intact complementary strand as a template (such as BER, SSB, NER, and MMR). DSBs, however, are believed to be the most toxic and mutagenic DNA damage experienced in cells since both strands are broken leaving no intact strand to provide a template for the repair. On one hand, the failure to repair as little as one single DSB can kill a cell if it hits and inactivates an essential gene or causes chromosomal degradation. On the other hand if repaired improperly, it can result in a variety of mutations including deletions, insertions, translocations, and chromosome fusions that cause genome instability. These mutations may lead to tumorigenesis if for example, the deleted sequence encodes a tumour suppressor gene or if the translocation leads to gene fusion that desregulates the function of specific proto-oncogene.

DSBs come about as a result of either endogenous or exogenous events. They are generated as a result of exogenous insults such as exposure to ionizing radiation (IR) or DNA-damaging drugs which are used in medicine for treating cancer patients. DSB can also be generated endogenously during various forms of site specific DNA recombination induced by nucleases, including yeast mating-type switching (Paques and Haber 1999), mammalian V(D)J recombination (Franco, Alt et al. 2006), immunoglobulin class-switch recombination (Chaudhuri, Basu et al. 2007), and meiotic recombination (Keeney and Neale 2006).

In addition, DSBs can also arise during DNA replication; when a replication fork encounters a template that contains another DNA damage type, i.e., a single-strand break. At this position a DSB is created with only one end. In addition the replication machinery dissociates from the DNA, a process called replication fork collapse (Jeggo 1998; Morgan, Corcoran et al. 1998; Olive 1998).

Introduction

Noteworthy, IR and some chemotherapeutic drugs can induce DSB either directly, when they hit the structure of DNA or indirectly via introducing many types of lesions that converted to DSB upon replication (Olive 1998).

1.2.1. DSB signalling

The DNA damage response (DDR) is a common term for a variety of pathways including that recognizes the damage but also reactions to arrest the cells cycle and repair the damage, or to kill the cell if the damage is too severe. DDR involves three groups of proteins that act in concert to translate the signal of damaged DNA into the response (Khanna and Jackson 2001). These groups include: (a) sensor proteins that directly or indirectly recognize the damaged DNA, initiating a biochemical cascade of activity; (b) transducer proteins, that transfer and amplify the signal from the sensors, and (c) effector proteins which involve in many cellular processes including activation of cell cycle checkpoints, repair of the damage, i.e. DSB, and cell death, such as apoptosis (Figure 1A). However, there is no absolute demarcation between the three groups involved in the DDR. For example, some proteins can participate in more than one step of the DDR. Recent studies have clarified the contribution of another class of molecules called mediators (also called adaptors). These proteins lack the catalytic activity but facilitate the signalling by promoting physical interactions between other proteins.

Cell cycle checkpoints are regulatory pathways responsible for slowing down the progression through the cell cycle to provide time for repair thus preventing DNA damage from being propagated to next generations. In case of severe damage the cells might initiate apoptosis. In mammalian cells, there are three main cell cycle checkpoints namely; G1/S, intra-S and G2/M checkpoints. Although they are distinct, the damage sensors appear to be shared by these checkpoints.

Currently, there are two models explaining how DSBs are recognized. The first model hypothesizes that ATM (ataxia telangiectasia mutated) is the sensor which is activated by the changes in chromatin structure induced by DSB (Bakkenist and Kastan 2003). In the second model, the MRN (Mre11/Rad50/Nbs1) complex first detects the DSB as a sensor by binding to the broken ends recruiting and promoting the activation of ATM (Lee and Paull 2005). Regardless of which protein first recognizes the DSB, both models lead to ATM activation (Lim, Kim et al. 2000) (Gatei, Young et al. 2000) (Lee and Paull 2005). ATM activation leads to phosphorylation and activation of many target proteins that involved in cell cycle control and DNA repair (Figure 1B). Within minutes of DSB recognition, activated ATM phosphorylates the H2AX histone over a region of megabases surrounding a DSB

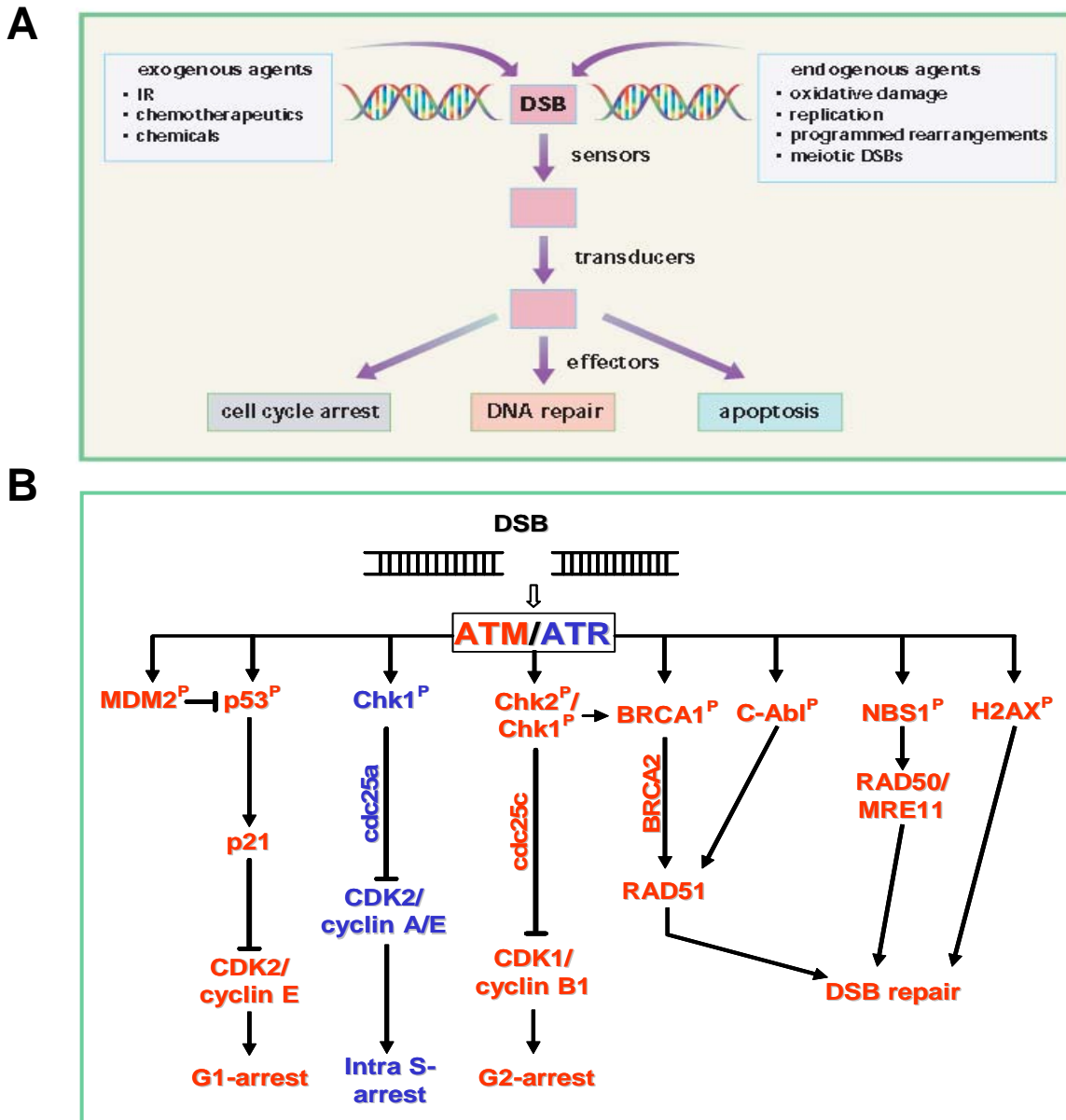


Figure 1. Signalling of double strand breaks (DSBs). A) The general organization of the DSBs response pathway. DSBs are recognized by sensors, which then transmit the signal through the transducers to a series of downstream effectors. These effectors include molecules involved in cell cycle arrest (cell cycle checkpoints), in DNA repair and in apoptosis (Khanna and Jackson 2001). B) ATM and ATR play a central role in the cellular response to DSBs. Activated ATM/ATR signals the presence of DNA damage by phosphorylating targets involved in cell-cycle arrest and DNA repair (ATM targets are depicted in red while in blue for ATR). H2AX is phosphorylated by ATR as a response of stalled replication fork.

Introduction

(Rogakou, Boon et al. 1999; Burma, Chen et al. 2001). In a similar manner, ATR (Ataxia telangiectasia and Rad3 related) responds to the presence of ssDNA or stalled replication forks by phosphorylating H2AX (Ward and Chen 2001). ATM or ATR phosphorylation of H2AX is believed to be a major signal for repair proteins to be recruited to the sites of DSBs (Celeste, Petersen et al. 2002). The activation of ATM/ATR leads to phosphorylation of a variety of downstream targets including p53, Chk1 (checkpoint kinase 1), and Chk2 (checkpoint kinase 2). p53 can be directly phosphorylated by ATM or indirectly by ATM phosphorylation of Chk2 which then phosphorylates p53 (Caspari 2000). These phosphorylations lead to p53 stabilization by interfering with p53 binding to its negative regulator MDM2 that targets p53 for degradation (Caspari 2000). The stabilized p53 controls G1/S arrest via trans-activation of the cyclin-dependent kinase inhibitor p21 and influences apoptotic regulators such as Bcl2 and Bax (Chao, Saito et al. 2000). The ATM-mediated phosphorylation of Chk1 and Chk2 kinases controls the G2-M checkpoint via phosphorylation of Cdc25C phosphatase. This phosphorylation leads to Cdc25C degradation which hinders the activation of CyclinB/CDK1 (cyclin-dependent kinase 1) preventing entry into mitosis. As a result of replication-associated DSB, ATR phosphorylation of Chk1 causes intra-S checkpoint through the phosphorylation and degradation of Cdc25A phosphatase. This leads to inactivation of CyclinE/CDK2 (cyclin-dependent kinase 2). ATM also phosphorylates BRCA1 (breast cancer gene 1) and c-Abl (Baskaran, Wood et al. 1997). BRCA1 is a component of many complexes including those that are involved in sensing the DSBs (BASC; BRCA1 associated genome surveillance complex) (Wang, Cortez et al. 2000) and in chromatin remodelling (Bochar, Wang et al. 2000). BRCA1 can, through its interaction with BRCA2 (breast cancer 2), modulate the function of repair proteins such as Rad51. Together, BRCA1 is a multifunctional protein that coordinates important branches of DSB signalling and repair (Khanna and Jackson 2001). C-Abl can regulate the function of Rad51 in both positive (Chen, Yuan et al. 1999) (Yuan, Chang et al. 2003) and negative (Yuan, Huang et al. 1998) manners, indicating that ATM, the critical modulator of c-Abl is hence also regulating Rad51. Another downstream target of ATM/ATR is Nibrin a member of the MRN complex which is directly involved in repair by stimulating the nuclease activity of Mre11 (van den Bosch, Bree et al. 2003). Noteworthy, MRN complex is working both upstream, as damage sensor which activates ATM, and downstream ATM.

1.2.2. DSB repair pathways

In order to avoid the detrimental effects of DSBs, cells have developed two mechanistically distinct repair pathways: nonhomologous end-joining (NHEJ) and homology-directed repair (HDR). The latter can be either a conservative mode such as gene conversion (GC) or non-conservative like single-strand annealing (SSA). NHEJ and HDR differ in their

requirement for a homologous DNA template and in the fidelity of the repair. There are three basic enzymatic activities commonly required for all repair processes: (1) nucleolytic removal of damaged DNA by nucleases, (2) limited DNA synthesis by polymerases to replenish, and (3) ligation to restore the phosphodiester backbone. Beside these basic enzymatic activities, a variety of cofactors are required that facilitate the respective repair processes.

- **Nonhomologous end-joining (NHEJ)**

NHEJ is the most simple repair mechanism for a DSB as it directly and sequence-independently rejoins the two DNA ends and that is why it is called nonhomologous end-joining (Weterings and van Gent 2004). In essence, NHEJ uses little or no sequence homology in an error-prone process that may lead to small deletions or insertions (1-3 nucleotides). The use of this error-prone process to repair DSBs in critical coding sites in the genome can potentially compromise genetic information (Gu, Forster et al. 1990; Lieber, Ma et al. 2003).

In mammalian cells, the majority of DSBs in G0/G1 are repaired by NHEJ. However, NHEJ functions throughout all cell cycle phases (Takata, Sasaki et al. 1998). The importance of NHEJ is illustrated by the fact that it exists in all living organisms including many prokaryotes (Gong, Bongiorno et al. 2005). Moreover, NHEJ is largely conservative from yeast to man (Gong, Bongiorno et al. 2005). In the last decade, the mechanistic steps of NHEJ have been extensively studied. Three steps have been suggested for the repair of DSBs via NHEJ as illustrated in Figure 2: (i) end binding in which the two ends are held in proximity to form a synapse, (ii) end processing by nucleases and polymerases that act on the ends to make them available for the last step which is (iii) ligation.

Two main complexes are involved in NHEJ namely the DNA-dependent protein kinase (DNA-PK) and the ligase complex. DNA-PK complex consists of DNA binding and kinase subunits. It has been shown that the *X-ray cross complementation* genes XRCC5, XRCC6 and XRCC7 encode the DNA-PK complex. XRCC5 and XRCC6 encode the 80 and 70 kDa subunits of Ku70/80 heterodimer (the DNA binding subunit of DNA-PK) while, XRCC7 encodes the 460 kDa DNA catalytic subunit of protein kinase (DNA-PKcs) (Weaver 1996; Chu 1997). The ligase complex is composed of DNA ligase IV (LigIV) and two cofactors XRCC4 and XLF (XRCC4-like-factor).

NHEJ starts with binding of the Ku70/Ku80 heterodimer to both DNA ends (end binding step) keeping them in proximity to facilitate the repair process (Pierce, Hu et al. 2001). The Ku70/80 heterodimer forms a close-fitting asymmetrical ring that threads onto a free end of DNA (Walker, Corpina et al. 2001). The end-bound Ku occupies approximately 16-18 bp as indicated by crystallography (Walker, Corpina et al. 2001), DNase footprinting

Introduction

and ultraviolet crosslinking assays (Yoo, Kimzey et al. 1999). Although, it tends to cling to the DNA end, Ku can translocate into the interior allowing the recruitment of multiple heterodimer molecules (Mimori and Hardin 1986). Once bound to DSB ends, Ku recruits other proteins including DNA-PKcs, XRCC4 and ligase IV to the DNA ends forming the repair synapse. Structural studies by electron crystallography indicate that DNA-PKcs also has an open channel that could accommodate approximately 12 bp of double stranded DNA (dsDNA) (Chiu, Cary et al. 1998; Leuther, Hammarsten et al. 1999). Upon recruitment of DNA-PKcs to the ends, it occupies the extreme ends of DNA, displacing Ku about 10 bp to the interior (Yoo, Kimzey et al. 1999). Once the catalytic subunit binds to Ku forming the DNA-PK complex on a DNA ends, the kinase activity of this complex is activated (Smith and Jackson 1999; Mari, Florea et al. 2006). Activated DNA-PKcs phosphorylates itself (autophosphorylation) producing a change in its conformation (Shrivastav, De Haro et al. 2008) which presumably regulates the accessibility of the DNA ends for further processing (Meek, Douglas et al. 2007).

Many DSB-inducing agents, such as IR, create a large variety of DNA ends including damaged bases or sugar residues that need processing before they can be ligated. This end processing step involves either removal and/or addition of a few nucleotides in order to render such ends ligatable.

Artemis is one of the target proteins of DNA-PK (Weterings and Chen 2008). Artemis exhibits an intrinsic 5' to 3' exonuclease activity (Pannicke, Ma et al. 2004). Phosphorylation of Artemis by DNA-PK, in addition, stimulates its endonucleolytic activity so that it becomes capable of opening hairpin loops (Ma, Pannicke et al. 2005; Ma, Schwarz et al. 2005) and cleaving off protruding single-stranded regions at DNA ends (Noordzij, Verkaik et al. 2003).

DSB ends, in some cases, need synthesis of limited number of nucleotides before they are ligated. Addition of nucleotides to a DSB is believed to be catalyzed by the polymerases pol μ and pol λ which have partially overlapping specificities (Lee, Blanco et al. 2004; Nick McElhinny, Havener et al. 2005). pol μ , in combination with purified Ku and XRCC4–LigIV, could carry out gap filling and end-joining during NHEJ in vitro (Mahajan, Nick McElhinny et al. 2002). Previous data suggested that pol λ interacts with XRCC4-DNA ligase IV via its N-terminal BRCT domain and this interaction stimulates the DNA synthesis activity of pol λ (Fan and Wu 2004). To permit DNA polymerization and ligation, a 3'-hydroxyl (3'-OH) and a 5'-phosphate need to be present at DNA ends. Polynucleotide kinase is recruited to the ends, by interaction with XRCC4, to remove 3'-phosphate and add 5'-phosphate

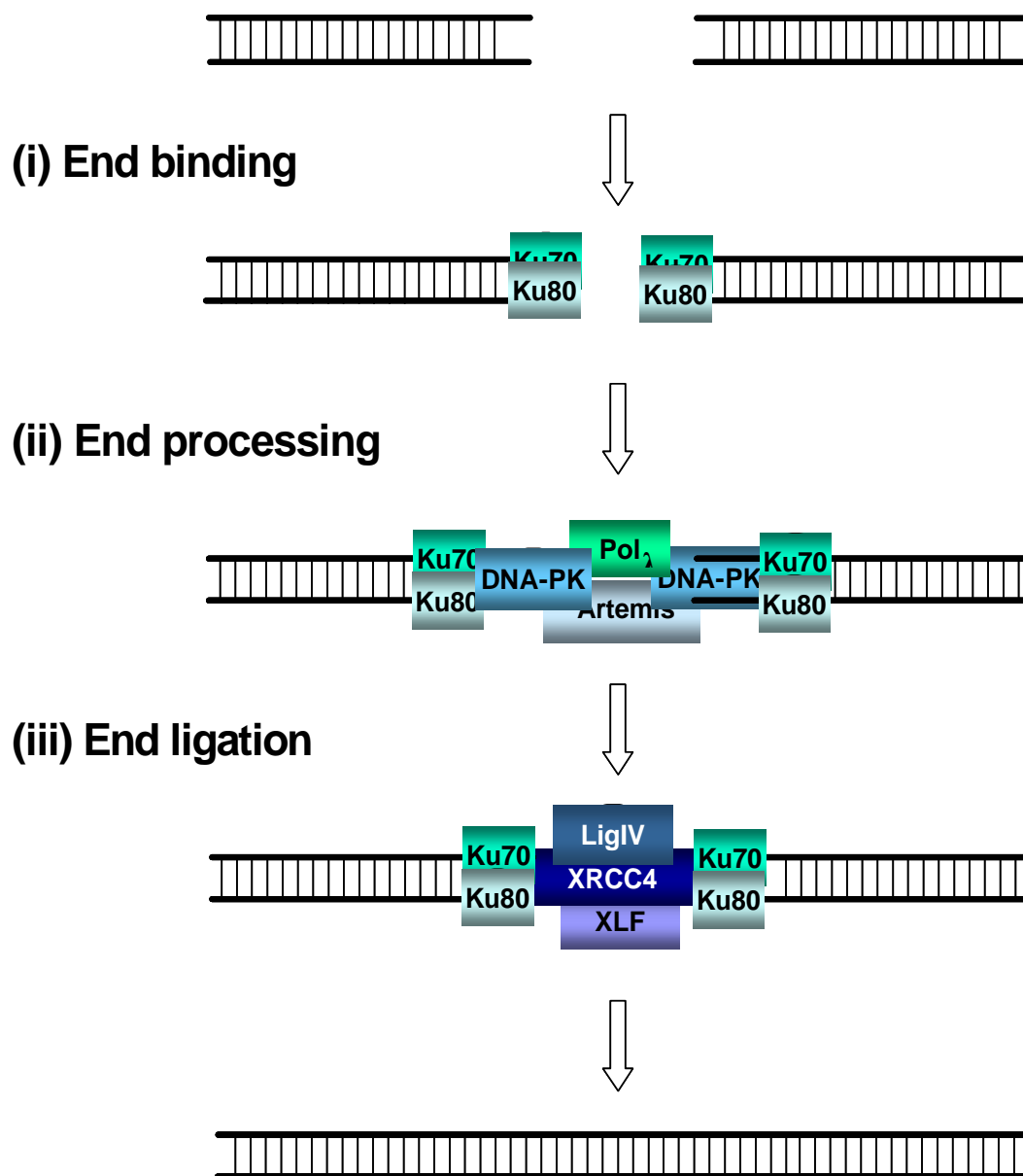


Figure 2. Model of key steps of nonhomologous end-joining (NHEJ). In the first step (end binding step, Ku70/80 heterodimer binds to both ends which then recruits DNA-PKcs to form the synapse complex. In most cases the ends are not ligatable and need some processing by Artemis nuclease trimming out some bases, or by pol λ adding some bases, to make them ligatable (end processing step). The synapse complex recruits the ligase complex (XRCC4/ligaseIV/XLF) to seal the DNA ends (ligation step).

Introduction

(Koch, Agyei et al. 2004). Compatible DNA ends, however, can be joined directly by the ligase complex without previous processing. The final step in NHEJ pathway is the ligation step which is mediated by the ligation complex XRCC4/LigIV. The ligation creates a phosphodiester bond between the 3'-OH of a nucleotide of one DSB end and the 5'-phosphate of another nucleotide on the other DSB end. XRCC4 is absolutely required not only for the stability of LigIV but also for its correct recruitment to DSBs (Grawunder, Wilm et al. 1997; Bryans, Valenzano et al. 1999; Chen, Trujillo et al. 2000). Interactions between XRCC4 and Ku70/80 heterodimer protein have been shown to be important for efficient NHEJ (Chen, Trujillo et al. 2000; Drouet, Delteil et al. 2005; Mari, Florea et al. 2006). DNA-PKcs provides even an additional stability to the ligase complex through interactions with XRCC4. However, the ligase complex assembly or its activity does not absolutely require this catalytic subunit. The ligation step is enhanced by the presence of XLF/Cernunnos protein which is recruited to DNA ends by Ku (Yano, Morotomi-Yano et al. 2008).

- **Homology-directed repair mechanisms (HDR)**

While NHEJ functions independently of sequence homology for rejoining two broken ends, the first requirement for HDR is to have homologous sequences elsewhere in the genome. Depending on where such sequences can be found, there are two major homologous recombination pathways. If the sequences surrounding the break can find homologies elsewhere in the genome (e.g. sister chromatides), this intact homologous sequence will be copied to the site of DSB. This process is basically conservative and called gene conversion (GC). However, if direct repeats are flanking the DSB, repair can occur by an exclusive non-conservative process called single-strand annealing (SSA) which results in the loss of one repeat and all of the intervening sequences.

- Gene Conversion

GC is error-free process that predominates in the late S/G2 phase of the cell cycle. In order to repair a DSB by GC, a second DNA molecule with homology to the region to be repaired must be available to serve as a repair template. Sister chromatides are the most preferable source of homology for GC (Moynahan and Jasin 1997; Richardson, Moynahan et al. 1998; Johnson and Jasin 2000). As illustrated in Figure 3, GC is carried out by a series of successive steps, (i) presynapsis, in which a resection of 5' ends of the DSB to expose free 3' single stranded DNA (3'-ssDNA) ends, (ii) synapsis, in which a physical connection between the DSB and the homologous sequences is generated by invasion of the 3'-ssDNA end(s), forming a structure called displacement loop (D-loop) and (iii) postsynapsis which includes a restoration of contiguous DNA strands by DNA synthesis using the invading 3'-

Introduction

overhang as the primer (Cao, Alani et al. 1990). After completion of strand extension, the newly synthesized strands unwind from the template and “reanneal” with each other. Gaps eventually remaining are replenished by further synthesis and the final nick is resealed by DNA ligase I or III.

The first event to occur during GC is resection of the DNA to yield 3' single stranded DNA overhangs. The nucleolytic component of the Mre11/Rad50/Nbs1 (MRN) complex (Paull and Gellert 1998; Tauchi, Kobayashi et al. 2002), exonucleases like exonuclease 1 (Exo1) (Nimonkar, Ozsoy et al. 2008) and C-terminal binding protein interacting protein (CtIP) (Takeda, Nakamura et al. 2007) are believed to be the main players of this resection step. After generation of the 3'-ssDNA tails, they became stabilized by replication protein A (RPA). The key step of GC is the invasion of the homologous sequence by the 3'-ssDNA overhang produced from resection step. The main protein that guides strand invasion in mammalian cells is Rad51 (Haber 2000). It is functional as a long helical polymer that wraps around the ssDNA to form a nucleoprotein filament (Figure 3) (Ogawa, Yu et al. 1993). In order to form this nucleoprotein filament, Rad51 must displace the RPA protein on the 3'-ssDNA overhang. By itself, Rad51 can hardly displace RPA protein while in the presence of Rad52 protein, the displacement of RPA from ssDNA by Rad51 protein is accelerated (Sigurdsson, Van Komen et al. 2001). Other proteins facilitate this displacement such as Rad54 and Rad51 paralogs including Rad51B, Rad51C, Rad51D, Xrcc2 and Xrcc3 (Sigurdsson, Van Komen et al. 2001). Moreover, the BRCA2 is required for the nuclear localizing and loading of Rad51 to DSB sites (Moynahan, Pierce et al. 2001; Powell, Willers et al. 2002).

The resulting nucleoprotein filament (Rad51-ssDNA) invades the sister chromatid, replacing its identical strand in the duplex forming heteroduplex DNA (displacement loop; D-loop) (Helleday, Lo et al. 2007). The stability of this heteroduplex DNA is mediated by Rad54 via introducing topological changes to the recipient duplex DNA that favour invasion of the incoming ssDNA molecule (Tan, Essers et al. 1999; West 2003). The invading end functions as a primer for DNA synthesis properly by DNA polymerase η (McIlwraith, Vaisman et al. 2005), which is consistent with the observation that cells lacking polymerase η showed a defect in homologous recombination (Kawamoto, Araki et al. 2005). A cross-stranded structure called Holliday junction (HJ) (Helleday 2003) is formed at the transition between hetero- and homoduplex (Figure 2). Sliding of the HJ in either direction which is called 'branch migration' can release the invading strand and the newly synthesized 3' single-stranded end can then anneal to the other side of the DSB. Many proteins have been shown to bind and/or resolve HJ in vitro (e.g., WRN, BLM, p53, RAD54, BLAP75 and hMSH2-hMSH6) (Lee, Cavallo et al. 1997; Mohaghegh, Karow et al. 2001; Subramanian and Griffith

Introduction

2002; Bugreev, Mazina et al. 2006; Raynard, Bussen et al. 2006). Final processing to remove flaps, fill in gaps, and ligate remaining nicks completes this pathway. Several proteins are involved in this final step including polymerase η and ϵ , PCNA, and DNA ligase I (Batty and Wood 2000).

In this model, only one strand needs to invade the template DNA. This model is called synthesis dependent strand annealing (SDSA) (Figure 3, left handed panel). Additionally, there is another more complex model according to which both Rad51-nucleofilaments invade the homologous DNA template forming a double HJ (Figure 3, right handed panel). Double Holiday junctions are resolved into unbranched recombinant molecules in either of two ways. If the two junctions are resolved in the same "plane" (both horizontal or both vertical, both brown arrows or both green arrows in Figure 3), the DNA sequence continuity is reserved in both strands resulting in noncrossing over event. Whereas, if the two junctions are resolved in opposite "planes" (one horizontal and one vertical, one brown and one green arrows) a crossover results. Importantly, crossover products have been rarely observed in mammalian cells after DSB induction and repair (Johnson and Jasin 2000). It has been observed that both human Bloom syndrome protein (hBLM) and topoisomerase III may resolve double HJs to avoid crossover products (Wu and Hickson 2003; Raynard, Bussen et al. 2006).

- Single strand annealing (SSA)

Single strand annealing (SSA) is a process that is initiated when a double strand break is introduced between two repetitive sequences oriented in the same direction. Four steps have been suggested for the repair of DSBs by SSA (Figure 4): (i) An end resection step which, in common with GC, is needed for the formation of long 3'-ssDNA, (ii) annealing step in which the two repetitive sequences are annealed together forming a flap structure, (iii) a 2nd resection step in which the flap structures which is formed by the regions between the repeats are resected and finally (iii) ligation of the ends.

Although SSA is well characterized in yeast (Haber and Leung 1996; Ivanov, Sugawara et al. 1996; Sugawara, Ira et al. 2000), its role in mammalian cells is not yet extensively studied. In common with GC, the SSA pathway is initiated by resection of the broken ends to create 3'-ssDNA which is properly mediated by the same nucleolytic components also involved in GC (Tauchi, Kobayashi et al. 2002). This resection step extends to the repeated sequences (Figure 4). RPA protein is then recruited to the ssDNA overhangs forming a filament. The Rad52 protein is believed to have a key role in SSA (Symington 2002) as it promotes the annealing of complementary single strands (Mortensen, Bendixen et al. 1996; Reddy, Golub et al. 1997; Shinohara, Shinohara et al. 1998; Sugiyama, New et al. 1998).

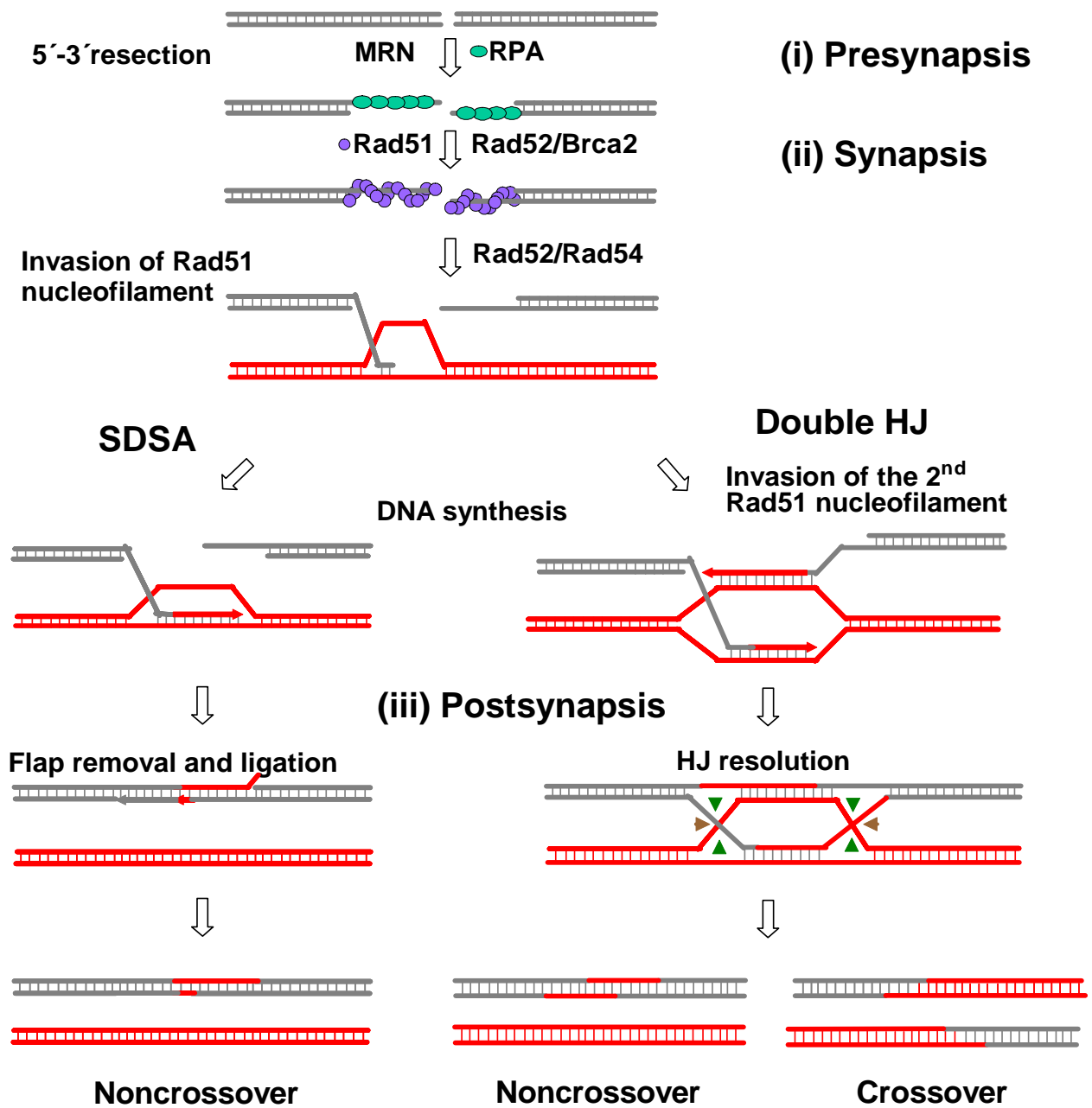


Figure 3. Schematic illustration of DNA double strand break (DSB) repair by gene conversion (GC). This pathway is initiated by a 5'-3' resection step to create a 3'-single-stranded (3'-ssDNA) tail which is then coated and stabilized by RPA protein. Rad51 by the help of both Rad52 and Brca2 replaces RPA protein forming two Rad51 nucleofilaments. Two possible mechanisms of GC can take place namely Synthesis-dependent strand annealing (SDSA) or double holiday junction (HJ). SDSA takes place when only one filament invades the homologous sequence in the intact homologous chromatid forming the D-loop following by DNA synthesis and releasing of the newly synthesized strand. Double HJ takes place when two filaments invade the homologous chromatid resulting in formation of double HJ structure. If the two junctions are resolved in the same "plane" (both horizontal; brown triangles or both vertical; green triangles), no crossover will be generated (non-crossover configuration), whereas if the two junctions are resolved in opposite planes (one horizontal and one vertical), a crossover is produced.

Introduction

Biochemical studies indicate that the N-terminus of Rad52 possesses ssDNA annealing activities, while its C-terminus contains the Rad51-binding domain (Symington 2002). It has been demonstrated that seven molecules of Rad52 form a heptamer ring structure which binds to the resected DNA termini. The ssDNA lies in the groove of the Rad52 ring such that the phosphodiester backbone is distorted and exposed to outward (Singleton, Wentzell et al. 2002). In this way, the protein would present the DNA to allow homologous pairing with a complementary strand, thus promoting strand annealing. SSA *in vivo* occurs presumably by two heptamer rings of Rad52 recruited to each 3'-ssDNA terminus. These complexes present the bases of the complementary strands outward and hence facilitate pairing of the complementary bases (Singleton, Wentzell et al. 2002). Visualization of the intermediates and products of the SSA reaction reveals that, after annealing, Rad52 remains bound to the heteroduplex DNA intermediate (Van Dyck, Stasiak et al. 2001). When the repeats annealed, the sequences between the repeats will be flapped out on either side (see Figure 4). These flap ends are cleaved off by the ERCC1/XPF endonuclease (Sargent, Rolig et al. 1997; Sargent, Meservy et al. 2000). The functional involvement of ERCC1 was confirmed in ERCC1-deficient hamster cells which showed a high frequency of rearrangements (Al-Minawi, Saleh-Gohari et al. 2008) at a tandem repeat locus of the adenine phosphoribosyltransferase (APRT) which stimulates recombination by SSA (Sargent, Brenneman et al. 1997). Moreover, it has been reported that ERCC1/XPF forms a stable complex with human Rad52 which stimulates the DNA structure-specific endonuclease activity of ERCC1/XPF (Motycka, Bessho et al. 2004).

The final ssDNA gap is closed by a ligase which has not yet been identified, perhaps ligase III. It is noteworthy that SSA is associated with loss of one of the repeats and the intervening sequence between them and hence obligating mutagenic behaviour of this pathway.

1.3. DSB repair pathways and cancer

DSBs are the potent inducers of chromosomal instability (CIN) which is characterized by the gross rearrangement of chromosomes. Common chromosomal aberrations include the loss or gain of whole chromosomes or chromosome fragments, and the amplification of chromosome segments. Loss of large regions of a chromosome can lead to the inactivation of tumour suppressor genes (for example, by loss of heterozygosity) (Lengauer, Kinzler et al. 1998), whereas amplification of chromosomal regions might promote tumourigenesis by the activation of proto-oncogenes (Lengauer, Kinzler et al. 1998). A different type of gross chromosomal aberration often observed in tumours is translocation caused by exchange of parts of nonhomologous chromosomes.

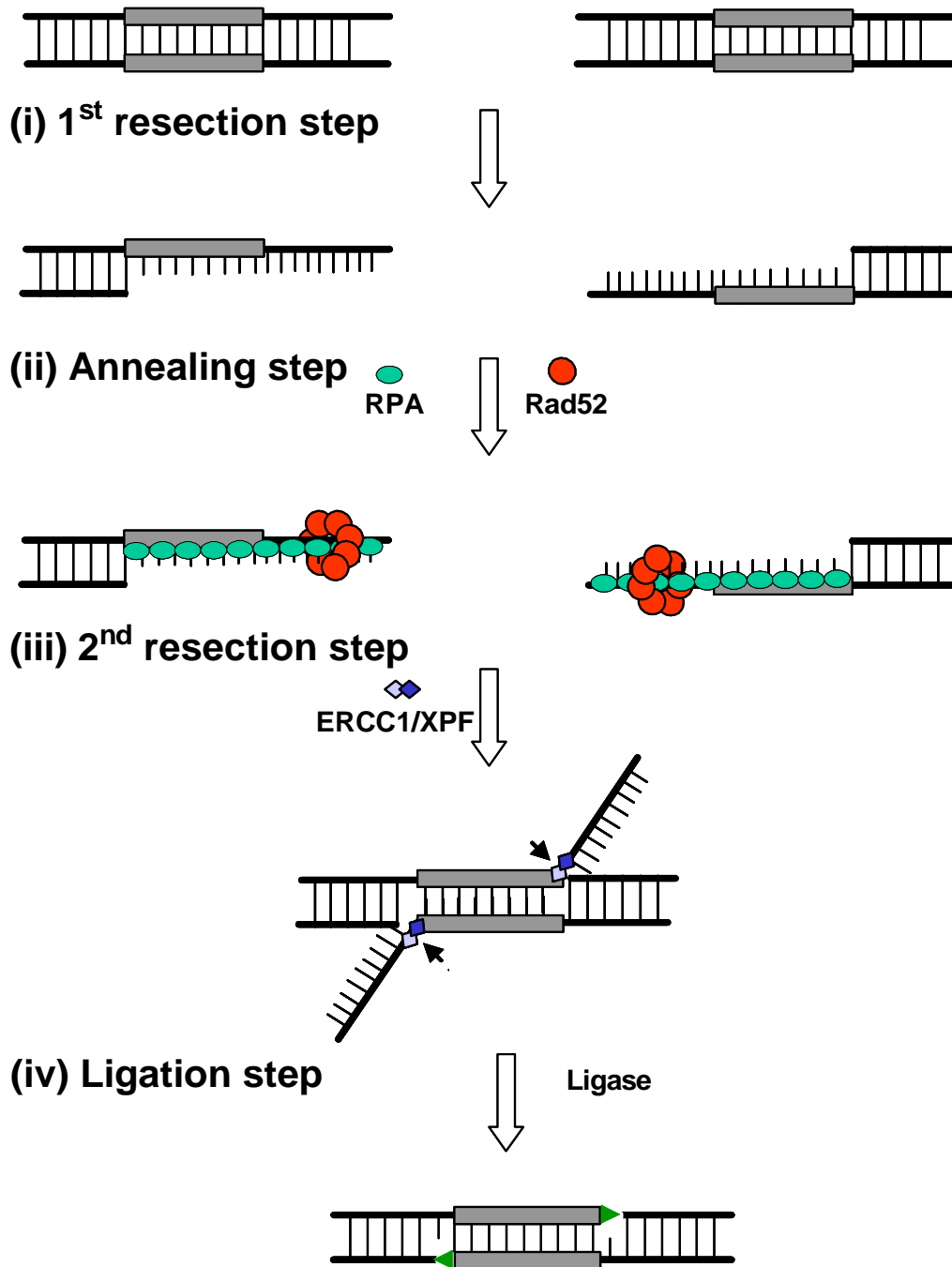


Figure 4. Schematic illustration of DNA double strand break (DSB) repair by single strand annealing (SSA). This pathway is initiated by a 5'-3' resection step to create a 3'-single-stranded (3'-ssDNA) tail (1st resection step). This ssDNA overhang is then coated and stabilized by RPA protein. Rad52 forms heptamer ring structure which binds to the ends stimulating the annealing of the complementary repetitive sequences (annealing step). The annealing of the two repeats, results in the formation of flapped structures that are removed by the endonucleolytic activity of ERCC1/XPF (2nd resection step). The gaps are filled-in by polymerases and the nicks are then ligated by DNA ligase (ligation step).

Introduction

These rearrangements can be associated with the deregulation of gene expression or the fusion of two genes that then acquires oncogenic potential (de Klein, van Kessel et al. 1982). The mechanism by which these translocations are produced is believed to be initiated by two different DSBs on the two participating chromosomes. Many types of CIN have been observed in different types of tumour, for example tumours of lymphoid origin (Vanasse, Concannon et al. 1999). In many well-characterized cases, chromosomal translocations with one of the breakpoints in either an Ig or a T-cell receptor (Tcr) locus have been found. The location of these breakpoints indicates that there might be a link between the chromosomal rearrangement and V(D)J recombination (at the Ig or Tcr loci) or class-switch recombination (at the *IgH* locus). So, DSBs are implicated in the generation of translocations in lymphoid tumours, at least on chromosomes 2, 7, 14 and 22 that carry the Ig and Tcr loci (Vanasse, Concannon et al. 1999). However, numerous translocations that involve other loci have also been documented. Other evidence for the involvement of DSBs in chromosomal aberrations comes from studies in which cells or animals have been exposed to ionizing radiation. Although this treatment generates a spectrum of DNA damage, including DNA single-stranded breaks, the most genotoxic lesions caused by ionizing radiation are DSBs. At relatively low doses, ionizing radiation does not cause extensive cell death, but it does contribute to chromosomal instability.

Repair of the DSBs is critical for maintaining genomic stability (Johnson and Jasin 2000) (Karanjawala, Grawunder et al. 1999; Ferguson, Sekiguchi et al. 2000; Sharpless, Ferguson et al. 2001; Nickoloff 2002; Tong, Cortes et al. 2002; Zha, Alt et al. 2007). Expectedly, loss or defects in key proteins involved in either of these pathways lead to repair deficiency which may increase carcinogenic risk.

NHEJ deficient cells have high rates of spontaneous chromosome breaks (d'Adda di Fagagna F 2001). DNA-PKcs and Ku70 mutant mice have high incidence of T-cell lymphomas (Smith and Jackson 1999). Ku70^{-/-} mice have increased rates of fibroblast transformation with chromosomal instability including breakage, translocations and aneuploidy (Smith and Jackson 1999). Ferguson et al. have reported that mouse cells lacking LigIV undergo numerous chromosome translocations after DNA damage by ionizing radiation, but wild-type cells do not (Ferguson and Alt 2001). A loss of single allele of LigIV in mouse cells exhibit gross chromosomal instability involving deletion, amplification and translocation and ultimately results in elevated incidence of soft tissue carcinoma (Sharpless, Ferguson et al. 2001). Moreover, it has been reported that mice lacking Ku or Xrcc4, as well as the p53 tumour suppressor protein, invariably develop pro-B lymphomas that result from translocations between the IgH locus and c-myc (Difilippantonio, Petersen et al. 2002; Zhu, Mills et al. 2002). Consistently, spontaneous chromosomal aberrations and oncogenic c-

Introduction

myc/IgH translocations are observed even in the absence of Ku or the ligase complex component Xrcc4 (Jankovic, Nussenzweig et al. 2007). Furthermore, patients with hypomorphic mutations in the Artemis gene have been found to develop thymic lymphomas, showing that a decrease in nonhomologous end-joining capacity can increase the risk of cancer in humans as well as mice (Moshous, Pannetier et al. 2003). From these data it is obvious that deficiencies of the NHEJ components are significantly associated with cancer.

Recent more details analyses have evolved a progress in the understanding of the connection between NHEJ and cancer which involve the repairing of the DSB improperly with more errors (misrepair). Analysis of translocation breakpoints in many types of tumours such as lymphoma, leukemia and sarcoma has revealed that most junctions have been performed by NHEJ associated with deletions and/or insertions (Morris and Thacker 1993; Difilippantonio, Zhu et al. 2000; Rothkamm, Kuhne et al. 2001; Zhang and Rowley 2006; Soutoglou, Dorn et al. 2007). Several studies reveal that programmed DNA breaks created during assembly of antigen receptor genes can be channelled into an erroneous NHEJ that is implicated in the chromosomal translocations of lymphoid cancers (Corneo, Wendland et al. 2007; Soulas-Sprauel, Le Guyader et al. 2007; Yan, Boboila et al. 2007). NHEJ defects are also encountered in manifest human tumours. For example high grade bladder tumours have been shown to frequently repair DSB by a highly mutagenic end-joining pathway, a process that may contribute to further genomic instability of bladder cancer (Bentley, Diggle et al. 2004).

SSA is a mutagenic pathway as it introduces large deletions. This may lead to carcinogenesis if this deletion has occurred in an area which contains a tumour suppressor gene. In fact, abundant repetitive elements (such as Alu, LINE and SINE repeats) in higher eukaryotes (Lander, Linton et al. 2001) should render SSA a suitable repair option but it is not known to which extent it actually contributes to overall DSB repair. However, SSA has also been identified as a significant pathway leading to translocations frequently inflicted in human cancers (Haber and Leung 1996; Ivanov, Sugawara et al. 1996; Strout, Marcucci et al. 1998; Sugawara, Ira et al. 2000; Elliott, Richardson et al. 2005; Weinstock, Elliott et al. 2006).

GC is usually error-free if the homologous repair template is provided by the nearby sister chromatid in the S- or G2-phase of the cell cycle. In contrast, GC initiated in the G1-phase carries a high risk of chromosomal rearrangements because the homologous template can only be found on a distant chromosomal locus, i.e. the homologous chromosome (2nd allele) or a pseudogene (Golding, Rosenberg et al. 2004; Saleh-Gohari and Helleday 2004). Given the high need of assuring accurate repair of DSBs, it is not surprising that defects in key proteins involved in GC are also associated with an increased risk of cancer (Thompson

Introduction

and Schild 2002). Increased expression of Rad51 has been reported in immortalized and tumour cells, which could alter recombination pathways to contribute to the chromosomal rearrangements found in these cells (Richardson, Stark et al. 2004). Increased Rad51 expression promotes aneuploidy and increases the level of crossing over events leading to chromosomal translocations (Richardson, Stark et al. 2004). Rad54, another recombinational protein, is required for accumulation of Rad51 molecules in so called foci at the sites of DSB. In addition, Rad54 facilitates the invasion step of the Rad51-nucleofilament into the donor helix. Accordingly, Rad54 deficient embryonic stem cells are hypersensitive to DSB inducing agents and have defective GC (Essers, Hendriks et al. 1997). Mutations of Rad54 have been observed in lymphoma, colon cancer and breast cancer suggesting a possible causative link (Matsuda, Miyagawa et al. 1999).

Other proteins that modulate homologous recombination are known to be cancer genes. For example, BRCA2 plays a central role in GC as it facilitates displacing RPA and loading of Rad51 onto ssDNA (Davies, Masson et al. 2001). Deficiency in BRCA2 which in turn causes GC deficiency (Stark, Pierce et al. 2004) results in the accumulation of chromosome aberrations (Patel, Yu et al. 1998), which is quite similar to what has been observed in vertebrate cells depleted of Rad51 (Lim and Hasty 1996). Furthermore, inappropriate HJs resolution couples crossover events to GC, resulting in deletions, inversions, loss of heterozygosity (LOH), or gene amplification (Moynahan and Jasin 1997; Richardson, Moynahan et al. 1998), all of which potentially promote carcinogenesis (Lasko, Cavenee et al. 1991). BLM is a helicase that is involved in resolution of HJ. BLM mutant cells are proficient in initiating homologous recombination, but the outcome of these repair events is apparently shifted toward exchange-associated events (Chaganti, Schonberg et al. 1974; Wu and Hickson 2003). The resulting increase in exchanges between homologous chromosomes leads to increased rates of LOH, which has been proposed to be the driving force behind the increased risk of cancer in Bloom's syndrome patients (Chaganti, Schonberg et al. 1974; Luo, Santoro et al. 2000).

In addition to the above mentioned proteins which are directly involved in either of these pathways, there are other proteins which are implicated in both pathways. A good example for that is BRCA1 whose involvement in HDR is mediated by its interaction with BRCA2 (Chen, Silver et al. 1998; Chen, Silver et al. 1999) which gives it a supporting role in GC. In addition, BRCA1 regulates NHEJ end processing by Mre11 endo- and exo-nuclease activity (Paull, Cortez et al. 2001) enhancing the accuracy of NHEJ (Durant and Nickoloff 2005; Gudmundsdottir and Ashworth 2006), possibly through its phosphorylation by Chk2 (Zhuang, Zhang et al. 2006). BRCA1 is a tumour suppressor gene that is frequently mutated in many tumours, preponderantly breast, ovarian and prostate. A possible mechanism by

which the loss of function of the mutated BRCA1 promotes genomic instability by promoting error-prone NHEJ and by inhibiting the error-free GC.

1.4. Regulation of DSB repair pathways

In mammalian cells, the majority of DSBs induced in the genome are repaired by NHEJ (Sargent, Brenneman et al. 1997). However, GC has been shown to be important in repairing DSBs during replication in all cellular organisms (Sonoda, Sasaki et al. 1998; Cox 2001; Kraus, Leung et al. 2001; Michel, Flores et al. 2001; Lundin, Erixon et al. 2002). It is important for the cells to control not only the choice between the DSB pathways but also the fidelity of each pathway in order to optimize repair efficiency and to minimize the risk of genetic alterations. Several factors affect the choice between repair pathways. One clear factor is the phase of the cell cycle at which DSBs are generated. It is well known that the ratio between NHEJ and GC changes during the cell cycle (Shrivastav, De Haro et al. 2008). GC is favoured in the late S and G2 phases of cell cycle when the entire sister chromatid is available (Rothkamm, Kruger et al. 2003; Stark, Pierce et al. 2004); while NHEJ is favoured in G1 phase but it can be used in all cell cycle phases (Takata, Sasaki et al. 1998). Evidence has been presented by Chen et al. that the preference of GC in S/G2 phase is actively regulated by the expression of Rad51 and Rad52 proteins which increase during S-phase (Chen, Nastasi et al. 1997). However, the level of Rad51 protein in G1 is sufficient to form Rad51 foci and so may initiate GC in G1 phase (Kim, Krasieva et al. 2005; Al-Minawi, Saleh-Gohari et al. 2008). Several studies suggested that the initiation of GC is tightly linked to cyclin-dependent kinases (CDKs) which are activated during S and G2 phases (Aylon, Liefshitz et al. 2004; Ira, Pellicoli et al. 2004; Esashi, Christ et al. 2005). CDK activity regulates both the generation of the 3'-ssDNA overhang and loading of Rad51 by regulating BRCA2 phosphorylation (Esashi, Christ et al. 2005). This mechanism may ensure that GC is restricted to S and G2 phases (Aylon, Liefshitz et al. 2004). On the other hand, the participation of SSA during cell cycle is not clear. A single recent study has reported low frequency of SSA in G1-arrested cells (Al-Minawi, Saleh-Gohari et al. 2008). The same study showed that inhibition of CDKs had no impact on SSA level. Together it remains an open question whether activity of SSA in mammalian cells is cell cycle dependent.

The uncontrolled use of SSA in mammalian cells may result in many types of mutations such as deletions and translocations. ~50% of mammalian genome is comprised of repeat sequences (Schmid 1996) and harbours many repetitive elements, e.g., there are $>10^6$ Alu repeats in the human genome (Batzer and Deininger 2002). One possible mechanism to regulate the use of SSA inside these repeats is the fact that these repeats exhibit sequence diversity (Smit 1996) possibly resulting in mismatches which in turn may

Introduction

help to suppress SSA (Elliott, Richardson et al. 2005) However, it has been found that SSA between Alu repeats can efficiently occur in the human genome (Sugawara, Ira et al. 2000)

The replication fork is stalled when it encounters a DNA lesion such as SSB, forming a one-ended DSB which are repaired by GC. The cell needs to ensure that NHEJ does not work on this type of DSBs, since this activity could promote misjoining between this one ended-DSB and another DSB at a different locus giving rise to an asymmetric translocation. Possibilities for ensuring that the one-ended DSBs are not accessed by NHEJ include the fact that on the one hand such breaks in the lagging strand whose replication is discontinuous could have a relatively long 3' single-stranded extension that could prevent Ku70/80 binding (Ristic, Modesti et al. 2003). On the other hand, such breaks in the leading strand may exploit a hand-off mechanism from the replication machinery to the homologous recombination pathway as both pathways share some proteins such as RPA and polymerases. A third mechanism of controlling NHEJ in S-phase is DNA-PKcs activity and phosphorylation which are critical for NHEJ (Kurimasa, Kumano et al. 1999; Chan, Chen et al. 2002; Ding, Reddy et al. 2003). Importantly, the phosphorylation and the activation of the DNA-PK are reduced in irradiated S-phase cells (Chen, Chan et al. 2005), representing a possible mechanism that down regulates NHEJ in S-phase.

Collectively, the regulation of the repair pathways is one of the current hot topics in biology. This regulation is achieved in many levels starting from sensing the double strand breaks following by recruiting the appropriate repair proteins. Furthermore, cell cycle plays an important role in the regulation of the DSB repair. Many, facts and data have been reported for these levels of regulation; however, a complete comprehensive picture is still missing. In the current study we have addressed another level of regulation for DSB repair which may be mediated by a possible cross-talk between the different repair pathways to ensure the employment of the appropriate pathway that faithfully repairs the DSB.

2. MATERIALS AND METHODS

2.1. Materials

2.1.1. Laboratory equipments

Provider

Apparatus

Olympus Optical Co., LTD, Japan

- Inverted-phase microscope (Olympus CK2)

Carl Zeiss Werk, Göttingen, Germany

- Axioplan2 imaging fluorescence microscope

Biometra, Germany

- BioDoc II, Gel documentation

Eppendorf, Hamburg, Germany

- Bio-photometer
- Eppendorf centrifuge 5415 D
- Centrifuge 5810R
- Hot-plate thermostat 5320

Beckman Instruments GmbH, Munich, Germany

- Refrigerated microcentrifuge R.
- pH meter 300

Kendro, Hanau, Germany

- Hera cell 240 CO2 incubator
- Heraeus type B15 incubator
- Hera Saf Type HS12/2 laminal flow

BD Bioscience, Heidelberg, Germany

- FACScan
- FACS Calibur

Bio-Rad Laboratories, Hercules, CA, USA

- Criterion Precast Gel System (Criterion electrophoresis cell and Citerion Blotter)
- Gene Pulser II. Electroporator

Materials and Methods

| | |
|--|---|
| | – E.coli Pulser |
| Amersham Pharmacia, Buckinghamshire, UK | – Western blots developing Cassette |
| MWG Biotech, Ebersberg, Germany | – Primus thermalcycler |
| | – Robocycler Gradient 40 |
| Stratagene, Amsterdam, the Netherlands | |
| Berthold Technologies GmbH&Co. KG, Bad Wildbad, Germany | – Light sensitive CCD camera system (Night-OWL) |
| Gulmay Medical LTD, Oxford, UK | – X-ray generator type RS225 research system |
| Beckman Coulter, Krefeld, Germany | – Coulter Counter model Z1 |
| Labortechnik Fröbel GmbH, Lindau /Bodensee, Germany | – Consort E455 power supply |
| | – Consort E802 power supply |
| Mettler-Toledo GmbH, Giessen, Germany | – Analytical balance P1200 |
| | – Analytical balance AE160 |
| Johanna Otto GmbH, Hechingen, Germany | – Edmund Bühler shaker model KM-2 |
| | – Edmund Bühler shaker model SM-30 |

2.1.2. Plasmids

| | |
|--------------------|--|
| • pEGFP-N1 | Clontech, BD Bioscience, Heidelberg, Germany |
| • pPHW2 | Previously constructed by our group |
| • pGC | Previously constructed by our group |
| • pEJ | Previously constructed by our group |
| • pEJ2 | Previously constructed by our group |
| • pEJSSA | Specifically constructed for this study |
| • pCMV3xnlS-I-SceI | A kind gift from M. Jasin |

Materials and Methods

- pCMV-neo Modified after pCMV-p53, Invitrogen GmbH, Germany

2.1.3. Software

- CellQuest Pro 4.0.2; Becton Dickinson, Heidelberg
- Optimas 6.51; Media Cybernetics, Silver Spring, USA
- Prism 4.03 for Windows, Graphpad software, Inc

2.1.4. Chemicals, reagents and kits

| <u>Provider</u> | <u>Substance</u> |
|--|--|
| Sigma-Aldrich Chemie GmbH, Deisenhofen, Germany | – β -Mercaptoethanol |
| | – 2-propanol |
| | – Acetic acid |
| | – 4-(2-hydroxyethyl)-1-piperazine ethanesulfonic acid |
| | – (HEPES) |
| | – Boric acid |
| | – Aprotinin |
| | – Pepstatin |
| | – Phenylmethylsulfonyl flouride (PMSF) |
| | – Bovine serum albumin (BSA) |
| | – Bromphenol blue |
| | – Calcium chloride CaCl ₂ |
| | – Di Methyl Sulfoxide (DMSO) |
| | – Ethanol absolute |
| | – Methanol |
| – Ethidium bromide | |

Materials and Methods

- Ethylene diamine tetracetic acid (EDTA)
- Agarose
- Glucose
- Glycine
- Magnesium chloride (MgCl_2)
- Potassium chloride (KCl)
- Di-sodium hydrogen phosphate (Na_2HPO_4)
- Sodium hydrogen phosphate (NaH_2PO_4)
- Sodium chloride (NaCl)
- Potassium dihydrogen phosphate (KH_2PO_4)
- Sodium Dodecyl Sulfate (SDS)
- Sucrose
- Trizma-base
- Crystal violet stain
- Coomassie brilliant blue R250
- Coomassie brilliant blue G250
- Bromophenol Blue
- Xylene Cyanol
- Dithiothreitol (DTT)
- PARP1 inhibitors (NU1025, and DIQ)

**Amersham Pharmacia Biotech
Europe GmbH, Freiburg, Germany**

- Enhanced chemiluminescence (ECL)
western
- X-ray films

**Invitrogen GmbH, Karlsruhe,
Germany**

- Trypsin-EDTA

Qiagen GmbH, Hilden, Germany

- Qiagen plasmid Mini kit
- Qiagen plasmid Maxi kit

Materials and Methods

- | | |
|---|--|
| | – DNeasy Blood and Tissue extraction kit |
| Merck Biosciences GmbH, Bad, Soden, Germany | – Glycerol |
| | – Tween 20 (polyoxyethylene (20) sorbitan monolaurate) |
| | – Hydrochloric acid (HCl) |
| Roche Diagnostics GmbH, Mannheim, Germany | – Mycoplasma PCR Elisa Kit |
| New England Biolabs GmbH, Frankfurt am Main, Germany | – Restriction enzymes |
| Promega Corporation, Madison, WI, USA | – Wizard SV gel and PCR clean-up system |
| PeQ Lab Biotechnology GmbH, Erlangen, Germany | – PeQ lab PCR Master-Mix (1.25U Taq-DNA Polymerase per 25 µl, 0.4 mM dNTPs, 40 mM Tris-HCl (pH 8.55 at 25 °C), 32 mM (NH ₄) ₂ SO ₄ , 0.02% Tween 20 and 4 mM MgCl ₂) |
| Applied Biosystems, CA, USA | – Big Dye mixture |
| | – Half term buffer |
| Tetenal, Norderstedt, Germany | – X-ray film developer (1 : 10) Eukobrom |
| | – X-ray film fixer (1 : 5) Superfix |
| Pierce Biotechnology, Rockford, IL, USA | – BCA Protein Assay |
| Bio-Rad Laboratories, Hercules, CA, USA | – PROTEAN II Ready Gel precast gels |

Materials and Methods

2.1.5. Molecular weight markers

- **Protein markers**
 - Bench Mark prestained protein ladder (Invitrogen, Karlsruhe, Germany)
 - Magic Mark Western standard (Invitrogen, Karlsruhe, Germany)
- **DNA marker**
 - 1kb DNA ladder, Invitrogen, Karlsruhe, Germany

2.1.6. Buffers and solutions

For all buffer preparations double distilled water was used. Ultra pure RNase free water (Invitrogen, Karlsruhe, Germany) was used for RNA-interference experiments.

- **Protein extraction buffer**

| | | |
|-----|---------|-------------------|
| 20 | mM | Hepes (pH 7.8) |
| 450 | mM | NaCl |
| 50 | mM | NaF |
| 25 | % (v/v) | glycerol |
| 0.2 | mM | EDTA |
| 0.5 | mM | DTT |
| 0.5 | mM | PMSF |
| 0.5 | µg/ml | Leupeptin |
| 0.5 | µg/ml | Pepstatin A |
| 1.0 | µg/ml | Trypsin Inhibitor |
| 0.5 | µg/ml | Aprotinin |
| 40 | µg/ml | Bestatin |

- **Agarose gel (1%)**

| | | |
|---|---|------------------------------------|
| 1 | g | Agarose / 100 ml TBE-buffer (0.5x) |
|---|---|------------------------------------|

- **Coomassie-blue staining solution**

| | | |
|---|----|-------------------------------|
| 2 | mM | Coomassie brilliant blue R250 |
|---|----|-------------------------------|

Materials and Methods

| | | |
|------|----|-------------------------------|
| 0.6 | mM | Coomassie brilliant blue G250 |
| 42.5 | % | Ethanol |
| 10 | % | Acetic acid |

- **Blocking buffer**

| | | |
|----|---------|-------------------------------------|
| 10 | % (w/v) | Non-fat milk powder/100 ml PBS (1x) |
|----|---------|-------------------------------------|

- **Crystal violet staining solution**

| | | |
|-----|---------|------------------------------------|
| 0.1 | % (w/v) | Crystal violet/dd.H ₂ O |
|-----|---------|------------------------------------|

- **Destaining solution**

| | | |
|----|---|-------------|
| 13 | % | Methanol |
| 10 | % | Acetic acid |

- **DNA loading buffer**

| | | |
|------|---|------------------|
| 30 | % | Glycerol |
| 0.25 | % | Bromophenol Blue |
| 0.25 | % | Xylene Cyanol |

- **10x Tris-glycine buffer (TG-buffer)**

| | | |
|------|---|-------------|
| 1.92 | M | glycine |
| 0.25 | M | Trizma base |

- **Electrophoresis buffer (1x)**

| | | |
|-----|------|---------------|
| 100 | ml/l | 10x TG-buffer |
| 10 | ml/l | 10% SDS |

- **PBS (phosphate buffered saline)**

| | | |
|-----|----|----------------------------------|
| 140 | mM | NaCl |
| 3 | mM | KCl |
| 8 | mM | Na ₂ HPO ₄ |

Materials and Methods

1.5 mM KH_2PO_4

- **PBST (0.05% Tween 20)**

0.5 ml Tween 20

995 ml PBS

- **5x protein loading buffer**

250 mM Tris-HCl; pH6.8

500 mM DTT

10 % SDS

0.5 % Bromophenol blue

50 % Glycerol

Aliquots stored in -20°C

- **10x TBE buffer**

1.8 M Tris-base

1.8 M Boric acid

20 mM EDTA

- **Transfer buffer**

200 ml 10x TG buffer

400 ml Methanol

10 ml 10% SDS

1.4 l cold dd.H₂O

2.1.7. Oligonucleotides sequence

- **Primer sequence** (MWG Biotech, Ebersberg, Germany)

Materials and Methods

| | |
|-----|--------------------------------|
| P1 | 5`-AATGGGCGGTAGGCGTGTA-3` |
| P2 | 5`-GGC ATG GCG GAC TTG AA-3` |
| S1F | 5`-GGAGTTCCGCGTTACATAACT-3` |
| S1R | 5`-ACCGTACACGCCTACCGCCCATTT-3` |
| S2F | 5`-GGAGCGAACGACCTACACCGAACT-3` |
| S2R | 5`-CCTGACGAGCATCACAAAAAT-3` |

- **siRNA sequence** (Qiagen GmbH, Hilden, Germany)

| | |
|---------------|--------------------------------|
| RAD51-siRNA | 5`-GCUGGUUCCAUAACGGUGG dTdT-3` |
| Scrambled RNA | 5`-UAGGCAUUGCGCGUGUGUC dTdT-3` |

- **SA repetitive sequences** (MWG Biotech, Ebersberg, Germany)

| | |
|------|---|
| SSA1 | 5`- <u>CTCGAGG</u> CAACCGCTCATACGACCGACAACCGACCGCGCA TCACGCCGCAAGA TCTT <u>GATCA</u> -3` |
| SSA2 | 5`- <u>CGATCGG</u> CAACCGCTCATACGACCGACAACCGACCGCGCA TCACGCCGCAGTCGAC <u>ACCGGT</u> -3` |

The underlined sequences indicate the restriction sites used for cloning; XhoI-BclI for SSA1 and PvuI-AgeI for SSA2.

2.1.8. Cell lines

CHOK1 (wild type) and xrs5 (Ku80-deficient) cells, derived from Chinese hamster ovary, were used in this study. xrs5 cells were generated from the wild type CHOK1 in the lab of P. A. Jeggo by ethyl-methan-sulfonat-(EMS)-mutagenesis (Jeggo, Kemp et al. 1982; Jeggo and Kemp 1983). CHOK1 and xrs5 were grown at 37°C with 5% CO₂ in alpha-medium

Materials and Methods

supplemented with 10% fetal calf serum, 100 U/ml penicillin and 100 µg/ml streptomycin. The cells have been regularly tested for mycoplasma infection.

2.1.9. Antibodies

- **Primary antibodies**

- Rabbit anti-Rad51 monoclonal IgG (mAb-51Rad01), Calbiochem, Darmstadt, Germany.
- Mouse anti-β-actin monoclonal IgG (clone AC-15), Sigma-Aldrich Chemie GmbH, Deisenhofen, Germany.
- Mouse anti-PAR monoclonal IgG (clone C2-10), Trevigen Inc. MD, USA

- **Secondary antibodies**

- ECL anti-rabbit IgG, horseradish peroxidase-linked whole Ab (from donkey) (GE Healthcare Limited, UK).
- ECL anti-mouse IgG, horseradish peroxidase-linked whole Ab (from sheep) (GE Healthcare Limited, UK).
- Alexa fluor 594 anti-mouse monoclonal IgG (H+L), Invitrogen GmbH, Karlsruhe, Germany

2.1.10. Transfection

Two different transfection methods were used.

- Chemical transfection for siRNA using TransIt-TKO (Mirus, Madison, WI, USA).
- Electroporation for plasmid transfection using Gene Pulser II and bacterial electrotransformation using E.coli Pulser.

2.1.11. Reagents and media for cell culture (Invitrogen GmbH, Karlsruhe, Germany)

- Geneticin Selective Antibiotic G418 Sulphate
- Preservation solution 10% DMSO in FCS
- Foetal calf serum (FCS)
- OA-medium MEM-α-powder, 0.22% (w/v) NaHCO₃

Materials and Methods

- α -Medium
To 1l with RNase-free water
MEM- α -powder, 0.22% (w/v) NaHCO₃
1% (v/v) Penicillin-Streptomycin
To 1l with dd.H₂O
- Pinicillin-Streptomycin
10,000 U/ml Penicillin, 10,000 μ g/ml Streptomycin

2.2. Methods

2.2.1. Cell manipulation

- **Cell culture**

All cell culture work is done in a sterile Laminar flow hood to avoid contamination. The cells growth was examined under inverted-phase microscope. All cells used in this study were grown in standard α -medium. For cell passaging, the medium is removed from the flasks leaving the cells adhered to the growth surface of the flask. The cells were washed by 5-10 ml of prewarmed sterile PBS. After removing the PBS, 1-3 ml trypsin were added to the cells and incubated for 3 minutes at 37°C to detach them from the surface. The bottom of the flask was stroked sharply with the palm of the hand to help dislodge the remaining adherent cells. After all cells have been detached, α -medium containing serum was added to the cells to inactivate the trypsin. Gently the cells were pipetted up and down to break up cell clumps. The cells were then counted using cell counter and appropriate number of cells was distributed to fresh flasks for subculturing.

- **Cell preparation**

Cells were prepared by trypsinizing cultures using 0.05% trypsin/0.02% EDTA solution for 3 minutes at 37°C. Trypsin was inactivated by adding 5 ml α -medium/10%FCS and the cells were collected by centrifugation at 1,300 rpm for 4 min. The cell pellet was washed by adding 5 ml prewarmed sterile PBS and the number of cells in the suspension was counted by using a coulter counter. The cell suspension was centrifuged at 1,500 rpm for 10 minutes. After centrifugation, the supernatant was removed and the cell pellet was used for the experiments.

- **Cell preservation**

Materials and Methods

Sub-confluent cells were used for the preservation. The cells were trypsinized and suspended in freshly-prepared preservation solution. The cells suspension was then aliquoted in cryo-tubes ($3\text{-}5 \times 10^6$ cells/tube) and incubated 2h at -20°C , overnight at -80°C and finally stored in liquid nitrogen (-196°C). For re-culturing of stored cells, the cells were thawed, suspended in 10 ml α -medium and centrifuged at 1,200 rpm / 4°C for 4 minutes. The cell pellet then was re-suspended in standard α -medium.

2.2.2. G418 toxicity test

In order to select clones that have stably integrated the reporter constructs pEJ and others (see below) the neomycin/G418-resistance gene have been used. In a first step, the toxicity of G418 for non-transfected was determined by growing 5×10^4 cells in concentrations of G418 ranging between 0.25 – 2 mg/ml. After one week flasks were examined for colony growth. At a concentration of 0.8 and 1.2 mg/ml neither xrs5 nor CHOK1, respectively, showed any viable colonies. For further experiments a slightly higher concentration of 1.5 mg/ml was commonly used for selection of resistant clones.

2.2.3. Colony formation assay

Colony formation assays have been developed (Puck and Marcus 1956) to study the effect of a specific treatment on the cells' ability to form colonies, i.e. to continuously produce offsprings. In the current work, the effect of an inhibitor of the repair protein PARP1 on the colony forming capability after exposure to irradiation was assessed. An appropriate number of cells was seeded and incubated for about 2-3h to allow for adhesion. Thereafter, the specific inhibitor (DIQ or NU1025) was added and the cells were incubated at 37°C for 2h before irradiation. After irradiation (200 keV, 15mA, additional 0.5mm Cu filter at a dose rate of 2 Gy/min), the cells were then incubated for 2 weeks for colony formation. Thereafter, the clones were washed with 0.9 % NaCl_2 and stained with 0.1% crystal Violet stain. The plating efficiency (PE) was measured as the number of colonies formed divided by the number of cells seeded. As control, DMSO was used instead of the inhibitor at the same concentration.

2.2.4. Immunofluorescence

Immunofluorescence is a technique allowing the visualization of a specific protein or antigen in cells or tissue sections by binding a specific antibody chemically conjugated with a fluorescent dye. Stained samples are examined under a fluorescence microscope providing monochromatic light at desired wavelength. We applied this technique to visualize the subcellular levels of poly-(ADP-ribose) moieties. The cells were grown on culture slides, treated and fixed using 4% paraformaldehyde in PBS. This fixation step is needed to ensure

Materials and Methods

free access of the antibody to its antigen. The cells were washed in PBS three times each for 5 min before placing the slides for 30 min in a solution containing 1 % BSA in PBS in order to block nonspecific sites on the cells where the antibody might bind. The anti-PAR antibody was added to the slides for 1h in a final dilution of 1:100 in 0.5% BSA and 0.1% Tween 20 in PBS. The slides were gently washed twice each for 5 min with 0.2% Tween 20 in PBS to remove excess, unbound primary antibody. From here on, the all steps are performed in dark. The secondary antibody (Alexa fluor 594 anti-mouse monoclonal IgG) was then added to the slides in a 1:600 dilution in 0.5% BSA and 0.1 % Tween 20 in PBS and incubated for 1h. This antibody has a fluorescent tag at the other end that is responsible for emitting the signal (Alexa fluor 594). Thereafter, the slides were washed again twice for 5 min with 0.1% Tween 20 in PBS. A cover slip was placed over the cells and sealed with nail polish to preserve the samples. The slides were then examined and photographed under a fluorescent microscope where the fluorescent tag is excited with the proper wavelength (590/617 nm) and emits a fluorescent signal.

2.2.5. Repair substrates

Four GFP-based repair substrates were used in this study: pEJ and pEJ2 to monitor NHEJ efficiency for non-cohesive and cohesive ends respectively, pEJSSA for SSA together with NHEJ, and pGC for GC. All these reporters rely on restitution of GFP gene expression upon repair of the induced DSB. The end-joining substrate, pEJ, is designed similar to the previously described substrate pPHW2 (Dahm-Daphi, Hubbe et al. 2005; Willers, Husson et al. 2006) containing two I-SceI sites inserted in opposite direction into the 5' untranslated region of the GFP transcript. Between both I-SceI sites, an artificial start codon (ATG_{art}) was placed out of frame with the original ORF, hence preventing translation of GFP (Figure 4A). pEJ2 has the same structure except that both I-SceI sites are oriented in the same direction (Figure 4A). After induction of double strand break by I-SceI endonuclease leading to the deletion of the ATG_{art} site, the cell can repair this double strand break by NHEJ resulting in GFP expression.

pEJSSA as illustrated in Figure 5B, has the same structure as pEJ except from two 50 bp homologous repeats (SSA1 and SSA2) which flank the two I-SceI recognition sites. Both repeats are located 39 and 41 nts distant from the DSBs. The cells can repair the induced double-strand break either by NHEJ using the few most proximal bases for annealing or by SSA employing the two long repetitive sequences SSA1 and SSA2. Both repair events will result in a reconstituted translation of the GFP.

Materials and Methods

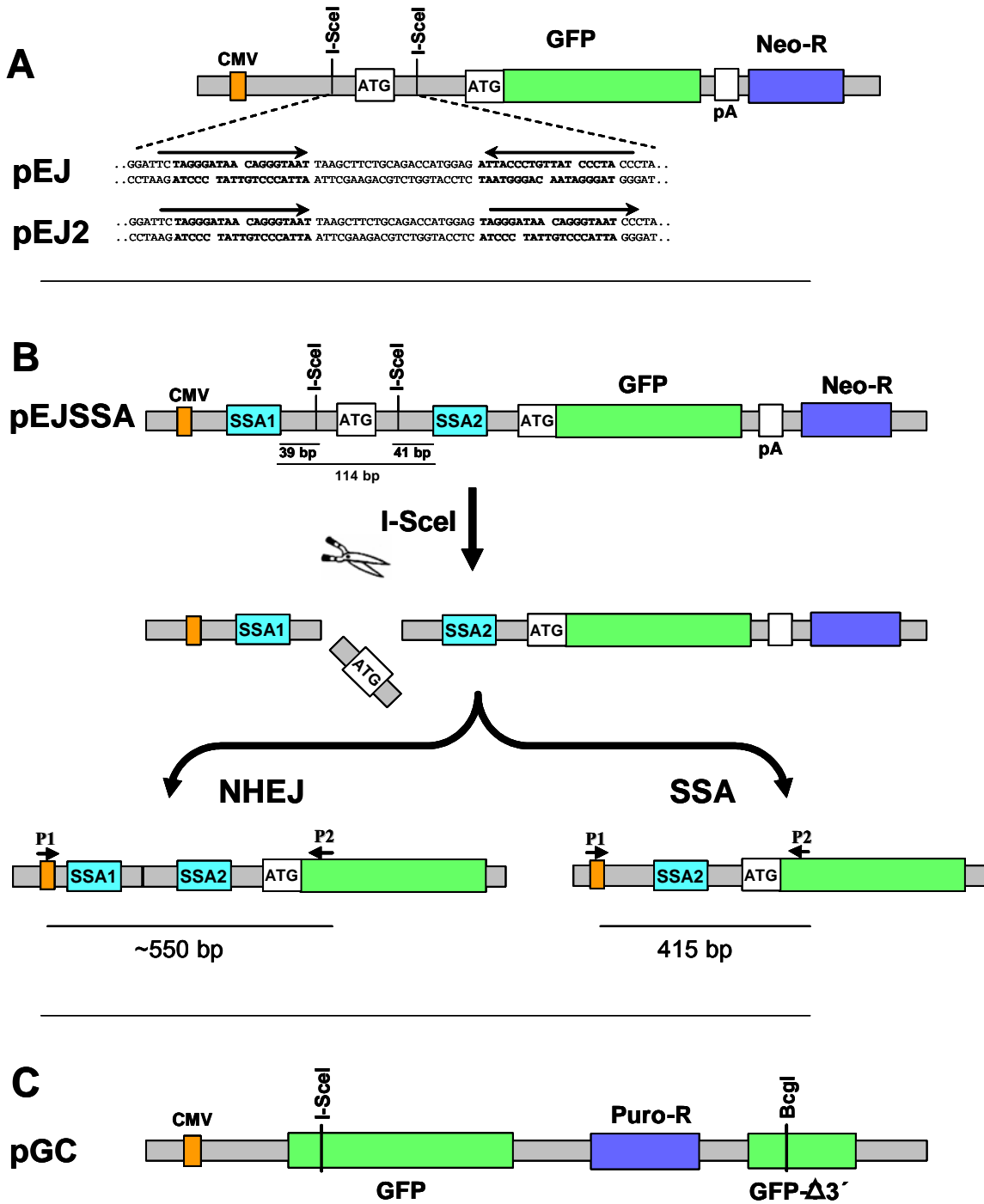


Figure 5. Reporter constructs. A) Schematic structure of the NHEJ substrates pEJ and pEJ2. Translation of GFP is prevented by an insert between the CMV promoter and the open reading frame (ORF), which is flanked by two inverted (for pEJ) or direct (for pEJ2) repeat I-SceI recognition sequences. Repair of the I-SceI-induced DSB by NHEJ restores GFP translation (see text for details). The insert illustrates the sequences flanking the two I-SceI sites (bold). B) The pEJSSA substrate for monitoring repair either by NHEJ or by SSA. pEJSSA is identical to pEJ, except for the presence of two additional 50-bp direct repeats (SSA1 and SSA2) flanking the I-SceI recognition sites. Simultaneous cleavage of both I-SceI sites leads to pop out of the artificial ATG. Repair by either pathway leads to green fluorescence. PCR analysis of NHEJ events using the primers P1 and P2 generates a fragment of about 550 bp. SSA events result in loss of one of the two SSA-cassettes and yields a PCR fragment size of exactly 415 bp. C) The pGC reporters with two non-functional GFP copies that share 520 bp of homology. DSB repair proceeds by gene conversion resulting in functional GFP. Constructs are not drawn to scale

Materials and Methods

pGC substrate consists of two inactive GFP genes (Figure 4C). The first copy is inactivated by an insertion of the 18-bp I-SceI recognition site into the unique Bcgl site of the GFP-coding sequence. The second copy is a truncated fragment of GFP (inactive). The truncated GFP copy is located 2.2 kb downstream of the mutated GFP fragment sequence and placed in the same orientation. The homology shared by both cassettes is 520bp long with 219 bp upstream and 301 bp downstream of the I-SceI recognition site.

2.2.6. Transfection Techniques

- **siRNA transfection (Trans-IT-TKO transfection agent)**

RNA interference (RNAi) is a mechanism that inhibits gene expression at the level of translation. The RNAi pathway is initiated by the enzyme dicer, which cleaves long, dsRNA molecules into short fragments of 20–25 base pairs called small interfering RNA (siRNA). These double stranded siRNA are recognized by another enzyme complex, the RNA-induced silencing complex (RISC), which uses one strand to target complementary mRNA molecules for degradation. Synthetic siRNA introduced into the cells against a gene of interest can be likewise used to drastically decrease the expression of selected gene through degradation of its mRNA. Since RNAi may not totally abolish expression of the gene, the method of using synthetic siRNA is technique is referred to as a "knockdown", to distinguish it from "knockout" procedures.

Free RNA molecules given into regular medium may be immediately destroyed by traces of RNase. In order to prevent this, the cells were grown for 5 passages in RNase-free α -medium. In this study, siRNA duplexes against Rad51 (siRad51) or control siRNA ("scrambled" scRNA) were synthesized by Qiagen. $4\text{-}5 \times 10^6$ confluent cells were seeded in T75 flask and incubated for 2h under optimum growth conditions (37°C, 5% CO₂). The transfection solution was prepared by diluting siRad51 or scRNA in OA-medium (108 μ l siRNA + 792 μ l OA-medium) to a final oligonucleotide concentration of 200 nM. In parallel, Trans-IT-TKO was diluted also in OA-medium (66 μ l TKO + 759 μ l OA-medium) and incubated in dark at RT for 5min. The diluted siRNA was carefully mixed with the diluted Trans-IT-TKO reagent and incubated in dark for 20 min at RT to form a transfection complex between siRNA and transfection reagent. 1.5 ml of this complex was added to the cells in a final volume of 7.5 ml α -medium/1% FCS without antibiotics.

- **Plasmid transfection (Electroporation)**

Electroporation was used to stably integrate the repair substrates in CHO cells and to transiently transfect I-SceI-expressing vector (pCMV3xnlS-I-SceI) in order to induce DSB. The goal of stable, long-term transfection is to isolate and propagate individual clones

Materials and Methods

containing transfected DNA. Therefore it is necessary to distinguish non-transfected cells from those that have taken up the exogenous DNA. This screening can be accomplished by genes that encode resistance to a lethal drug when an appropriate drug resistance marker is included in the transfected DNA. Only the individual cells that survive under the drug treatment have taken the transfected DNA.

In order to achieve chromosomal integration, the cells were electroporated with the linearized form the plasmid pEJ, pEJ2 and pEJSSA were linearized by AflIII. For linearization of pGC, XmnI was used. Complete digestion was verified by electrophoresis and the DNA band containing the linearized fragment was excised from the gel using a scalpel under UV-light. The DNA was purified from the gel using Wizard SV gel and PCR clean-up system according to manufacturer's instructions.

The cells (CHOK1 and xrs5) were trypsinized and collected in PBS with cell density of 4×10^6 /ml. 3×10^6 cells were mixed very well by pipetting with 0.5 μ g of either linearized substrate in a total volume of 800 μ l. The mixture was transferred into a 1 ml electroporation cuvette (BioZym Scientific GmbH, Oldendorf, Germany) and electroporated at 250 V and 950 μ F with constant time 11–13 seconds using Gene Pulser II Electroporator, immediately mixed with full medium and incubated for 2-3 days. The cells were then trypsinized and replated in α -medium containing 1.5 mg/ml of G418 to select for cells that have kept the plasmids pEJ, pEJ2 or pEJSSA integrated in their chromosomes. For pGC integration, puromycin was used at concentrations of 1.5 mg/ml. After 2-3 weeks, all cells without integrated plasmids died and distinct clones of "survivors" were seen. Individual colonies were trypsinized and transferred to multi-well plates for further propagation in the presence of selective medium.

2.2.7. Transfection efficiency

Transfection efficiency is cell type-dependent. We wanted to test the difference in the transfection efficiency between CHOK1 and xrs5 cells. 30 μ g of pEGFP-N1 plasmid that encodes for the GFP protein were used for electroporation of 4 independent clones of each cell line. 24h post transfection, the percentage of green fluorescent cells (GFP⁺) cells was assessed using flow cytometry (FACScan, BD Bioscience, Heidelberg, Germany). As seen in Figure 6, CHOK1 and xrs5 cells showed $70.8 \pm 3.9\%$ and $64.2 \pm 8.4\%$ of GFP⁺ cells, respectively. All repair results of xrs5 cells were corrected for this 1.1-fold lower transfection efficiency as compared to CHOK1.

2.2.8. Analysis of the repair

- **Induction of DSB in vivo and measuring repair efficiency**

Materials and Methods

In order to analyze repair, DSB has to be induced in the cells harbouring either one of the repair substrates. For that purpose, 50 µg of I-SceI-expression vector (pCMV3xnlS-I-SceI) or an empty control vector (pCMV-neo) was transfected into about 3×10^6 cells. Thereafter, the cells were immediately resuspended in prewarmed α -medium. Twenty-four hours later the medium was replaced with fresh one supplemented with 10% FCS. Twenty-four hours later, the cells were trypsinized, washed with and resuspended in PBS in a cell density of at least 1×10^6 cells/ml for FACS analysis or sorting of GFP⁺ cells. The fraction of GFP⁺ cells indicates the efficiency of the repair by NHEJ in cells harbour either pEJ or pEJ2. For cells that carry pGC, the GFP⁺ cells represent the repair by GC. For cells with pEJSSA, the GFP⁺ cells represent both NHEJ and SSA events.

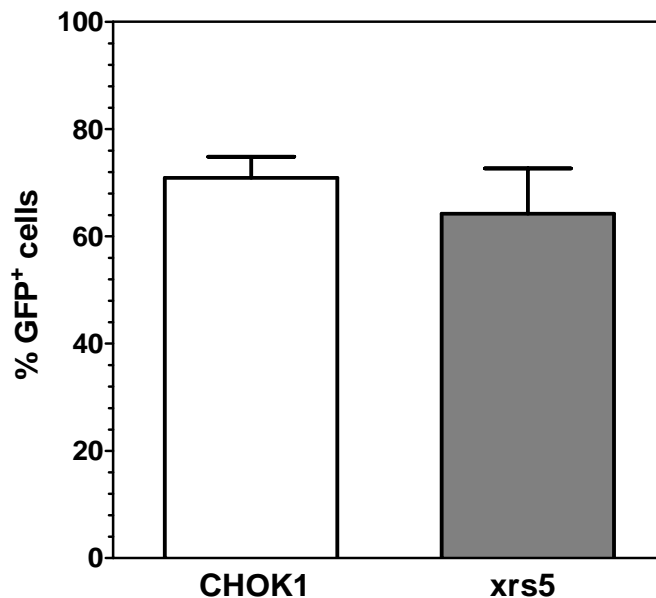


Figure 6. Transfection efficiency in CHOK1 and xrs5 cells. 30µg pEGFPN1 was electroporated into exponential growing cells. 24h post transfection, the percent of formed green fluorescence positive (GFP⁺) cells were assessed in 4 different clones of each CHOK1 (white) and xrs5 (grey) independently using FACS. CHOK1 and xrs5 cells showed 70.8±3.9% and 64.2±8.4% of GFP+ cells, respectively. All repair results were corrected for the 1.1 fold lower transfection efficiency of xrs5 cells.

- **Repair distribution between NHEJ and SSA**

In order to distinguish between NHEJ and SSA pathways in cells containing pEJSSA, GFP⁺ cells were sterile sorted by FACS, immediately reseeded in Petri dishes, raised to individual colonies which were then picked out and further expanded as described for DNA isolation.

Materials and Methods

The repair junctions were amplified from the DNA isolated from individual colonies using the primers P1 and P2 (Figure 4A). PCR conditions used included an initial denaturing step at 96°C for 2 min and amplification by 35 cycles at 96°C for 20 sec, 68°C for 20 sec, and 72°C for 80 sec, and a post-amplification extension for 7 min at 72°C. 5µl of DNA loading buffer were added to the PCR product, and were electrophorized on 1 % agarose gel supplemented with 0.5 µg/ml ethidium bromide at 100V for 1 h. The ethidium bromide signals were visualized using BioDoc II Gel documentation (Biometra, Germany). NHEJ and SSA events were further confirmed by sequencing (see below).

- **Topo-Cloning analysis**

As alternative to raising repair clones individually the TOPO-TA-cloning method was used to assess the distribution between NHEJ and SSA. To this end, genomic DNA was extracted from the whole sorted GFP⁺ population. Repair junctions were PCR amplified as described in the previous section using P1 and P2 primers. The PCR products which contain both NHEJ and SSA events were ligated into TOPO-TA vector according to the manufacturer's protocol (TOPO-TA cloning kit). Briefly, the commercially available Topo-TA vector carries a Topoisomerase I molecule which is covalently bound via its tyrosyl residue (Tyr-274) to each of the 3' phosphate end. This phospho-tyrosyl bond is subsequently attacked by the 5' hydroxyl group of the PCR product, releasing topoisomerase I (Shuman 1994). The ligated products were electroporated (1.8 kV, at a time constant of 4-5 sec) into "one shot TOP10" electro-competent E.coli. The transformed bacteria were incubated in LB medium for 1h at 37°C with agitation (225 rotations/min), spread on LB plates containing 0.8 mg/ml Ampicillin and incubated overnight at 37°C. Single clones were then picked from the plates and directly subjected to PCR using P1 and P2 primers at conditions described before.

- **Analysis of the repair fidelity**

NHEJ fidelity was assessed by sequencing of the end-joining junctions. The principle of DNA sequencing reactions is to use labelled dideoxy nucleotides (ddNTP) that lack the 3'-hydroxyl group necessary for chain extension. Whenever a dideoxy nucleotide is incorporated into a growing DNA chain, it terminates chain growth. An actual sequencing reaction mixture contains thousands of DNA template strands, which are all being sequenced simultaneously. Simply by chance, some annealed primers will only be extended a few nucleotides before the chain extension is terminated by the addition of a ddNTP. However, other primers will form a longer chain of DNA before a ddNTP is incorporated. Thus, after complete PCR, amplification products of all possible length are generated which carry one labelled terminal base. The sequencing reaction is performed in a thermal cycler in order to

Materials and Methods

increase the yield by repeating the sequencing reaction many times in one experiment. We applied an automated sequencing using different fluorescent labels attached to each of the four dideoxy nucleotides (ddATP, ddCTP, ddGTP and ddTTP). Consequently, each terminated DNA chain is coloured according to the nucleotide at its end, enabling us to determine the terminal base in each fragment of DNA.

The PCR products after Topo-cloning were subjected to this sequencing PCR using only the P1 primer in the presence of "Half-term" buffer and "Big-Dye" mixture containing beside the labelled and unlabelled nts a high fidelity polymerase for 35 cycles at 96°C for 50 sec, at 55°C for 50 sec, and at 64°C for 240 sec. The product was precipitated in sodium acetate and subjected to capillary electrophoresis in the UKE service lab on a ABI 377 automated sequencer.

2.2.9. Western Blot

The knockdown of Rad51 expression using siRNA technology was examined by Western blot. The total protein was extracted from the cells transfected with siRad51 and 50 µg of total protein were electrophorized on 12% SDS-PAGE, and then transferred onto PVDF membrane. Rad51 protein expression was detected using an anti-Rad51 antibody.

- **Protein extraction and quantification**

All extract preparation steps were performed at 4°C. The total protein extraction was achieved according to Finnie et al (Finnie, Gottlieb et al. 1995). $1-3 \times 10^7$ cells were collected by trypsinization, and centrifuged. The pellet was resuspended in 100 µl of protein extraction buffer and 4 times shock frozen on liquid N₂ and re-thawing at 30°C. The lyses mixture was centrifuged at 12,000 rpm / 4°C for 15 minutes. The supernatant, containing the total soluble protein was transferred to a new tube and stored in -80°C.

BCA-method was used to determine total protein concentration (Smith, Krohn et al. 1985) which based upon the use of Biuret-reaction. The Biuret reagent (copper sulphate dissolved in a strong base) changes to brown colour upon reaction with peptide bonds. The BCA Protein Assay reagent was prepared by mixing reagent A and reagent B in a ratio of 50:1. Two µl of protein extracts were added to 48 µl dd.H₂O. 50 µl of dd.H₂O was used as a blank. One ml of the colour reagent was added to the diluted samples and the blank as well and after vortexing, they were incubated at 37°C for 30 minutes. The colour intensity was determined using a spectrophotometer at a wave length of 562 nm.

- **Sodium Dodecyl sulfate-polyacrylamide gel electrophoresis (SDS-PAGE) and blotting onto PDVF membrane**

Materials and Methods

For the electrophoresis, 50 µg of total protein with 5X loading buffer and dd.H₂O in a final volume of 20 µl were mixed very well together. The samples were denatured at 100°C for 10 minutes, spun down and immediately placed on ice. The samples were loaded onto SDS- polyacrylamide gels. For molecular weight determination, Magic Mark Western Protein Standard was used. The electrophoresis was run at 100 V for 5 min to collect the proteins through stacking gel and at 200 V for 55 min for separation.

The electrophorized proteins were transferred onto PDVF membranes with 0.2 µm pores. The membrane was activated by submersion in methanol for 10 seconds and then washed for 5 minutes in dd.H₂O. Both, gel and membrane were equilibrated in transfer buffer for 5 min. Transfer was performed by electro-blotting for 30 min at 100 V and 4°C. After the blotting, the gel was stained in Coomassie-Blue staining solution for 30 min to confirm the completeness of transfer.

- **Detection of proteins**

After blotting, the membrane was blocked for 1 h in blocking solution at RT to prevent any unspecific protein binding to the PVDF material that would create a high background. All following incubations were performed on a shaker platform to achieve optimum contact of solutions and membranes. The membrane was then incubated for 5 min in PBST solution at RT followed by incubation for 1h at RT with anti-Rad51 antibody in a final dilution of 1:100 in 5% w/v non-fat milk in PBS. The membrane then was washed three times for 10 min each in PBST solution at RT. Thereafter, the secondary antibody (ECL anti-rabbit IgG) was added in 5 % (w/v) non-fat milk (1:1000) and incubated for 1h at RT. The membrane was washed again three times with PBST solution in order to remove unbound secondary antibodies from the membrane. For signal detection, the membrane was incubated for 1 min with ECL- solution (consisting of equal volumes of solution 1 and 2 of the Amersham ECL kit). X-ray film was exposed to the membrane and the chemo-luminescence signal was detected after the film has been developed fixed and extensively rinsed in pure water. Alternatively, the chemo-luminescent signals were quantified directly by a sensitive CCD-camera (NightOWL). After detection of the Rad51 signal on the membrane, the signal of the housekeeping protein β-actin, as a control, was measured analogously to verify equal loading of the samples.

The relative Rad51 expression was evaluated after normalization to β-actin signal and extracting the background signal as follows:

$$\text{Relative protein signal} = \frac{(\text{protein1 signal} - \text{Background signal}) / (\beta\text{-actin signal} - \text{Background signal})_{\text{siRNA}}}{(\text{protein signal} - \text{Background signal}) / (\beta\text{-actin signal} - \text{Background signal})_{\text{scRNA}}} \times 100$$

3. RESULTS

In the current study, 4 GFP-based repair reporters were used namely; pEJ&pEJ2 for assessing NHEJ, pGC for GC and pEJSSA for monitoring both NHEJ and SSA. The first three reporters (pEJ, pEJ2 and pGC) were previously constructed in this laboratory, while design and cloning of pEJSSA was part of this study.

3.1. pEJSSA cloning

pEJSSA is a GFP-based reporter which has been designed to investigate single strand annealing (SSA) and NHEJ in the chromosomal context. It relies on reactivation of GFP expression upon repair of single I-SceI endonuclease-induced DSBs. It has the same structure as of pEJ, however, to make SSA available, two 50 bp homologous sequences named SSAI and SSAIL were inserted as XhoI-BclII and PvuI-AgeI fragments, respectively.

3.1.1. Insertion of SSA1 and SSA2

For SSAI insertion, both pEJ and SSA1 were double digested by BclII and XhoI. BclII cleaves at the sequence TGATCA which is subject of dam methylation (CmATC) in bacteria. To avoid this methylation, which precludes BclII activity, the plasmid had to be amplified in dam⁻ bacteria. After transformation, pEJ was extracted from individual clones using mini-and maxi-prep kits according to the manufactures' protocols. 2 Units (U) of BclII were used to digest pEJ at 37°C for 2h. The digestion was confirmed using an agarose gel and the linear form was purified and restricted a second time by XhoI for 2h/37°C. Similarly, the oligonucleotide SSAI was digested in two steps using BclII and XhoI, the recognition sites of which flank the sequence on either site.

The XhoI-SSAI-BclII fragment (insert) was ligated to the double-digested plasmid (BclII-pEJ-XhoI) using T4 ligase. During this reaction, a variety of different products such as vector-vector or insert-insert dimers are formed beside the insert-vector ligation. The desired product (insert-vector) was distinguished from the other non-desired products on a agarose gel, purified and sequenced using Big-Dye method (see materials and methods). This intermediate was named pEJSSA1.

Following the same steps, SSAIL was inserted by ligating PvuI-SSAIL-AgeI fragment to the AgeI-pEJSSA1-PvuI-fragment forming pEJSSA. The successful insertion of both SSA1 and SSA2 was verified by sequencing pEJSSA using the P1 primer (for more details see materials and methods). As illustrated in Figure 7, both SSAI and SSAIL have been correctly inserted at the right positions flanking the two I-SceI sites.

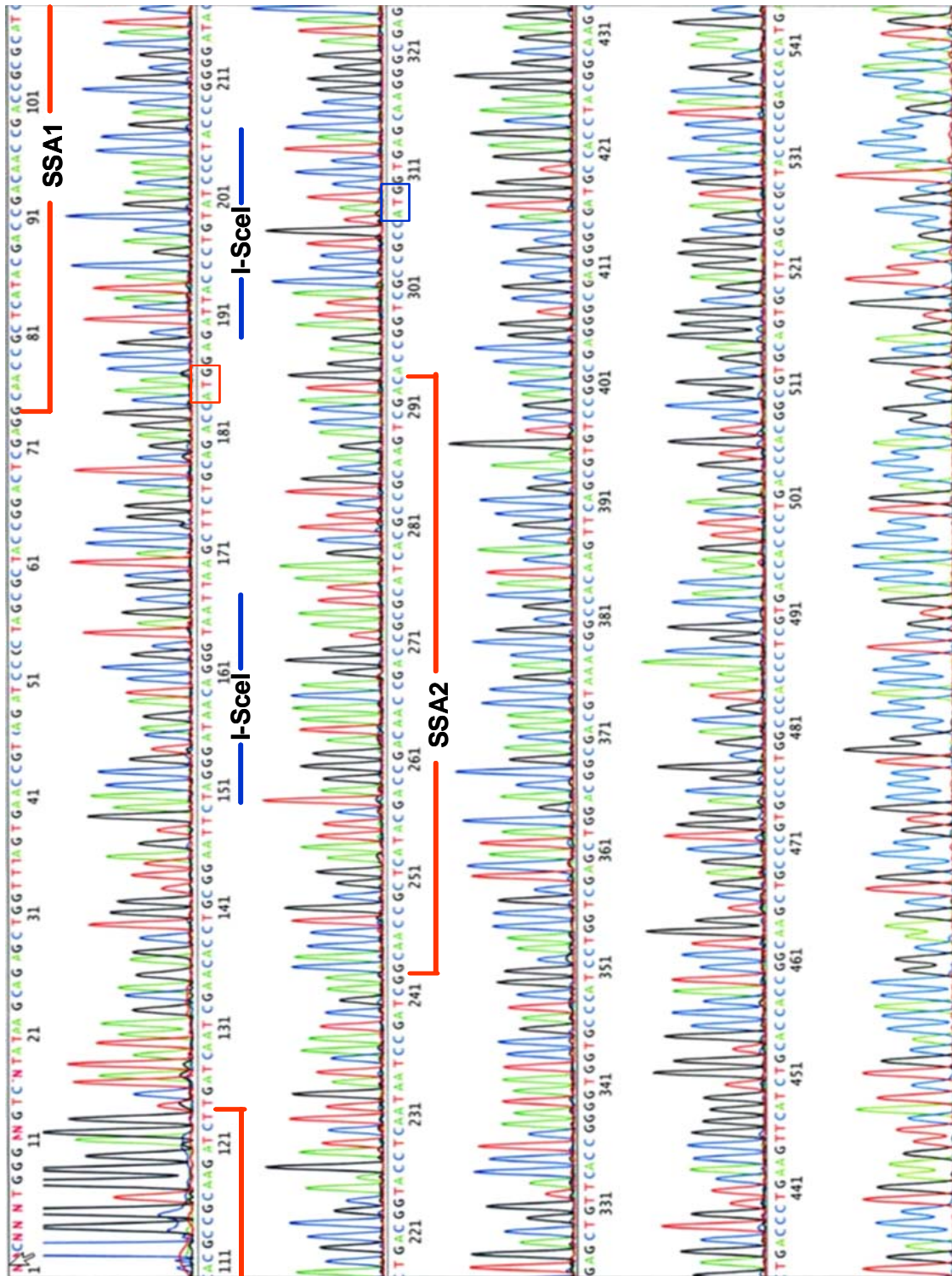


Figure 7. Sequencing analysis of pEJSSA. Successful insertion of both SSA1 and SSA2 was verified by Big-Dye labeled sequencing using P1 primer. Both SSA1 and SSA2 (red lines) flank the two 18-bp I-SceI sites (blue lines). Both ATG^{art} and ATG^{orig} are shown in red and blue squares, respectively.

3.1.2. Functional assay for pEJSSA

In the following pilot experiment we tested the functionality of pEJSSA by assessing the ability of the cells to repair the double strand break induced within the plasmid. The principle of this experiment is to induce DSB within the plasmid in vitro by digesting the plasmid by I-SceI endonuclease and transfecting the cells (*xrs5* in this case) with the linearized plasmid. 48h post-transfection the percentage of GFP-expressing cells (GFP⁺) cells was assessed by FACS, as indication for the occurrence of repair. Both undigested and AflIII-linearized plasmids were used as controls. As illustrated in Figure 8, transfection of the I-SceI-linearized pEJSSA resulted in 1.16 % GFP⁺ cells, while transfection of circular and AflIII-digested plasmids resulted in almost no GFP⁺ cells (0.03% and 0.04%, respectively). This 39-folds increase indicates that the cells have correctly reconstituted the expression of GFP by repairing the I-SceI-induced DSB and prove the pEJSSA functional.

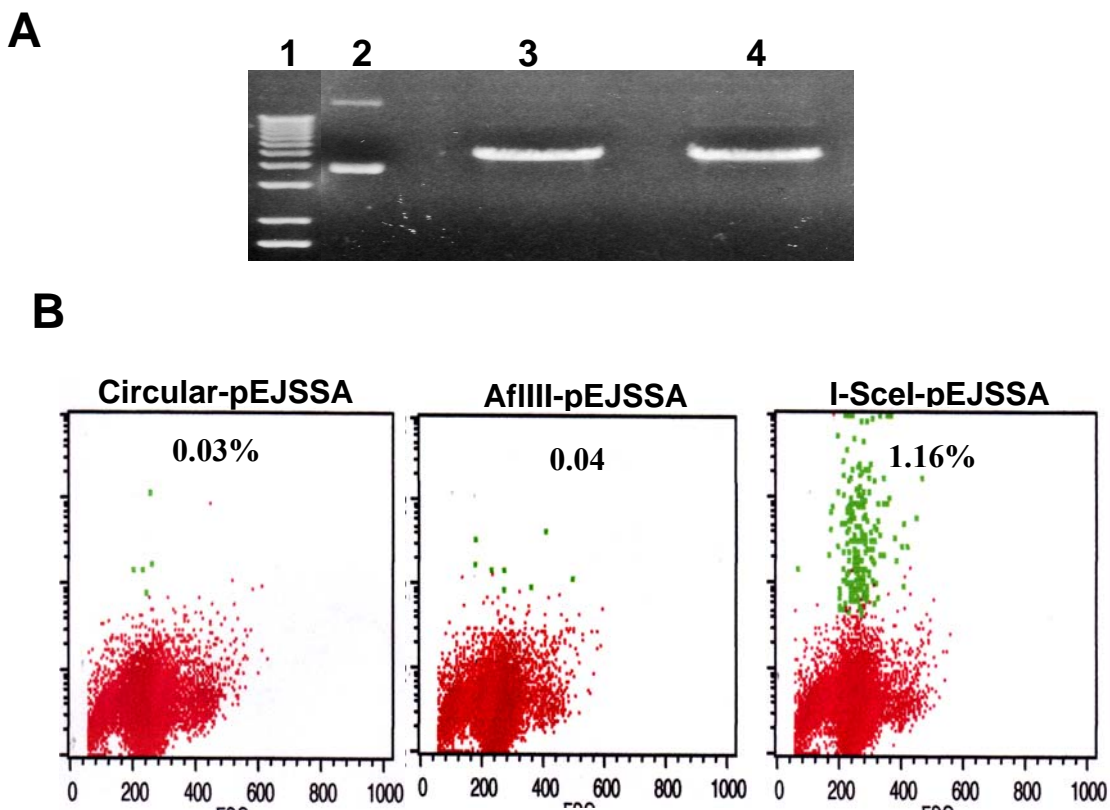


Figure 8. Functional assay for pEJSSA. A) Gel electrophoresis of undigested plasmid (lane 2), AflIII- (lane 3) or SceI- (lane 4) linearized pEJSSA. B) FACS analysis for GFP⁺ cells resulted 24h after transfecting *xrs5* cells with 30 µg of either circular, AflIII- or SceI-linearized pEJSSA. Transfection with either circular, AflIII-linearized plasmid resulted in 0.03 % and 0.04 % GFP⁺ cells respectively while in case of AflIII-linearized plasmid was 1.16 %.

3.1.3. Integration of pEJSSA in Hamster cells

Next, pEJSSA was integrated into chromosomes of CHOK1 and xrs5 cells in order to assess the ratio between NHEJ and SSA *in vivo*. To this end, 5 µg of pEJSSA was firstly linearized by AflIII (Figure 8A lane3), purified from the gel and quantified using a UV-spectrophotometer. Three different concentrations of AflIII-linearized pEJSSA (0.2, 0.5 and 1.0 µg) were used to transfect both CHOK1 and xrs5 cells using electroporation. The cells which harbour pEJSSA were selected by growth in medium containing 1.5 mg/ml G418. The resistant clones were picked by micro-trypsinization and expanded for further analysis.

3.1.4. Testing for intact stable integration

Next, we wanted to verify that pEJSSA has been integrated as an intact copy. pEJSSA as illustrated in Figure 9A contains (1) the GFP-gene (~701 bp), with its CMV-promoter (~589 bp), (2) the neomycin resistance gene (~794 bp) and its promoter (~380 bp), (3) plasmid replication origin (~643 bp) which enable the replication of the plasmid in bacterial cells, and (4) the repair cassette which span the 240 bp at the multiple cloning site (MCS). This cassette is located between the CMV-promoter and GFP gene and contain the two I-SceI sites flanking ATG^{art} and the two repetitive sequences (SSA1 & SSA2). Integrity of most of the elements were tested functionally and the regions flanking the AflIII site by sequencing.

Amplification of plasmids in bacteria guaranties an intact pUC origin of replication. Growth of hamster clones in G418 confirms that the neomycin resistance gene and its promoter are maintained correctly. These clones were then tested for intact copy of GFP gene by measuring the expression of GFP protein after DSB induction via I-SceI-expression. Figure 9B shows some representative CHOK1 clones tested by FACS for GFP-expression. Clones # 9, 64, 23 and 57 expressed GFP protein indicating an intact integrated copy of GFP gene and its CMV-promoter. On the other hand, clone #91 did not produce GFP⁺ cells upon DSB-induction which suggests a mutation with in the GFP gene or its promoter.

The intact repair elements have been tested via PCR using 3 different sets of primers (S1F&S1R, P1&P2, and S2F&S2R) (see Figure 9A). Shown in Figure 9B is the electrophoresis of the PCR products of some CHOK1 clones (#9, 91, 64, 23, and 57) using these primer sets. Clones #9, 64, 23, and 57 showed the right amplification pattern for all primer sets (lanes 2, 4, 5, and 6 respectively) while clone #91 gave no product with S1F&S1R primer set (lane 3 above panel), which indicates that at least part of this region may be deleted. This region contains a significant part of the CMV-promoter which explains as to why this clone did not express GFP (Figure 9B). All the clones which were used in the upcoming experiments have been analogously tested for the intact integration.

Results

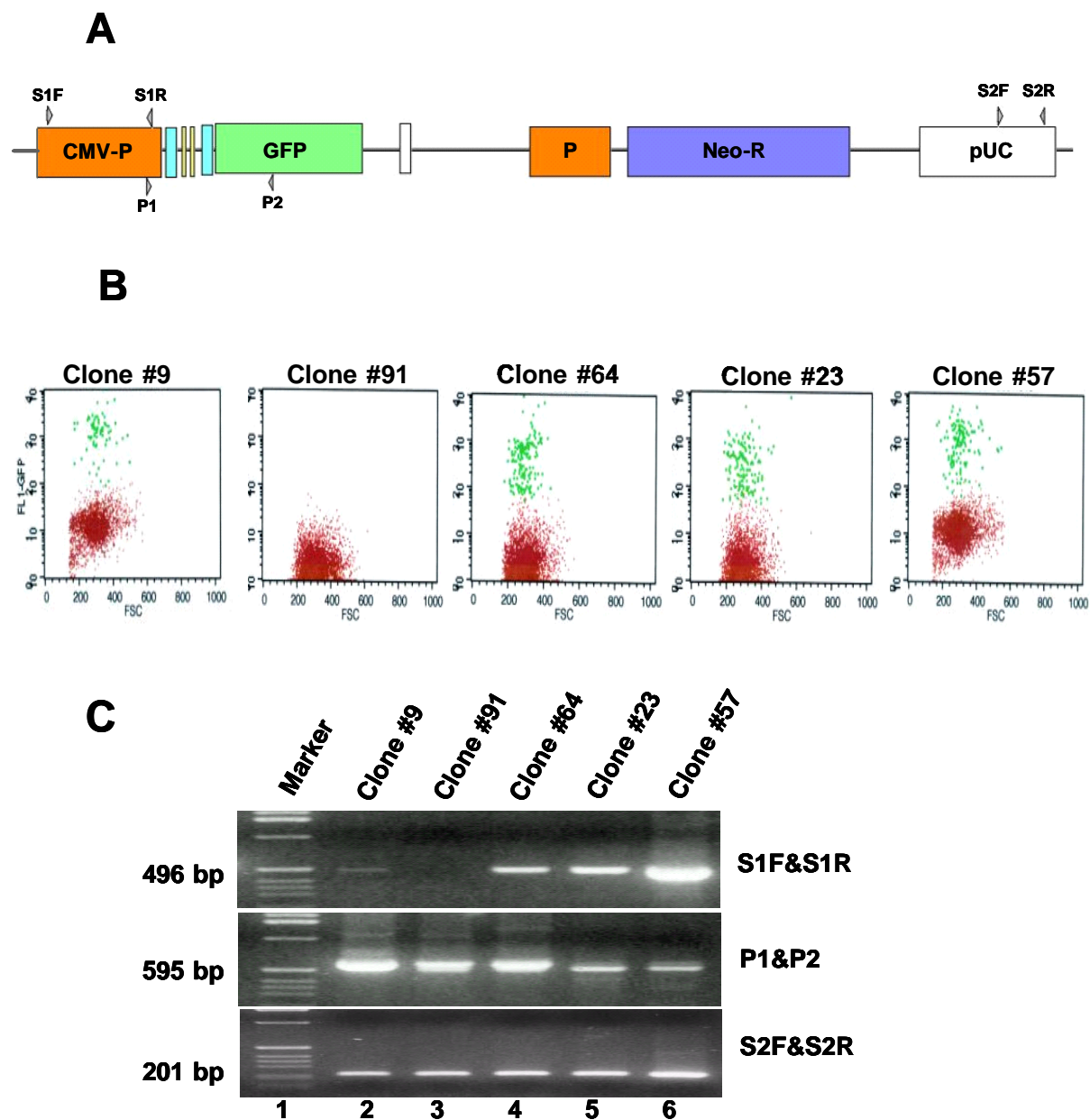


Figure 9. Intact integration of pEJSSA. A) To-scale-schematic representation for pEJSSA showing positions of S1F&S1R, P1&P2, and S2F&S2R. B) FACS analysis showing the GFP⁺ cells produced in the indicated CHOK1 clones after transfection with I-SceI-expressing vector. 24h-posttransfection, clones # 9, 64, 23, and 57 showed specific fraction of GFP⁺ cells while clone # 91 did not. C) Gel electrophoresis of PCR amplified fragments using S1F&S1R (471-bp, upper panel), P1&P2 (575 bp, middle panel) and S2F&S2R (222 bp, lower panel). Lane 1: 1kb DNA ladder.

3.2. Repair efficiency

3.2.1. NHEJ efficiency for cohesive and non-cohesive ends

Previous studies reported that the efficiency of NHEJ is affected dramatically by the structure of the DSB ends (Ma, Kim et al. 2003; Guirouilh-Barbat, Huck et al. 2004). To address this issue, pEJ and pEJ2 substrates with non-cohesive and cohesive ends respectively, were integrated in both CHOK1 and *xrs5* cells independently. Individual clones were harvested and expanded as described. A panel of clones were scored for green fluorescence 24h after transfection of I-SceI-expressing vector. Shown in Figure 10 A and B is the NHEJ efficiency of CHOK1 and *xrs5* cells that harbour either of pEJ or pEJ2. The mean value of 10 different pEJ clones from either strain showed a significantly higher repair efficiency in CHOK1 cells (3.0 ± 0.6 %) in comparison to its Ku80-deficient counterpart *xrs5* (0.71 ± 0.1 %). This ~ 4-fold decrease in NHEJ efficiency due to Ku80-deficiency was also observed in case of pEJ2 substrate (5.47 ± 1.1 % for 12 CHOK1 clones and 1.5 ± 0.3 % for 13 *xrs5* clones). This results revealed that CHOK1 cells repair the induced DSB with significant higher efficiency than *xrs5* cells regardless of whether the ends are cohesive ($p=0.0012$) or non-cohesive ($p=0.0025$). The data also showed that the overall joining efficiency was in both strains for cohesive ends slightly higher than for non-cohesive ends. However, the differences were statistically not significant ($p=0.13$ and $p=0.2$ for CHOK1 and *xrs5*, respectively).

3.2.2. NHEJ repair kinetics in both CHOK1 and *xrs5* cells

Previously, our lab reported a modest decrease (1.5-folds) in NHEJ efficiency in Ku80-deficient cells compared wild-type mouse fibroblasts (Schulte-Uentrop, El-Awady et al. 2008), while in the current study this reduction was more pronounced (~4-folds). Beside different cell systems and repair reporter constructs used the two studies measured the repair efficiency at different time intervals. Schulte-Uentrop allowed 48h for repair while in the current study as shown in Figure 10A and B cells were harvested 24h after transfection. In order to further study the effect of the repair time a continuous kinetics was recorded. The percentage of GFP⁺ cells was measured at 0, 6, 12, 24, 48, 72, and 96 h after transfection of the I-SceI expression vector. In CHOK1 cells earliest repair events were detectable after only 6h of repair incubation post-transfection for both pEJ and pEJ2. (Figure 10C). *xrs5* cells showed the first repair events about 6h later. The fraction of GFP⁺ cells steadily increased with time in both strains to reach 3.3 % in CHOK1 and 1.1 % in *xrs5* for pEJ 24h post transfection. This ~4-fold difference between both strains was also observed for pEJ2 (4.6 vs. 1.9 % in CHOK1 and *xrs5* cells, respectively) perfectly confirming the previous result

Results

(Figure 10A and B). 48h post-transfection, the number of GFP⁺ cells in CHOK1 increased slightly further to reach 4.2 % for pEJ and 5.1 % for pEJ2.

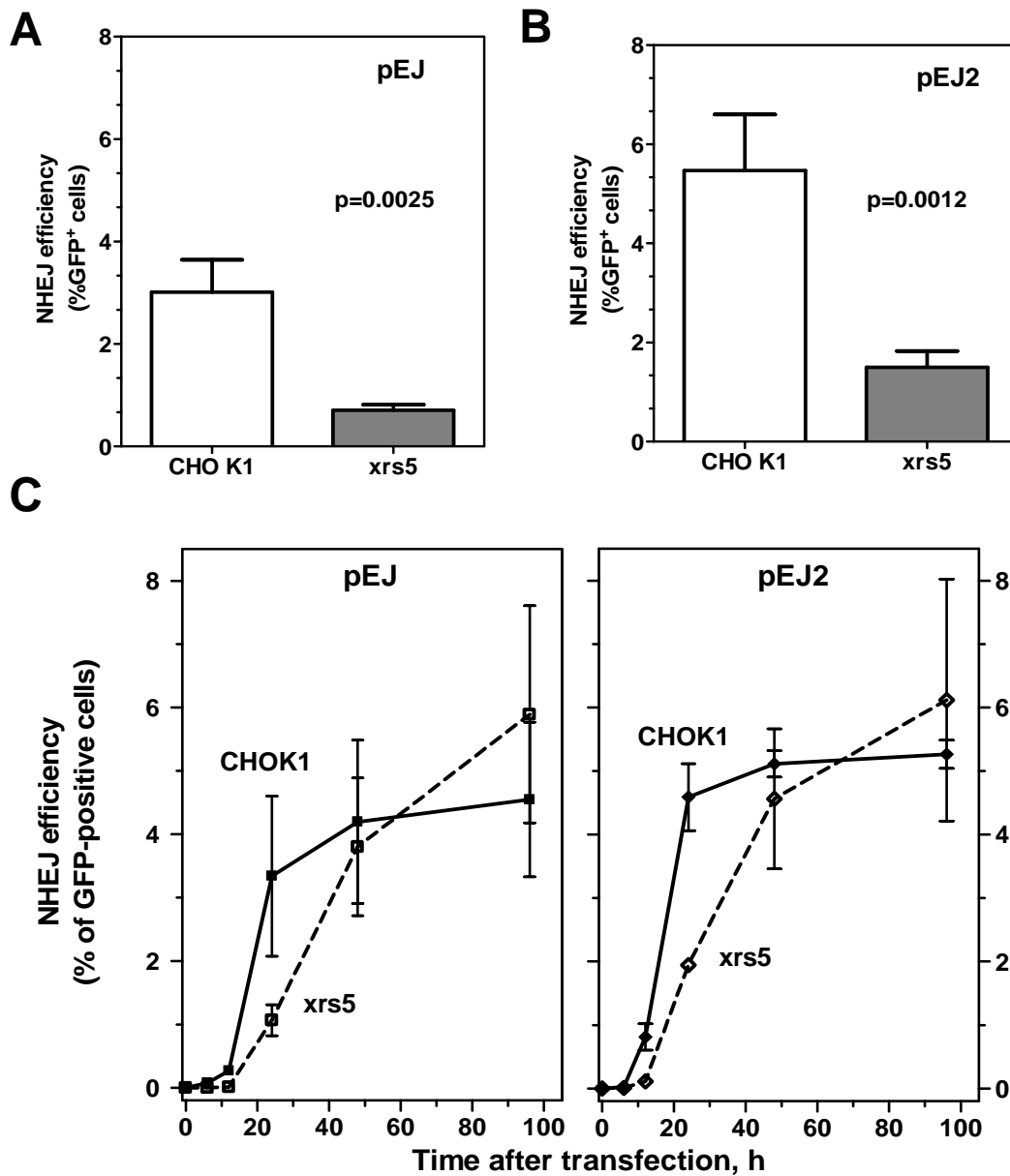


Figure 10. Effect of Ku80-deficiency on NHEJ efficiency. A) NHEJ repair efficiency of non-cohesive ends corresponds to the fraction of GFP⁺ cells produced 24h-post transfection with I-SceI-expressing vector. Shown are the mean values of 10 independent clones of either CHOK1 (white) or xrs5 (grey) harbouring pEJ. Difference between the two strains was significant (Mann-Whitney, $p=0.0025$). B) NHEJ repair efficiency of cohesive ends corresponds to the fraction of GFP⁺ cells produced 24h-post transfection with I-SceI-expressing vector. Shown are the mean value of 12 independent clones of CHOK1 (white) and 13 clones of xrs5 (grey) harbouring pEJ2. Difference between the two strains was significant (Mann-Whitney, $p=0.0012$). C) NHEJ repair kinetics showing efficient but slower end-joining in xrs5 (dashed line) compared to CHOK1 cells (solid line) for both pEJ (left) and pEJ2 (right).

Results

Strikingly, this increase was more pronounced in *xrs5* cells (3.8 % for pEJ and 4.6 % for pEJ2), approaching closely the values of the wild-type cells. After 96 h *xrs5* showed even more GFP⁺ cells higher than the wild-type, however the differences were not significant. These data demonstrate that Ku80-deficient cells (*xrs5*) repaired DSB efficiently but at a slower rate compared to their Ku80-proficient counterparts (CHOK1).

3.2.3. NHEJ repair fidelity in both CHOK1 and *xrs5* cells

Ku80 has been reported to affect not only the repair efficiency (see above, Schulte-Uentrop, El-Awady et al. 2008) but also repair fidelity (Kabotyanski, Gomelsky et al. 1998; Feldmann, Schmiemann et al. 2000; Guirouilh-Barbat, Huck et al. 2004; Kuhfittig-Kulle, Feldmann et al. 2007; Schulte-Uentrop, El-Awady et al. 2008). To address this, GFP⁺ cells of two different clones of each CHOK1 and *xrs5* cells harbouring either of the NHEJ substrates were sorted out using a FAC-Sorter and subjected to further analysis. By means of TopoTA-cloning, 190 repair junctions were scored. These junctions were PCR- amplified using P1 and P2 primers. Figure 11A (upper panel) revealed that almost all the amplified fragments from repair junctions in CHOK1 showed similar molecular weight as parental sequence (compare lanes 1-18 with lane 19). In contrast, amplified *xrs5* junctions (Figure 11A, lower panel) showed smaller molecular weight (lanes 1-10 and 12-19) compared with pEJ fragment (lane 11) indicating significant sequence loss during the repair. The junctions were sequenced for pEJ and pEJ2 of either strain after 24 and 48 h of transfection and depicted in an alignment chart (Figure 11B and C). The analysis of the spectrum deletion length at individual junctions for CHOK1-pEJ showed that 24h-post transfection, the majority of repair junctions (74%) were accomplished with no deletion (Figure 12A, left panel). Essentially, the same spectrum was observed 48h-post transfection (Figure 12A, left panel). Interestingly, not even a single repair junction was observed in *xrs5*-pEJ cells without any deletion (Figure 12A, right panel). 24h post transfection the majority of the repair junctions (73%) showed deletions of up to 20 bp and 27% those with more than 20 bp. Strikingly, 48h post transfection only 32% of the repair junctions in *xrs5* cells showed shorter deletions while 68% showed extremely long deletions (>20 bp, maximum 114 bp). Accordingly, the mean deletion length in *xrs5*-EJ cells was 17 ± 3 bp 24h post transfection and it increased significantly to 45 ± 7 bp 48h-post transfection ($p=0.003$) (Figure 12C). In contrast, the mean deletion length in their CHOK1 counterparts was 3.1 ± 2 bp 24h post transfection and had been not changed 24h later (1.4 ± 0.6 bp, $p=0.7$).

Deletions spectrum in cells containing pEJ2 showed essentially the same shift to more error-prone outcome after 48h of repair as described for pEJ (Figure 12B). The mean deletion length in *xrs5*-pEJ2 increased from 22.6 ± 6 bp after 24h to 45.5 ± 7.9 bp after 48h

Results

(difference, $p=0.003$) while deletion length remained constantly on a low level in CHOK1 cells ($p=0.8$). (Figure 12D).

These data unveiled that, in comparison to CHOK1, *xrs5* cells repair the DSB with more errors. Those errors, i.e. deletion length, increased with time indicating that in the absence of functional Ku80, the ends are subject of continuous degradation.

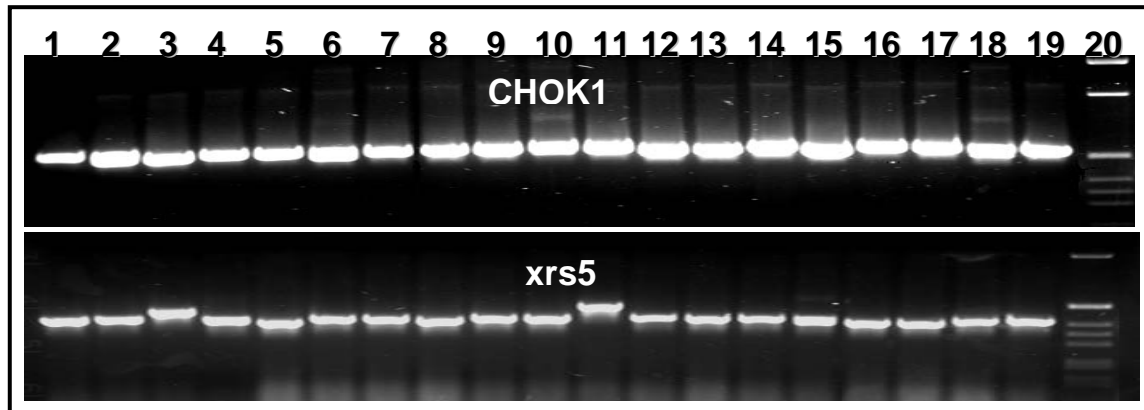
3.2.4. The role of PARP1 for DSB repair in Ku80-deficient cells

The above results can be explained in either of two ways. In the absence of Ku other NHEJ repair proteins recruited slower to the DSB ends which delays the completion of repair. In this case, except from Ku the pathway uses the same repertoire of enzymes including DNA-PKcs and XRCC4/LigaseIV/XLF. Due to slower recruitment of the DNA binding proteins the ends are more vulnerable to degradation by nucleases. Alternatively, in the absence of Ku cells use another genetically distinct end-joining pathway which operates more slowly and error-prone

Some recent reports have introduced poly(ADP-ribose) polymerase 1 protein (PARP1) as a potential player in an end-joining pathway based on its high binding affinity for DNA DSBs (Weinfeld, Chaudhry et al. 1997; D'Silva, Pelletier et al. 1999). PARP1 is involved in different cellular processes, including base excision and single-strand break repair (Bouchard, Rouleau et al. 2003). Upon binding to damaged DNA, PARP1 catalyzes the cleavage of its substrate NAD⁺ producing polymers of ADP-ribose moieties (PAR). These moieties bind to many target proteins such as XRCC1, histon H1, Ku70/80, p53 and PARP1 itself. These PAR residues form of high-molecular weight branched structures (adducts of > 40 molecules) on their targets which presumably serve as signals for further proteins recruitment. This post-translational modification is called poly(ADP-ribosyl)ation. A possible role of PARP1 in the repair of DSBs is supported by the following points. (i) Ku heterodimer does not represent the only DSB recognition complex in the cell because it was originally pointed out that PARP1 is activated in vitro by DSBs (Benjamin and Gill 1980). (ii) Purified PARP1 binds to DSBs with a higher efficacy than to SSBs (Weinfeld, Chaudhry et al. 1997) and with an affinity even greater than that of DNA-PK (D'Silva, Pelletier et al. 1999). (iii) PARP1 has been shown to interact with both subunits of DNA-PK (Ariumi, Masutani et al. 1999; Galande and Kohwi-Shigematsu 1999) catalyzing their poly(ADP-ribosyl)ation (Ruscetti, Lehnert et al. 1998; Li, Navarro et al. 2004). (iv) In cells, nuclear areas of poly(ADP-ribosyl)ation were induced concomitantly to the formation of direct DSBs via V(D)J recombination in the absence of functional DNA-PK (Brown, Franco et al. 2002).

Results

A



B

| Parental | n | Del (bp) | μh (bp) |
|---|----|----------|---------|
| AACACCTGCGGAATTC TAGGGATAACAGGGTAATTAAGCTTCTGCAGACCATGGAGATTACCTGTTATCCCTACCCGGGGATACTGACGG TTGTGGACGCCCTTAAGATCCCTATTGTCCCATTAATTGCGAAGCGTCTGTACCTCTAATGGGACAATAGGGATGGGCCCTATGACTGCC | | | |
| I-SceI-induced DSB AACACCTGCGGAATTC TAGGGATAA-----CCCTACCCGGGGATACTGACGG | | | |
| CHOK1-pEJ/24h | | | |
| AACACCTGCGGAATTC TAGGGAT-----tatCCCTACCCGGGGATACTGACGG | 12 | -1 | 1 |
| AACACCTGCGGAATTC TAGGGATAA-----tCCCTACCCGGGGATACTGACGG | 8 | -1 | 1 |
| AACACCTGCGGAATTC TAGGGATA-----CCCTACCCGGGGATACTGACGG | 7 | 0 | 0 |
| AACACCTGCGGAATTC TAG-----tCCCTACCCGGGGATACTGACGG | 1 | 5 | 0 |
| AACACCTGCGGAATTC TAGGGATAACAGGGTAATTAAGCTTCTGCAGACCATGGAGATTA-----CCCTACCCGGGGATACTGACGG | 1 | 9 | 4 |
| AACACCTGCGGAATTC TAGGGA-----CCCTACCCGGGGATACTGACGG | 1 | 2 | 2 |
| AACACCTGCGGAATTC TAGGGATAA-----G | 1 | 21 | 1 |
| AACACCTGCGGAATTC TAG----- | 1 | 49 | 1 |
| AACACCTGCGGAATTC TA-----GGGATACTGACGG | 1 | 15 | 3 |
| AACACCTGCGGAATTC T-----tatCCCTACCCGGGGATACTGACGG | 1 | 5 | 1 |
| CHOK1-pEJ/48h | | | |
| AACACCTGCGGAATTC TAGGGAT-----tatCCCTACCCGGGGATACTGACGG | 15 | -1 | 1 |
| AACACCTGCGGAATTC TAGGGATAA-----tCCCTACCCGGGGATACTGACGG | 9 | -1 | 1 |
| AACACCTGCGGAATTC TAGGGATA-----tCCCTACCCGGGGATACTGACGG | 4 | 0 | 2 |
| AACACCTGCGGAATTC TAGGGAT-----CCCTACCCGGGGATACTGACGG | 3 | 2 | 2 |
| AACACCTGCGGAATTC TAGGGATAA-----CCCTACCCGGGGATACTGACGG | 3 | 0 | 0 |
| AACACCTGCGGAATTC TAGGGATAACAGGGTAATTAAGCTTCTGCAGACCATGGAGATTACCTGTTA-----CCCTACCCGGGGATACTGACGG | 1 | 1 | 0 |
| AACACCTGCGGAA-----CCCTACCCGGGGATACTGACGG | 1 | 11 | 0 |
| AACACCTGCGGAA-----GGGATACTGACGG | 1 | 20 | 0 |
| AACACCTGCGGAATTC-----atCCCTACCCGGGGATACTGACGG | 1 | 8 | 2 |
| AACACCTGCGGAATTC TAGGGATAA-----TTAAGCTTCTGCAGACCATGGAGATTACCTGTTATCCCTACCCGGGGATACTGACGG | 1 | 8 | 3 |
| xrs5-pEJ/24h | | | |
| AACACCTGCGGAATTC TA-----CCCTACCCGGGGATACTGACGG | 1 | 7 | 0 |
| AACACCTGCGGAATTC T-----CCCTACCCGGGGATACTGACGG | 1 | 8 | 1 |
| AACACCTGCGGAATTC TAGG----- | 1 | 61 | 1 |
| AACACCTGCGGAATTC TA-----tCCCTACCCGGGGATACTGACGG | 1 | 6 | 2 |
| AACACCTGCGGAATTC T-----CTACCCGGGGATACTGACGG | 1 | 10 | 0 |
| AACACCTGCGGAATTC TA-----CCCGGGGATACTGACGG | 1 | 13 | 2 |
| AACACCTGCGGAATTC TA-----CGGGGATACTGACGG | 1 | 15 | 0 |
| AACACCTGCGGA-----GGGATACTGACGG | 1 | 23 | 0 |
| AACACCTGCGG-----GGGATACTGACGG | 1 | 24 | 1 |
| AACACCTGCGGAATTC-----CGGGGATACTGACGG | 1 | 17 | 1 |
| AACACCTGCGGAATTC TAG-----GGAGATTACCTGTTATCCCTACCCGGGGATACTGACGG | 1 | 33 | 6 |
| AACACCTGCGGAATTC TAGGGAT-----CCCTACCCGGGGATACTGACGG | 2 | 2 | 2 |
| AACACCTGCGGAATTC TAG-----aatt----- | 1 | 30 | 0 |
| AACACCTGCGGAATTC TAGG-----CCTACCCGGGGATACTGACGG | 1 | 6 | 0 |
| AACACCT----- | 1 | 51 | 4 |
| AACACCTGCGGAATTC TA-----CCCGGGGATACTGACGG | 1 | 12 | 3 |
| AACACCTGCGGAATTC TAGGGA-----attc-----CCCTACCCGGGGATACTGACGG | 2 | 8 | 0 |
| AACACCTGCGGAATTC TAG-----CCCTACCCGGGGATACTGACGG | 1 | 6 | 0 |
| AACACCTGCGGAATTC TAGGGATA-----CTGACGG | 2 | 16 | 6 |
| Xrs5-pEJ/48h | | | |
| AACACCTGCGGAATTC TAGGGA-----CCCGGGGATACTGACGG | 1 | 8 | 0 |
| AACACCTGCGGAATTC TAGGGAT-----ctg-----CCTACCCGGGGATACTGACGG | 1 | 48 | 0 |
| AACACCTGCGGAATTC TAGGGAT-----CCCTACCCGGGGATACTGACGG | 2 | 2 | 2 |
| AACACCTGCGGAATTC TA-----GATACTGACGG | 1 | 18 | 3 |
| -----GG | 2 | 55 | 2 |
| -----TTACCTGTTATCCCTACCCGGGGATACTGACGG | 1 | 103 | 1 |
| -----GACCATGGAGATTACCTGTTATCCCTACCCGGGGATACTGACGG | 1 | 123 | 5 |
| -----TTATCCCTACCCGGGGATACTGACGG | 1 | 21 | 1 |
| AACACCTGCGG-----TGACGG | 1 | 30 | 0 |
| AACACCTGCGGAA-----CTGACGG | 1 | 27 | 1 |
| ----- | 1 | 81 | 1 |
| ----- | 1 | 82 | 6 |
| ----- | 1 | 64 | 0 |
| -----CCTACCCGGGGATACTGACGG | 1 | 57 | 1 |
| AACACCTGCGGAATTC TAGGGATA----- | 1 | 30 | 0 |
| -----ACTGACGG | 1 | 64 | 2 |
| AACACCTGCGGAATTC TA-----GGGATACTGACGG | 2 | 15 | 3 |
| AACACCTGCGGAATTC TAGGG-----CCCGGGGATACTGACGG | 1 | 9 | 0 |

Results

C

| Parental | n | Del (bp) | t μ h (bp) |
|--|----|----------|----------------|
| AACACCTGCGGAATTC ATTACCTGTTATCCCTA GTGCACAAGCTTCTGCAGACC <u>ATGGAGATTACCTGTTATCCCTA</u> CCCGGGGATACTGACGG | | | |
| TTGTGGACGCCTTAAG TAATGGGACAATAGGGAT CACGTGTTTCGAAGACGCTGTGTACCTC TAATGGGACAATAGGGAT GGGCCCTATGACTGCC | | | |
| I-SceI-induced DSB | | | |
| AACACCTGCGGAATTC ATTACCTGTTAT ----- CCCTACCCGGGGATACTGACGG | | | |
| CHOK1-pEJ2/24h | | | |
| AACACCTGCGGAATTC ATTACCTGTTAT ----- CCCTACCCGGGGATACTGACGG | 14 | 0 | 0 |
| AACACCTGCGGAATTC ATTACCTGTTATCCCTA GTGCACAAGCTTCTGCAGACC <u>ATGGAGATTACCTGTTAT</u> - CCCTACCCGGGGATACTGACGG | 1 | 1 | 0 |
| AACACCTGCGGAATTC ATTACCTGTTAT ----- TGCACAAGCTTCTGCAGACC <u>ATGGAGATTACCTGTTAT</u> - CCCTACCCGGGGATACTGACGG | 1 | 7 | 0 |
| AACACCTGCGGAATTC ATTACCTGTTATCCCTA GTGCACAAGCTTCTGCAGACC <u>ATGGAGATTA</u> ----- TACCCGGGGATACTGACGG | 1 | 12 | 0 |
| AACACCTGCGGAATTC ATTA ----- GGGATACTGACGG | 1 | 18 | 0 |
| CHOK1-pEJ2/48h | | | |
| AACACCTGCGGAATTC ATTACCTGTTAT ----- CCCTACCCGGGGATACTGACGG | 17 | 0 | 0 |
| AACACCTGCGGAATTC ATTACCTGTTAT ----- CCGGGGATACTGACGG | 1 | 6 | 0 |
| AACACCTGCGGAATTC ATTACCTG ----- CTACCCGGGGATACTGACGG | 1 | 6 | 0 |
| AACACCTGCGGAATTC AT ----- TACCCGGGGATACTGACGG | 1 | 14 | 5 |
| xrs5-pEJ2/24h | | | |
| AACACCTGCGG ----- | 1 | 58 | 2 |
| AACACCTGCGGAATTC ATTACCTGTTATCCCTA GTGCACAAGCTTCTGCAGACC <u>ATGGAGATTACCT</u> ----- ACCCGGGGATACTGACGG | 1 | 10 | 1 |
| AACACCTGCGGAATTC ATTA ----- CCCTACCCGGGGATACTGACGG | 2 | 9 | 4 |
| AACACCTGCGGAATTC ATTACCTGTTAT ----- CCCTACCCGGGGATACTGACGG | 1 | 0 | 0 |
| AACACCTGCGGAATTC ATTACCTGTTA ----- CCCTACCCGGGGATACTGACGG | 1 | 1 | 0 |
| AACACCTGCGGAATTC ATTA ----- TACCCGGGGATACTGACGG | 1 | 12 | 2 |
| AACACCTGCGGAATTC ATTACCTG ----- GATACTGACGG | 1 | 15 | 1 |
| AACACCTGCGG ----- CGG | 1 | 37 | 0 |
| AACACCTGCGGAATTC ATTACCTG ----- CCTAGTGCACAAGCTTCTGCAGACC <u>ATGGAGATTACCT</u> ----- CCCTACCCGGGGATACTGACGG | 1 | 10 | 1 |
| AACACCTGCGGAATTC ATTACCTGTTATCCCTA GTGCACAAGCTTCTGCAGACC <u>ATGGAGATTACCT</u> ----- CCCTACCCGGGGATACTGACGG | 1 | 5 | 1 |
| ----- at CCCTACCCGGGGATACTGACGG | 1 | 33 | 2 |
| ----- TACCTGTTATCCCTA CCCGGGGATACTGACGG | 1 | 62 | 0 |
| AACACCTGCGGAATTC ATTACCTG ----- CCCTACCCGGGGATACTGACGG | 1 | 4 | 0 |
| AACACCTGCGG ----- <u>GGAGATTACCTGTTATCCCTA</u> CCCGGGGATACTGACGG | 1 | 46 | 2 |
| AACACCTGCGGAATTC ATTACC ----- CCCTACCCGGGGATACTGACGG | 1 | 7 | 2 |
| AAC ----- | 1 | 89 | 3 |
| xrs5-pEJ2/48h | | | |
| AACACCTGCGGAATTC ATTACC ----- CCTAGTGCACAAGCTTCTGCAGACC <u>ATGGAGATTACCTGTTATCCCTA</u> CCCGGGGATACTGACGG | 1 | 7 | 2 |
| ----- ACCCGGGGATACTGACGG | 1 | 52 | 2 |
| ----- ATTACCTGTTATCCCTA CCCGGGGATACTGACGG | 1 | 73 | 1 |
| AACACCTGCGGAATTC ATTACCT ----- CCTACCCGGGGATACTGACGG | 1 | 6 | 2 |
| ----- GGGGATACTGACGG | 1 | 63 | 0 |
| AACACCTGCGGAATTC ATTACCTGTTATCCCTA GTGCACAAGCTTCTGCAGACC <u>ATGGAGATTACCTG</u> ----- CCCTACCCGGGGATACTGACGG | 1 | 4 | 0 |
| AACACCTGCGGAATTC ATTACC ----- | 1 | 36 | 0 |
| ----- TACTGACGG | 1 | 79 | 0 |
| AACACCTGC ----- CCCTACCCGGGGATACTGACGG | 1 | 20 | 1 |
| AACACCTGCGGAATTC ATTACCTGTTATCCCTA GTGCACAAGCTTCTGCAGACC <u>ATGGAGATTACCT</u> ----- CCCTACCCGGGGATACTGACGG | 1 | 5 | 1 |
| AACACCTGCGGAATT ----- CCCGGGATACTGACGG | 1 | 19 | 1 |
| AAC ----- | 1 | 89 | 2 |
| AACACCTGCGGAATTC ATTACCT ----- CCCGGGATACTGACGG | 1 | 10 | 0 |
| ----- CCCTACCCGGGGATACTGACGG | 1 | 53 | 2 |
| ----- | 1 | 114 | 1 |

Figure 11. Sequences of NHEJ repair junctions obtained from CHOK1, xrs5 cells harbouring either pEJ or pEJ2. A) Gel electrophoresis of some representative repair junctions of pEJ amplified using P1 and P2 primers. Repair junctions in CHOK1 cells (upper panel) showed almost the same molecular weight as pEJ amplified fragment while xrs5 repair junctions (lower panel) showed smaller fragments. Lane 20: 1kb DNA ladder. B) Sequences of NHEJ repair junctions obtained from CHOK1, xrs5 cells harbouring pEJ. For the parental and the cleaved sequences both strands are given, for the repair products only the sense strand. I-SceI-recognition sites are depicted in bold. The artificial start codon is underlined in the parental sequence. Del indicates the net loss or gain of base pair, whereby both single-stranded overhangs were together counted as 4 bp double-stranded DNA. t μ h indicates the number of terminal microhomologies used for rejoining, n: indicates number of events. C) Sequences of NHEJ repair junctions obtained from CHOK1, xrs5 cells harbouring pEJ2.

In the current study, we have addressed whether or not the slow repair process observed here represents a PARP-dependent mechanisms. We reasoned that if PARP1 is involved in the end-joining observed in Ku80-deficient cells, its inhibition should unveil this contribution. Two specific competitive inhibitors namely; DIQ and NU1025 were used to

Results

inhibit the activity of PARP1. These inhibitors have been designed to mimic NAD⁺, the substrate of PARP1. Their inhibitory effects are achieved by interactions with the PARP1 catalytic domain preventing the utilization of NAD⁺ for poly(ADP-ribosylation).

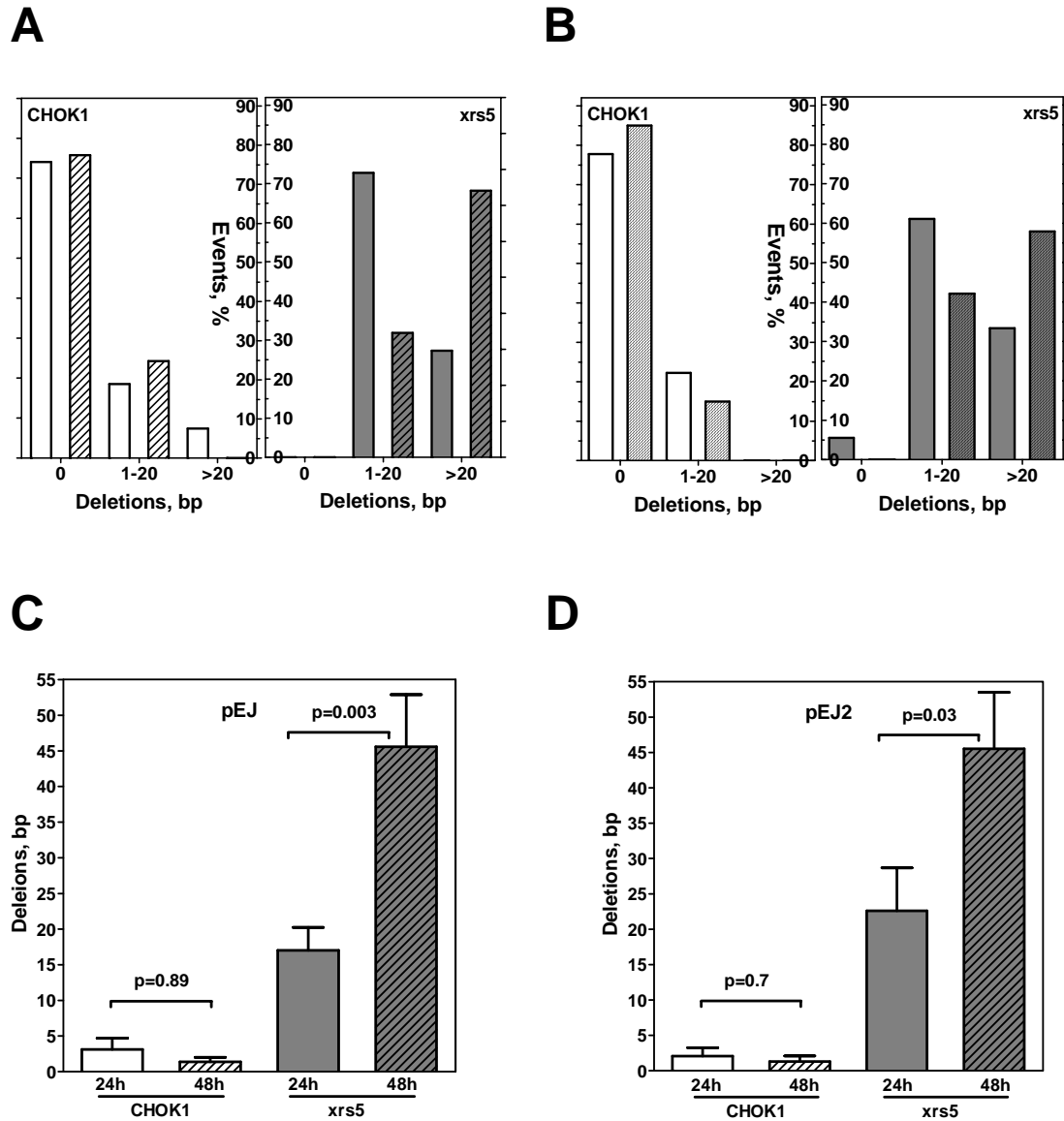


Figure 12. Effect of Ku80-deficiency on NHEJ fidelity. A) & B) Distribution of deletions length at individual junctions for both CHOK1 and *xrs5* clones harbouring pEJ and pEJ2. Deletions are defined as the sum of base pairs lost at both sites of the DSB hence, the 34-bp pop-out event in case of double I-SceI cleavage is not considered a deletion. C) Mean deletion length in both strains harbour pEJ substrate showing increase deletion length in Ku-deficient *xrs5* cells (grey) compared to their wild type CHOK1 (white). Notably, the mean deletion length in *xrs5* cells increased significantly 48h post-transfection (striated bars) (Mann-Whitney, $p=0.003$) while was not changed in CHOK1. D) Mean deletion length in both strains harbour pEJ2 substrate showing similar results as in pEJ.

Results

- **The Cytotoxicity of DIQ and NU1025**

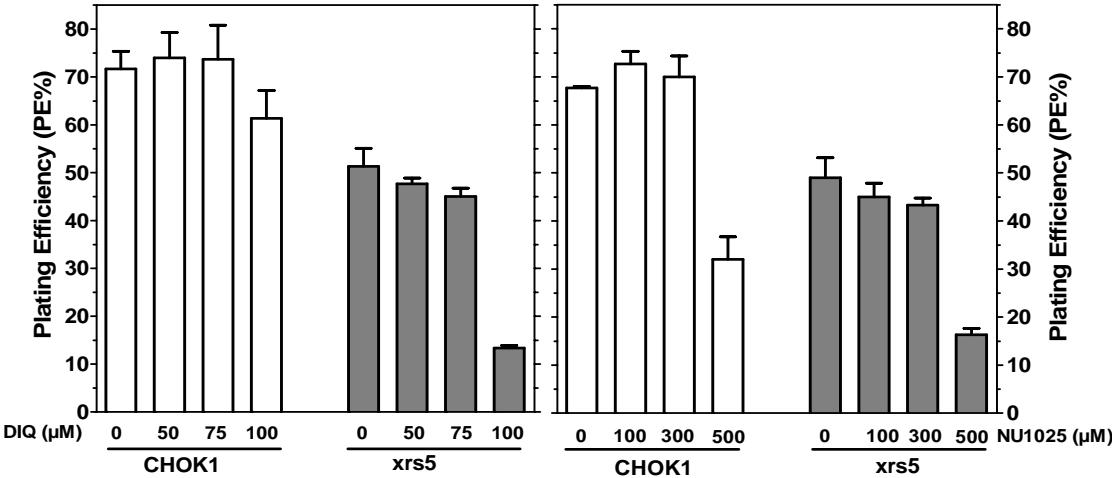
Before using the inhibitors for repair experiments their specific toxicity and their activity was determined. The colony formation assay was used to determine the cytotoxicity of both PARP1 inhibitors. Concentrations ranging between 25-100 μM for DIQ and between 100-300 μM for NU1025 were added independently to the cells and incubated for colony formation. Shown in Figure 13A is the plating efficiency for both strains in the presence of either DIQ (left panel) or NU1025 (right panel). Treating the cells with up to 75 μM of DIQ has almost no effect on the plating efficiency for both CHOK1 and xrs5. However at higher concentration (100 μM) the PE was decreased significantly in both strains. For NU1025, the maximum concentration which has no effect on the PE was 300 μM while at 500 μM the cell survival of both strains drastically decreased. In the following experiments, 75 μM and 300 μM of either DIQ or NU1025 were used because they proved for both strains to be not toxic.

Next we wanted to verify the effect of those inhibitors on PARP1 activity. Irradiating the cells with 20Gy led to dramatic increase in PAR signal. Pre-treating the cells with either 75 μM of DIQ or 300 μM of NU1025 has completely inhibited the accumulation of PAR molecules after IR as indicated by diminishing the immuno-fluorescent signal of PAR molecules. Shown in Figure 13B are PAR molecule signals after 20Gy in CHOK1 cells with or without (w/wo) treatment by either DIQ (left panel) or NU1025 (right panel) demonstrating almost complete inhibition of the signal after treatment by either of the inhibitors. Consistent results were also obtained for xrs5 cells. Altogether, these results indicate that both inhibitors are suitable to inhibit PARP1 activity without affecting the cell survival.

- **Effect of PARP1 inhibition on the Cytotoxicity of X-irradiation**

If PARP1 is a candidate for an alternative repair pathway of DSBs, its inhibition should have an impact on cell survival in response to double strand breaking agents such as IR. In order to test this, both colony formations of CHOK1 and xrs5 cells were examined after IR with or without PARP1-inhibitor. Figure 14A shows the dose response curves for both strains. The data were fitted to the linear quadratic equation (closed symbols). The dose modifying factor (DMF) at survival level of 0.37 was calculated for both strains. This survival level indicates the IR dose at which almost all cells get one hit in their genome (Hall and D. 1994). The evaluation of the DMF for both strains indicates that xrs5 cells were 4-fold more sensitive to IR in comparison to CHOK1 cells. Importantly, pretreating the cells with PARP inhibitors has increased the sensitivity by factor of 1.9 in xrs5 cells (open diamond symbols) while, almost has no effect on the sensitivity of CHOK1 (open inverted triangles). These data illustrates that PARP1 is involved at least partially in the repair of IR-induced DSBs in xrs5 cells.

A



B

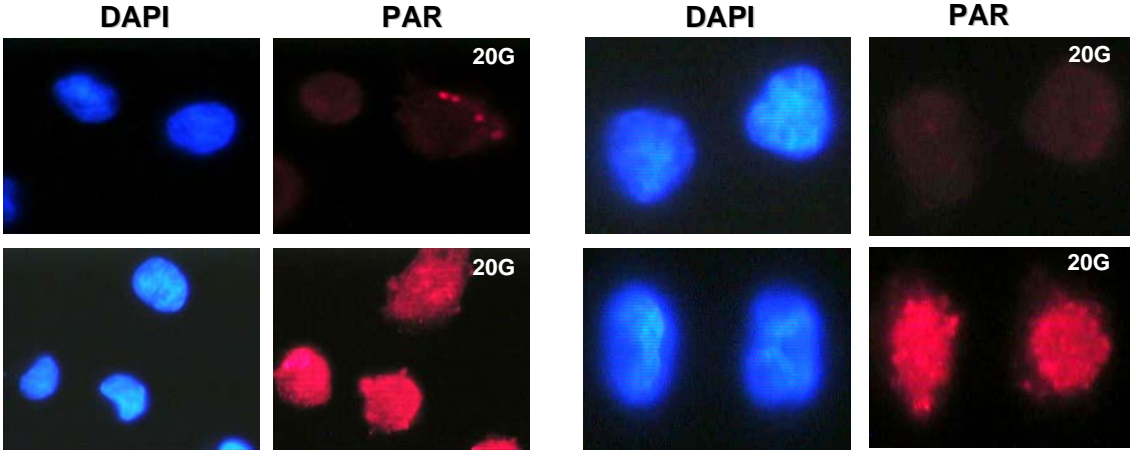


Figure 13. Inhibition of PARP1. A) Plating efficiency of CHOK1 (white) and xrs5 (grey) after treatment with the indicated concentrations of either DIQ (left panel) or NU1025 (right panel). The plating efficiency was measured as the number of colonies formed divided by the number of cells seeded. Shown are the mean value of 3 different experiments. B) Immunofluorescence signal of PAR in CHOK1 after 20 Gy is almost abolished after treatment by either 75μM of DIQ or 300μM of NU1025.

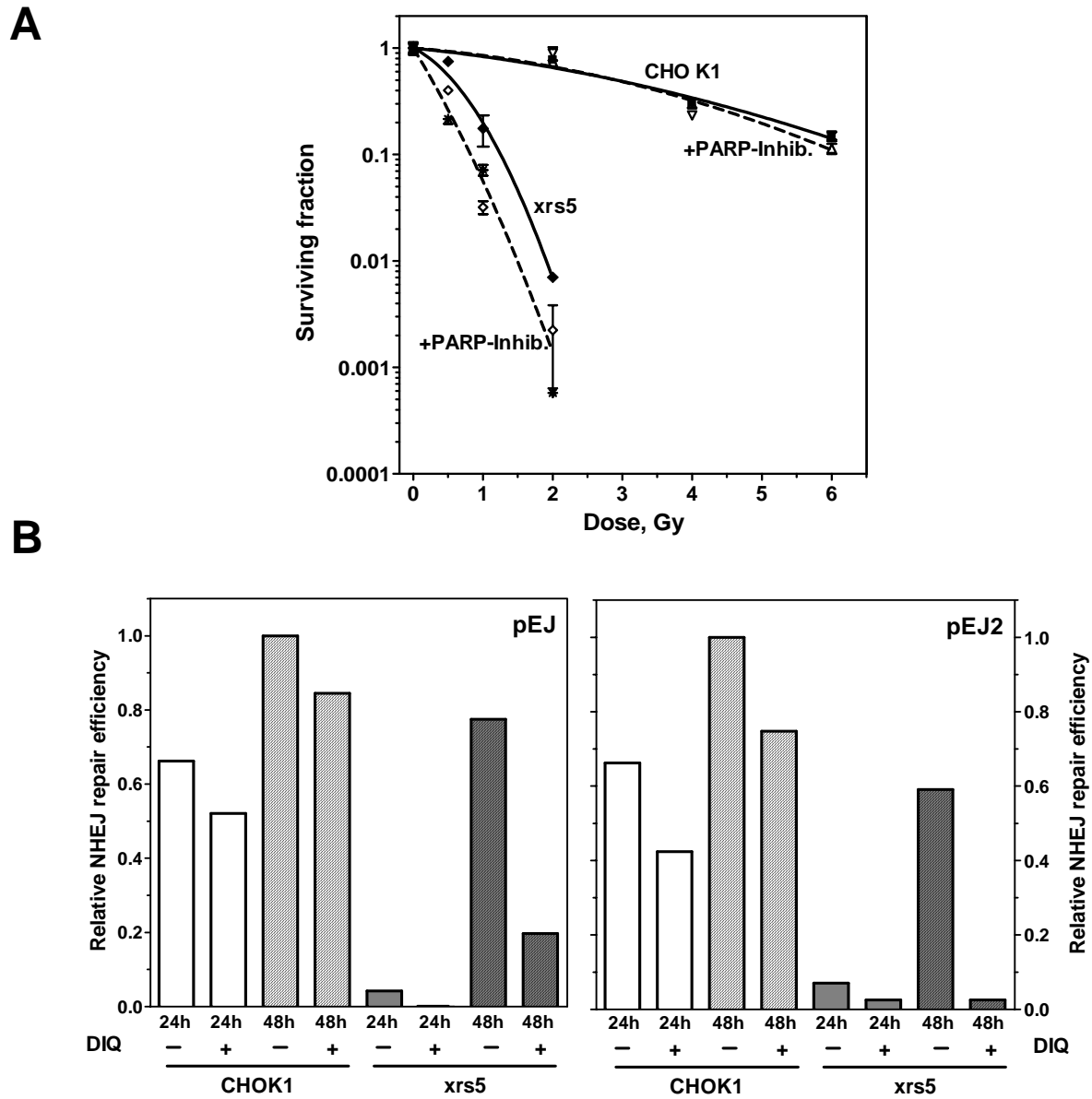


Figure 14. Role of PARP1 on NHEJ. A) Dose response curves of CHO K1 and xrs5 cells as indicated by the surviving fraction before (continuous lines) and after (dashed lines) treatment with the indicated concentrations of either DIQ or NU1025. Shown are the mean value of 3 independent experiments. Data were fitted to the linear quadratic equation $S/S_0 = \exp(-aD - bD^2)$. The parameters (a, b) obtained were used to calculate the mean inactivation dose D_{bar} (Fertil et al. 1984). B) After PARP1 inhibition using DIQ, the slow end-joining in xrs5 was exterminated while slightly decreased in CHO K1 for both pEJ (left panel) and pEJ2 (right panel).

Results

- **Effect of PARP1 inhibition on slow repair in xrs5 cells**

In order to directly address the role of PARP1 in the slow end-joining process observed in xrs5 cells (Figure 10) PARP1 was inhibited using DIQ and repair efficiencies were assessed 24h and 48h after transfection. Most of the repair (~70%) in pEJ-harboring CHOK1 was completed after 24h while, only 5% was completed in their Ku80-deficient counterparts (xrs5) cells. From Figure 13B, the end-joining efficiency of xrs5 cells increased during the following 24h and reached then ~80% of the level of CHOK1 cells, confirming the previous results (Figure 10B). In contrast to CHOK1, PARP1 inhibition in pEJ-harboring xrs5 cells almost completely abolished the end-joining 24h-post transfection which did not increase after 48h of repair. Essentially similar results were reported for pEJ2 substrate. Together, these results demonstrate that for both substrates almost all end-joining in the absence of Ku depends on PARP1 activity, indicating that PARP1 is an essential component of the slow end-joining process in Ku80-deficient cells.

3.2.5. SSA as an alternative pathway for NHEJ

Next, pEJSSA was employed to test whether or not SSA is an alternative option for DSB repair in addition to the PARP1-dependent end-joining. For that purpose, DSB was induced in both CHOK1 and xrs5 cells and the fraction of GFP⁺ cells was assessed 48h later by flow cytometry (example in Figure 15A). The mean value of seven independent wild type and seven xrs5 clones were 1.88 ± 0.49 % and 1.83 ± 0.37 %, respectively (Figure 15B). This indicates that Ku80-deficiency did not affect the repair efficiency using pEJSSA.

- **Impact of Ku80 on SSA**

Having established that, using pEJSSA, DSB repair was equally efficient with or without functional Ku80, we next examined the effect of Ku80-deficiency on SSA. To address this, the GFP⁺ cells from two independent clones from each CHOK1 and xrs5 were sorted by FACS, and the repair distribution between NHEJ and SSA was assessed using two different protocols. First, GFP⁺ cells were sorted and seeded in low density in order to raise well separated colonies on the plates. The clones were then picked and expanded individually. Genomic DNA was isolated from each clone and the repair junction was amplified using primers P1 and P2. Alternatively, the genomic DNA of the whole sorted green cells was isolated, the repair region amplified by PCR and the products were sub-cloned using TOPO TA cloning. Direct PCR amplification of the DNA of the individual bacterial colonies allows differentiating between NHEJ and SSA. Products of SSA event gave an exact fragments size of 415bp (Figure 15C lane 2 for CHOK1 and lanes 3, 6, and 9 for xrs5 cells), while for NHEJ

Results

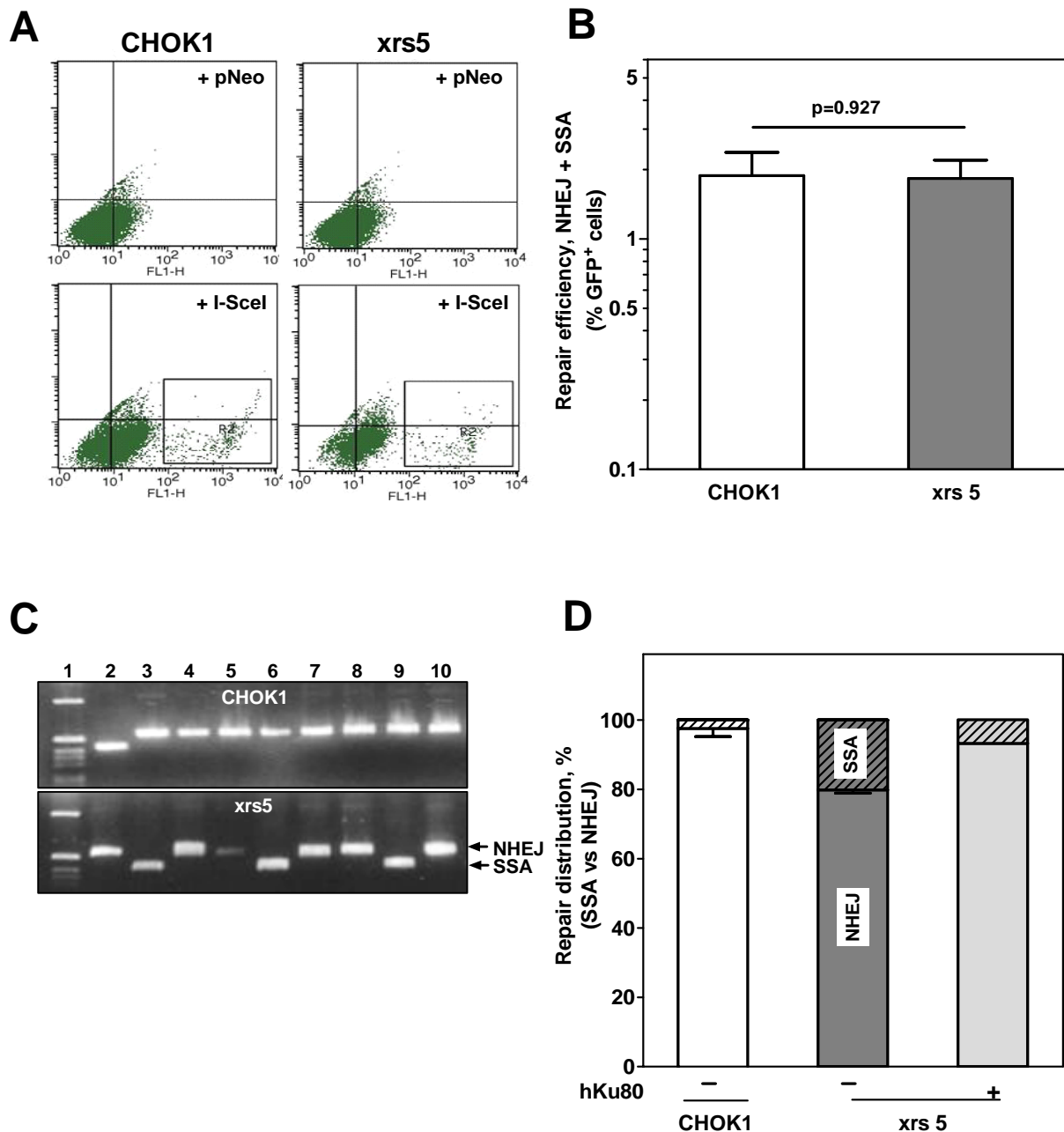


Figure 15. Impact of Ku80-deficiency on NHEJ and SSA. A) FACs analysis of GFP⁺ cells formed in CHOK1 and xrs5 cells harbouring pEJSSA 48h post-transfection of either the control vector (+ pNeo) or the I-SceI expression vector (+ I-SceI). GFP⁺ cells are highlighted by the R2-box. B) Total repair efficiency corresponds to % GFP⁺ cells produced after repair. Shown are the mean of 7 CHOK1 (white column) and 4 xrs5 (grey column) independent clones. Both strains showed similar repair efficiency (Mann-Whitney, $p=0.927$). C) Gel electrophoresis of some representative repair junctions amplified using P1 and P2 primers. CHOK1 cells (upper panel); lane 2: a 415 bp fragment corresponding to SSA event, lanes 3-8: close-to 550 bp fragments corresponding to NHEJ events. xrs5 cells (bottom); lanes 3, 6, 9: SSA events, lanes 2, 4, 5, 7, 8, 10: NHEJ events. D) Relative fractions of SSA (striated bars) and NHEJ events (open bars). Mean values are given for two independent CHOK1 and two xrs5 clones. For complementation, pcDNA3.1-hKu80 was co-transfected with the I-SceI expression plasmid. “Adding-back” hKu80 reverted the repair distribution to the wild type.

Results

event the molecular weight was of about 550 bp depending on the amount of end processing (lanes 3-8 for CHOK1 and lanes 2, 4, 5, 7, 8, 10 for *xrs5* cells). Our results revealed that CHOK1 cells showed a repair distribution of 97.6 ± 2.4 % NHEJ and 2.4 ± 2.4 % SSA events while the respective ratio for *xrs5* cells was 79.9 ± 1 % and 20.1 ± 1 %, representing an ~ 8-fold significant relative increase in SSA (Fisher's Exact test, $p < 0.001$). In order to ensure that the observed increase in SSA was a result of Ku80-deficiency, *xrs5* cells were transiently transfected with pcDNA3-hKu80 in order to complement the defected cells by expressing hKu80 protein. The complemented *xrs5* cells showed a repair distribution of 93.3% NHEJ and 6.8 % SSA events, representing reversion to the ratio observed in CHOK1 cells (Figure15D). This result indicates that in addition to its role in NHEJ, Ku80 controls the DSB repair by suppressing SSA.

3.2.6. NHEJ repair junctions in pEJSSA

The increased rate of SSA reported in *xrs5* could be explained in either of two ways. Firstly, the lack of end protecting Ku-protein leads to uncontrolled continuous degradation of the ends (see results of pEJ) which in turn stimulates SSA when it reaches homologous repeats (SSA1 and SSA2). Secondly, cells switch systematically to another pathway if they can not initiate NHEJ properly due to Ku80-deficiency. In order to test these possibilities, 125 different NHEJ junctions (61 in CHOK1 and 64 in *xrs5* cells) were sequenced (Figure16A). The deletion spectrum in *xrs5* cells showed more frequent deletions in comparison to their wild type counterparts (CHOK1). Moreover, the repair junctions in *xrs5* cells have significantly longer deletion length than in CHOK1 cells (Figure16C), i.e., 5.0 ± 0.7 bp vs. 0.9 ± 0.3 bp, respectively ($p < 0.0001$). To verify that this increase in the deletion length in *xrs5* cells was a consequence of Ku80-deficiency, *xrs5* cells were transfected with hKu80-expressing vector and 45 NHEJ junctions were sequenced (Figure 16A). Those cells showed a reversion to almost the same deletion length (0.73 ± 0.4 bp) and deletion spectrum as in CHOK1 (Figure 16B&C). These results indicate that the increased frequency of SSA was in fact due to a systematic switch to another repair pathway due to the release of the suppressive effect of Ku80 on SSA in Ku80-deficient cells rather than a result of uncontrolled end degradation (see discussion).

3.2.7. Impact of Ku80 on GC

From the preceding experiments the question arose whether or not the observed increase in SSA in Ku80-deficient cells reflects a general increase in homology-mediated repair activities. In order to address this GC was assessed in *xrs5* cells.

Results

A

Parental

CTGCCGAATTC **TAGGGATAACAGGGTAAT** TAAGCTTCTGCAGACCATGGAGATTACCCTGTATCCCTA CCCCGGGGATACTGA
 GACGCCTTAAGATCCCTATTGTCCCATTAATTCGAAGACGTCTGGTACCTC **TAATGGGACAATAGGGAT** GGGGCCCTATGACT

n Del (bp) tμh (bp)

I-SceI-induced DSB

CTGCCGAATTC **TAGGGATAA** ----- **CCCTA**CCCGGGGATACTGA
 GACGCCTTAAGATCCC ----- **AATAGGGAT**GGGGCCCTATGACT

CHOK1(n=61)

CTGCCGAATTC **TAGGGATA** ----- **tCCCTA**CCCGGGGATACTGA 14 0 2
 CTGCCGAATTC **TAGGGATAA** ----- **CCCTA**CCCGGGGATACTGA 13 0 0
 CTGCCGAATTC **TAGG**----- **tatCCCTA**CCCGGGGATACTGA 8 2 0
 CTGCCGAATTC **TAGGGAT**----- **CCCTA**CCCGGGGATACTGA 7 2 2
 CTGCCGAATTC **TAGGGA**----- **ttatCCCTA**CCCGGGGATACTGA 5 -1 1
 CTGCCGAATTC **TAGGGATAA**----- **tCCCTA**CCCGGGGATACTGA 5 0 1
 CTGCCGAATTC **TAGGG**----- **ttatCCCTA**CCCGGGGATACTGA 4 0 0
 CTGCCGAATTC **TAGGGAT**----- **ttatCCCTA**CCCGGGGATACTGA 3 2 0
 CTGCCGAATTC----- **CTA**CCCGGGGATACTGA 2 11 1

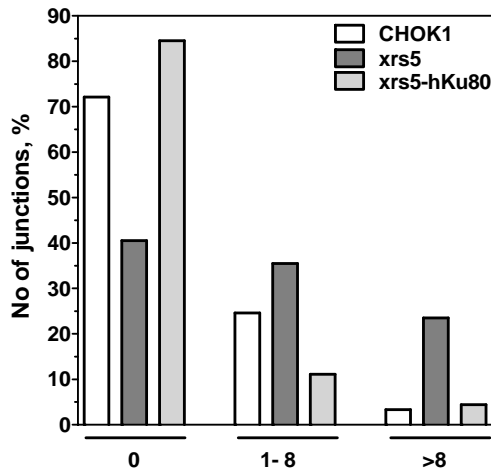
Xrs5 (n=64)

CTGCCGAATTC **TAGGGATAA**----- **CCCTA**CCCGGGGATACTGA 14 0 0
 CTGCCGAATT----- **CTA**CCCGGGGATACTGA 8 11 3
 CTGCCGAATTC**T**----- **CCCTA**CCCGGGGATACTGA 6 8 1
 CTGCCGAATTC **TAGGGA**----- **tatCCCTA**CCCGGGGATACTGA 5 0 1
 CTGCCGAATTC **TAGGG**----- **ttatCCCTA**CCCGGGGATACTGA 5 0 0
 CTGCCGAATTC **TAGGGA**----- TACTGA 4 17 4
 CTGCCGAATTC **TAGGGAT**----- **CCCTA**CCCGGGGATACTGA 4 2 2
 CTGCCGAATTC**TA**----- **tCCCTA**CCCGGGGATACTGA 3 6 2
 CTGCCGAATTC **TAGGG**----- **CCCTA**CCCGGGGATACTGA 3 4 0
 CTGCCGAATTC **TAGGGATA**----- CCGGGGATACTGA 3 6 2
 CTGCCGAATTC **TAGGGA**----- **CCTA**CCCGGGGATACTGA 2 4 0
 CTGCCGAATTC **TAGGGA**----- ACTGA 2 18 0
 CTGCCGAATTC **TAGGG**----- **tCCCTA**CCCGGGGATACTGA 2 3 1
 CTGCCGAATTC **TAGGGATAA**----- **g**----- **CCCTA**CCCGGGGATACTGA 2 -1 0
 CTGCCGAATTC**T**----- **CCTA**CCCGGGGATACTGA 1 9 0

hKu80-xrs5 (n=45)

CTGCCGAATTC **TAGGGATAA**----- **CCCTA**CCCGGGGATACTGA 11 0 0
 CTGCCGAATTC **TAGGGAT**----- **tatCCCTA**CCCGGGGATACTGA 9 -1 1
 CTGCCGAATTC **TAGGGATAA**----- **tCCCTA**CCCGGGGATACTGA 8 -1 1
 CTGCCGAATTC **TAGGGATA**----- **tCCCTA**CCCGGGGATACTGA 5 0 2
 CTGCCGAATTC **TAGGGATA**----- **CCCTA**CCCGGGGATACTGA 3 1 0
 CTGCCGAATTC **TAGGGAT**----- **atCCCTA**CCCGGGGATACTGA 3 0 1
 CTGCCGAATTC **TAGGG**----- **ttatCCCTA**CCCGGGGATACTGA 2 0 0
 CTGCCGAATTC **TAGGGAT**----- **CCCTA**CCCGGGGATACTGA 2 2 2
 CTGCCGAATTC----- **CCCTA**CCCGGGGATACTGA 1 9 0
 CTGCCGAATTC **TAGGGATA**----- CTGA 1 17 6

B



C

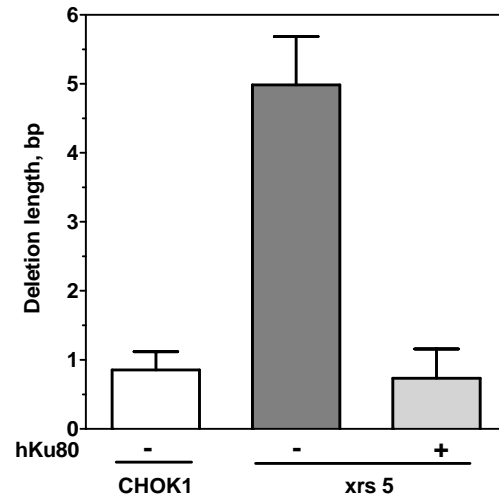


Figure 16. Loss of Ku80 increases inaccurate end-joining. A) Sequences of NHEJ repair junctions obtained from CHOK1 (white), xrs5 cells (grey) harbouring pEJSSA and xrs5 cells complemented by hKu80 (light grey). For the parental and the cleaved sequences both strands are given, for the repair products only the sense strand. SceI-recognition sites are depicted in bold. The artificial start codon is underlined in the parental sequence. Del indicates the net loss or gain of base pair, whereby both single-stranded overhangs were together counted as 4 bp double-stranded DNA. tμh indicates the number of terminal microhomologies used for rejoining, n: indicates number of events. B) Distribution of the length of deletions generated upon NHEJ. C) Mean deletion length. Differences between CHOK1 and xrs5 were significant (Mann Whitney, p=0.03)

Results

• Rad51-knockdown using siRNA

Since Rad51 is the central player of homologous recombination we decided to down-regulate Rad51 in order to modulate GC. Rad51 knockdown was achieved using siRNA. In order to elucidate the kinetics of the down-regulation, cells were transfected by 200nM of either control siRNA (“scrambled” scRNA) or siRNA against Rad51 (siRad51) using Tras-IT-TKO. Between 4 and 24 h after transfection, total protein was isolated and Rad51 was detected and semi-quantified by Western blotting. Figure 17 A shows Western blot analyses

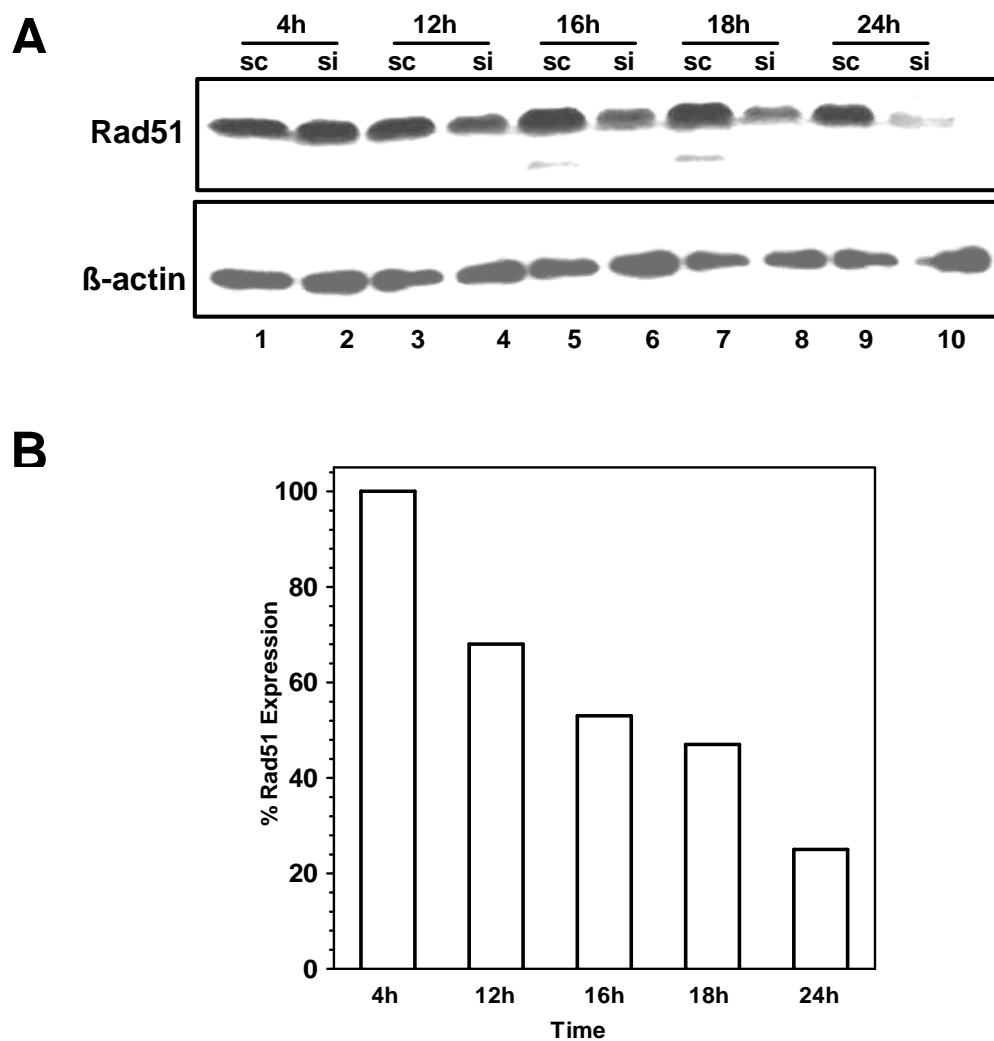


Figure 17. RAD51 knockdown using siRNA. A) Western blot showing expression of Rad51 (upper panel) and β -actin (lower panel) after the indicated time points of the treatment with either control siRNA (sc) or siRNA (si) against Rad51. B) The relative expression of Rad51 as measured from the equation indicated in the materials and methods section. Rad51 expression was decreased about 76% 24h-post transfection with siRNA.

Results

for both Rad51 (upper panel) and β -Actin (lower panel) after each indicated time points. After scRNA transfection the expression of Rad51 showed no difference (over the whole observation period). However, down-regulation of Rad51 starts between 4h and 12h reaching maximum inhibition (75%) after 24h of transfection (Figure 17B). In the following experiments, the time point 24h was used to knockdown Rad51.

- **Effect of Ku80-deficiency on GC**

In order to measure GC, pGC was stably integrated into both CHOK1 and *xrs5* cells. Transfection of the I-SceI expressing vector showed significantly more (~6-folds) GFP⁺ *xrs5* cells ($4.6 \pm 0.7\%$) compared to CHOK1 ($0.8 \pm 0.1\%$) ($p= 0.02$) (Figure 18A). As expected, pretreating the cells for 16h with siRad51 almost completely inhibited GC in both strains (Figure 18A). These data indicate that the presence of Ku80 prevents GC mechanism from acting on DSBs. The release of this suppressive effect in the absence of Ku80 makes GC an option for DSB repair.

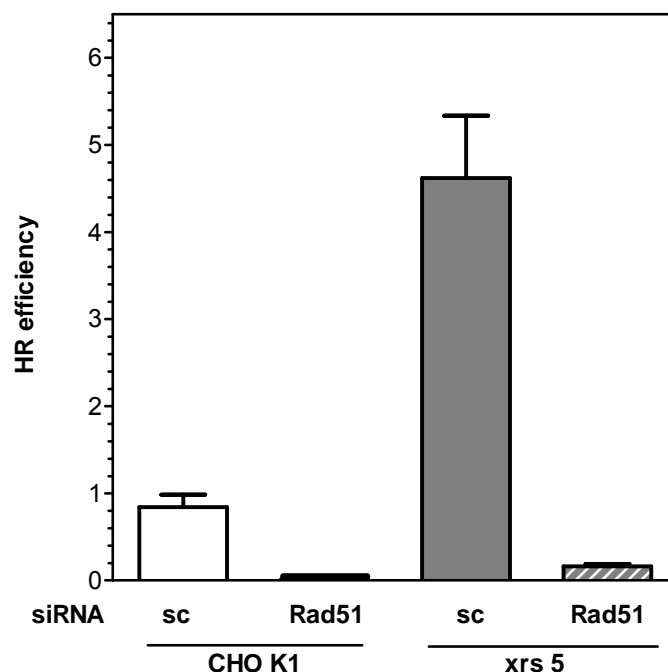


Figure 18. Impact of Ku80 deficiency on GC. A) Repair efficiency by gene conversion assessed by pGC substrate. Cells were transfected with I-SceI expression vector and the % GFP⁺ were assessed in 3 independent clones of each strain. For Rad51 knockdown, cells were pretreated for 16h with siRNA and then transfected with the I-SceI expression plasmid.

3.2.8. Interplay between GC and NHEJ

The above results show that some DSBs are repaired by GC when NHEJ is deficient due to Ku-defect. We asked whether or not can NHEJ analogously replace GC. For this purpose, Rad51 was knocked-down in CHOK1 and xrs5 cells that carry the pEJ substrate and the repair efficiency by NHEJ was measured. scRNA transfection did not affect NHEJ efficiency in either of CHOK1 or xrs5 cells (Figure 19) (4.3 ± 1.2 % and 3.0 ± 1.1 % for scRNA compared to 4.0 ± 1.2 and 3.1 ± 0.9 for siRNA). Importantly, Rad51 knockdown did not change the NHEJ efficiencies indicating that NHEJ by itself can not replace Rad51-dependent GC.

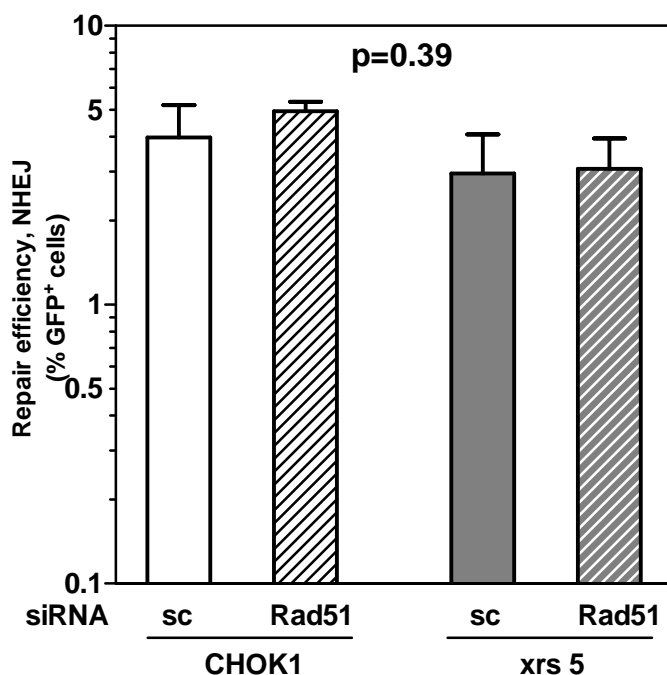


Figure 19. Impact of Rad51-knockdown on NHEJ. Total NHEJ efficiency using pEJ in CHOK1 and xrs5 cells without or with 16h of pretreatment with siRad51 or scRNA. Data represent the mean (\pm SE) of three clones each and two repeat experiments. Notably the repair efficiency of clones harbouring the pEJ was slightly higher compared to those with the pEJSSA.

3.2.9. Interplay between NHEJ, GC and SSA

Having shown the relationship between NHEJ and SSA and also between NHEJ and GC, we wanted to elucidate a possible interplay between GC and SSA. To address this, Rad51 was knocked down in CHOK1 and xrs5 cells carrying pEJSSA. Total repair efficiency

Results

(NHEJ plus SSA) was measured after induction of DSB in CHOK1 and *xrs5* cells without or with 16h of pretreatment with siRad51. Neither the single values were significantly different from each other nor was the mean of all CHOK1 versus all *xrs5* data ($p=0.97$) (Figure 20A). Next, the distribution between NHEJ and SSA was studied by PCR amplification of individual repair junctions. Interestingly, Rad51 knockdown in CHOK1 cells resulted in a small yet robust increase in the frequency of SSA by 11% (Figure 20B; second bar). Ku80-deficient *xrs5* cells showed, as expected, an increase in SSA by 26% (Figure 20B; third bar), confirming the above results (Figure 15D). Importantly, Rad51 knockdown in *xrs5* cells increased SSA in an additive manner (40%), i.e. 26% due to Ku80-deficiency plus 11-14% due to Rad51-knockdown. These results illustrate that Rad51 and Ku80 act synergistically to negatively regulate SSA use for DSB repair. On the other hand, SSA can be efficiently used as a back-up repair pathway in case both NHEJ and GC are impaired (double deficient background).

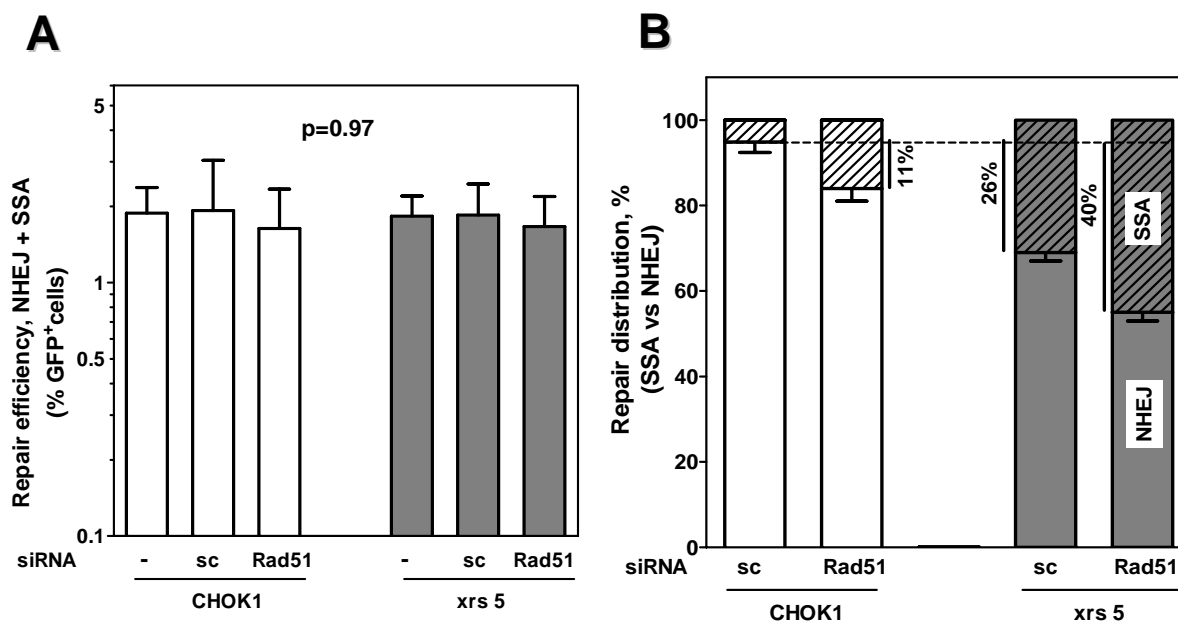


Figure 20. Interaction between NHEJ, SSA and GC. A) Total repair efficiency (NHEJ plus SSA) using pEJSSA in CHOK1 and *xrs5* cells without or with 16 h of pretreatment with siRad51. Experiments were carried out as before. Neither the single values were significantly different from each other nor was the mean of all CHOK1 versus all *xrs5* data (Mann-Whitney, $p=0.97$). siRNA experiments were performed with two independent clones of each strain. Data represent the mean of 3 repeat experiments. B) Relative distribution between SSA (striated bars) and NHEJ (open bars). Indicated is the difference in the respective fractions of SSA as compared to CHOK1 control cells (dashed line).

Results

A

Parental

CTGCGGAATTCTAGGGATAACAGGGTAATTAAGCTTCTGCAGACCATGGAGATTACCCGTGTATCCCTACCCCGGGGATACTGA
 GACGCCTTAAGATCCCTATTGTCCCATTAATTCGAAGACGTCTGGTACCTCTAATGGGACAATAGGGATGGGGCCCTATGACT

n Del (bp) t_μh (bp)

I-SceI-induced DSB

CTGCGGAATTCTAGGGATAA-----CCCTACCCCGGGGATACTGA
 GACGCCTTAAGATCCC-----AATAGGGATGGGGCCCTATGACT

CHOK1+siRad51 (n=40)

CTGCGGAATTCTAGGGATA-----tCCCTACCCCGGGGATACTGA 12 0 2
 CTGCGGAATTCTAGGGATAA-----CCCTACCCCGGGGATACTGA 11 0 0
 CTGCGGAATTCTAGGGAT-----tatCCCTACCCCGGGGATACTGA 8 -1 0
 CTGCGGAATTCTAGGG-----tatCCCTACCCCGGGGATACTGA 5 2 0
 CTGCGGAATTCTAGGGAT-----CCCTACCCCGGGGATACTGA 3 2 2
 CTGCGGAATTCTAGGGATAA-----tCCCTACCCCGGGGATACTGA 1 0 1

Xrs5+siRad51 (n=40)

CTGCGGAATTCTAGGGATAA-----CCCTACCCCGGGGATACTGA 10 0 0
 CTGCGGAATTCTAGGGAA-----TACTGA 7 17 4
 CTGCGGAATT-----CTACCCCGGGGATACTGA 7 11 3
 CTGCGGAATTCTAGGGATA-----tCCCTACCCCGGGGATACTGA 5 0 2
 CTGCGGAATTCT-----CCCTACCCCGGGGATACTGA 4 8 1
 CTGCGGAATTCTAGGGATAA-----tCCCTACCCCGGGGATACTGA 4 -1 2
 CTGCGGAATTCTAGGGAA-----ACTGA 1 18 0
 CTGCGGAATTCTAGGG-----CCCTACCCCGGGGATACTGA 1 4 0
 CTGCGGAATTCTAGGGATA-----CCCGGGGATACTGA 1 6 2

Xrs5+scRNA (n=18)

CTGCGGAATTCTAGGGATAA-----CCCTACCCCGGGGATACTGA 6 0 0
 CTGCGGAATTCTA-----tCCCTACCCCGGGGATACTGA 5 6 2
 CTGCGGAATT-----CTACCCCGGGGATACTGA 4 11 3
 CTGCGGAATTCT-----CCCTACCCCGGGGATACTGA 3 8 1

B

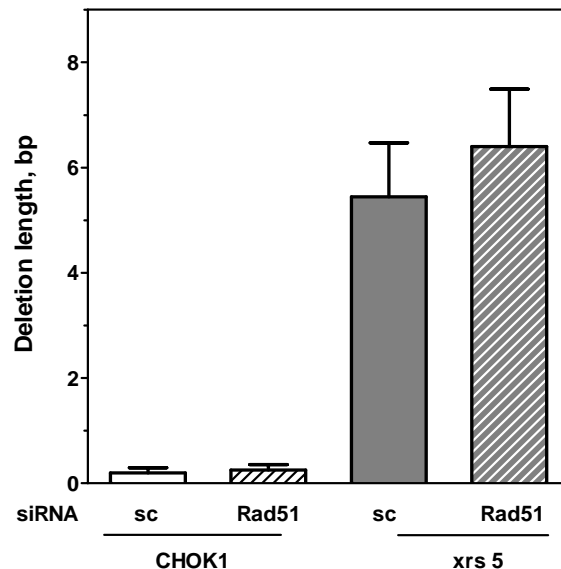


Figure 21. Impact of Rad51-knockdown on NHEJ fidelity. A) Sequences of NHEJ repair junctions obtained from CHOK1, xrs5 cells harbouring pEJSSA after Rad51-knockdown. For the parental and the cleaved sequences both strands are given, for the repair products only the sense strand. I-SceI-recognition sites are depicted in bold. The artificial start codon is underlined in the parental sequence. Del indicates the net loss or gain of base pair, whereby both single-stranded overhangs were together counted as 4 bp double-stranded DNA. t_μh indicates the number of terminal microhomologies used for rejoining. B) Mean deletion length. Differences between CHOK1 and xrs5 were significant (Mann Whitney, p=0.03). Rad51 knockdown did not affect the mean deletion length in both strains.

3.2.10. Effect of Rad51-knockdown on NHEJ fidelity

Worth to be mentioned is that Rad51-knockdown has increased SSA only at the expense of NHEJ which means that using the pEJSSA substrate inhibition of GC has indirectly decreased the NHEJ efficiency (Figure 20B). It was hence asked whether this effect also involves the fidelity of end-joining under those conditions. Shown in Figure 21A are the repair junctions of both CHOK1 and *xrs5* after siRNA treatment. The mean deletion length in CHOK1 was 0.3 ± 0.1 bp while in *xrs5* cells was 6.4 ± 1.1 bp showing almost the same mean deletion lengths reported previously (Figure 16C). This result indicates that Rad51-knockdown did not affect the repair fidelity of NHEJ in both strains.

4. DISCUSSION

Of the many types of DNA damage, DNA double strand breaks present a unique challenge to cells. On the one hand, DSBs are necessary for some vital processes such as meiotic recombination, V(D)J recombination and class switch recombination. On the other hand, they can be lethal if unrepaired or can create mutations and promote genomic instability if misrepaired. In general, two main pathways have been developed to repair DSBs in mammalian cells namely; NHEJ and HDR (GC and SSA). These pathways are critical for repairing the DSBs and maintaining the survival. However, if these pathways improperly repair the DSBs, they can be mechanisms for generating many types of mutations including point mutations, deletions, insertions and translocations which are hallmarks of cancer. Therefore, the cells need to regulate these pathways to faithfully repair DSBs not only to maintain the survival but also to avoid the mutations.

Early genetic evidence suggested competition between HR and NHEJ (Roth, Porter et al. 1985) which then was strengthened by the findings that HR proteins (RAD51, RAD52) and NHEJ proteins (Ku70, Ku80, DNA-PKcs) bind to the DNA ends at DSBs (Baumann and West 1998; Haber 2000; Haber 2000).

In the current study we aimed to investigate a possible cross-talk between NHEJ, GC and SSA repair mechanisms to employ the appropriate pathway that faithfully repairs the DSB and hence avoids the misrepair of the DSB. To that end, 4 GFP-based repair reporters (Figure 5) were employed to assess the fate of the repair by NHEJ, SSA, and GC of an I-SceI-induced DSB intra-chromosomally in hamster cell lines.

Ku protein is considered to function as a damage sensor. Moreover, Ku protein is a principal NHEJ core protein which critically determines the efficiency of DSB repair after ionizing irradiation. Having known that, we hence speculate that Ku protein is perhaps the protein which binds firstly after DSBs and thereby regulates the employment of the repair pathways. To test that, we have assessed the options in Ku80-deficient cells for repairing an I-SceI-induced DSB.

4.1. Molecular mechanisms for end-joining in Ku80-deficient and proficient cells

At first, it is important to define the term fidelity of NHEJ. I-SceI cleavage in pEJ2 produces 4-bp compatible 3'-overhangs. The end-joining process is termed "accurate" when the cells ligate the two overhangs restoring the original I-SceI restriction site. For the noncompatible ends (pEJ and pEJSSA), the four-base overhangs require modification before

Discussion

rejoining. This modification causes changes in the original sequence and hence the definition of "accurate" NHEJ of noncompatible ends is not self-evident. For that, the term "accurate" is reserved to the rejoining of the noncompatible DSB ends in such a way that not even one single base of the overhangs is deleted or inserted.

For the compatible ends, the majority (~82%) of the end-joining junctions in Ku80-proficient cells were formed by complete overlap of the four-base overhangs via an "accurate" NHEJ mechanism (Figure 22). By contrast, in Ku80-deficient cells only one junction (Figure 11, xrs5-pEJ2/24h line #4) was formed by "accurate" NHEJ while the rest of junctions were performed by "inaccurate" NHEJ. Importantly, the underlying end processing during the formation of the inaccurate junctions varied considerably in Ku80-deficient cells. Almost each junction is formed after a varied extent of nucleolytic degradation (see Figure 11). This reflects that the ends in Ku80-deficient cells are subjected to a random uncontrolled end processing that precedes the ligation.

Although it can not be error-free, the repair of the noncompatible ends was "accurate" in ~72% of the junctions in Ku80-proficient cells (Figure 22). Five different ways can explain the underlying mechanism of this "accurate" end-joining type in noncompatible ends (Figure 22 A-E). All these mechanisms rely on the formation of partial overlaps between the noncompatible bases followed by mismatches corrections. ~32% of these "accurate" junctions were performed by partial overlaps between the internal TA/AT (types A – C) leaving two external "A/A" mismatches. ~40% of the "accurate" junctions in Ku80-proficient cells were performed by overlaps between the TA/AT which flanks an "A/A" mismatch, leaving two gabs to be filled-in by polymerases (Figure 22 D and E). "A/A" mismatch is then corrected on either the sense (type D; 23.4%) or the antisense (type E; 16.1%) strand.

There are two different ways to explain the formation of accurate endjoining junctions via the mechanisms illustrated in Figure 22 types A - C: (1) Two "A/A" external mismatches are transiently formed which are then corrected on the sense strand (type C; 2.9%) or antisense strand (type B; 16.8%) or on both strands (type A; 13.1%) by mismatch repair system before the ligation step (Figure 22, right panel). This explanation is supported by the previous studies made by Pfeiffer co-workers who found that some mismatches between single bases are likely formed as intermediates during NHEJ (Pfeiffer and Vielmetter 1988; Pfeiffer, Thode et al. 1994). This way likely explains the underlying mechanism of the formation of the "accurate" junctions in the presence of Ku protein. Ku as an alignment factor keeps the ends in proximity and hence may guarantee the proper sittings of the mismatches (Pfeiffer and Vielmetter 1988; Pfeiffer, Thode et al. 1994). (2) The two terminal "A"s on both strands are firstly removed by an exonuclease then the overlap is formed between TA/AT followed by gab filling of unpaired bases (Figure 22, left panel).

Discussion

| Prevalent mechanism | | CHOK1 | xrs5 | | |
|--|--|-------|------|--------------|--------------|
| Complete overlap for compatible ends (pEJ2; n=38) | | | | | |
| | | 81.6% | 3.1% | | |
| Partial overlap for non-compatible ends (pEJ and pEJSSA; n=137) | | | | | |
| A) | | OR | | 13.1% | 4.6% |
| B) | | OR | | 16.8% | 12.3% |
| C) | | OR | | 2.9% | 4.6% |
| D) | | | | 23.4% | 0% |
| E) | | | | 16.1% | 0% |
| Total | | | | 72.3% | 21.5% |

Figure 22. Prevalent molecular mechanisms for "accurate" NHEJ. For compatible ends, accurate end-joining junctions are formed by complete overlapping of the complementary bases to align DNA ends for end-joining. However, accurate end-joining junctions in noncompatible ends which contain mismatches at internal or external positions, are formed by partial overlaps followed by mismatches correction, gap filling of the unpaired bases and then nick ligation (A-E). For more details see the text.

Significantly low rate of accurate NHEJ was observed in Ku-deficient cells (~21%). The mechanism of the formation of such accurate junctions in xrs5 cells is exclusively mediated by the formation of partial overlaps between TA/AT (types A – C). While the "accurate" NHEJ junctions in Ku-proficient cells were formed by either partial overlapping of terminal or internal mismatches (types A-E), the "accurate" junctions in Ku-deficient cells have been formed by partial overlapping of terminal mismatches (types A-C). The majority of the junctions in Ku-deficient cells were mediated by "inaccurate" NHEJ mechanism which

Discussion

accompanied with long deletions and variable spectra of deletions (Figure 11). Accordingly, the formation of the "accurate" NHEJ junctions in the Ku-deficient cells is properly mediated by removing one or the two terminal "A"s on both strands as described above (the second explanation).

Importantly, the ~21% accurate NHEJ junctions in Ku-deficient cells were exclusive to pEJSSA while pEJ showed no accurate junction. We conclude that the presence of the nearby tandem copies are recognized and actively guide the resection step to these repetitive sequences in order to guide the repair towards SSA. Ramsden and Gellert have suggested a competition between end-joining and processing which will be shifted to the ligation by NHEJ in the presence of Ku (Ramsden and Gellert 1998). However, Rad52 may also control this competition in favour of annealing by SSA. Given that SSA is a repair option in case of pEJSSA, the formation of the accurate junctions may be an indirect effect of the end binding by Rad52 that directs the repair to SSA. Once bound to the ends, Rad52 programs the end degradation to reach the two repetitive sequences to stimulate SSA. However, because NHEJ still is an option even in the absence of Ku, it can work on these protected ends.

4.2. Switch to PARP1-dependent end-joining in Ku80-deficient cells

In the current study we reported the earliest repair events in Ku-proficient cells after 6h of DSB induction (Figure 10C). However, Ku-deficient cells showed the first repair events after 12h, indicating a delay in the repair in these cells. Moreover, the repair in Ku-deficient cells had a slower kinetics (Figure 10) and accompanied with longer deletions (Figures 11 and 12) compared with the repair in wild-type cells. In the absence of Ku, the recruitment of the repair proteins to the DSB ends is slower which delays the completion of repair. Consequently, the ends stay longer open which makes them available for degradation by the action of nucleases. These results are in consistence with the experiments conducted in human tumour cell lines which have provided evidence for a Ku-independent "alternative" end-joining mechanism (DiBiase, Zeng et al. 2000) (Wang, Perrault et al. 2003). One of the former studies that reported the inaccurate characteristics of this alternative end-joining mechanism was made by Liang and Jasin 1996 who reported for the Ku80-deficient hamster cells (xrs6) that the recovery of products with precisely joined ends is reduced with a concomitant increase in the recovery of products containing deletions (Liang, Romanienko et al. 1996). Together with our own, these results indicate that in the absence of functional Ku proteins, the repair is switched to an alternative "inaccurate" and slower end-joining mechanism.

Discussion

During the process of carcinogenesis, the cells sequentially accumulate genetic alterations such as translocations that may generate new oncogenic fusion proteins, inactivate tumour suppressor genes and consequently become malignant over time. These genetic instabilities are critical features that enable tumour progression, Because of its nonconservative manner; we introduce the alternative end-joining as a mechanism for the tumour cells to accumulate such genetic instabilities. A good support to this assumption is the fact that NHEJ-deficient mice are characterised by high rate of translocations between the Ig heavy chain (IgH) locus and c-Myc which lead to lymphomas (Barnes, Stamp et al. 1998; Frank, Sekiguchi et al. 1998; Gao, Sun et al. 1998; Riballo, Critchlow et al. 1999). Surprisingly, analysis of the junctions of these translocations revealed that they still appear to be the result of end-joining activity which accompanied with large deletions, pointing at the alternative end-joining. In line with that, some recent studies have found that when the classical NHEJ is compromised, this alternative pathway in mammalian cells became robust during class switch recombination (CSR) (Soulas-Sprauel, Le Guyader et al. 2007; Yan, Boboila et al. 2007) and V(D)J recombination (Corneo, Wendland et al. 2007) resulting in a high rate of translocations. Furthermore, It has been found that targeted disruption of one allele of Ku70/80 gene in human colon cancer cell line HCT116 leads to an increase in chromosomal instability (Li, Nelsen et al. 2002).

The observations that this alternative pathway is often associated with genomic instability and cancer (Corneo, Wendland et al. 2007; Soulas-Sprauel, Le Guyader et al. 2007; Yan, Boboila et al. 2007), promoted us to verify its genetic attributes. In the current study and for the first time intrachromosomally, we have reported that this alternative end-joining is completely PARP1 dependent because the inhibition of PARP1 using specific competitive inhibitors has completely abrogated the slow-rate end-joining mechanism in Ku80-deficient cells (Figure 14). Our results are confirmed by the in vitro studies conducted by Salles and Iliakis laboratories who have reported that PARP1 functions independently of Ku or DNA-PKcs on the joining of two DSB ends (Audebert, Salles et al. 2004; Wang, Rosidi et al. 2005; Wang, Wu et al. 2006).

The findings that PARP1 is engaged to DSB repair when Ku is absent (Figure 14), can be explained by a possible competition between Ku and PARP1 proteins for end binding. This competition normally goes in favour of Ku protein properly because of its high end binding affinity. However, if Ku is absent the ends are free for PARP1 binding. Supporting this competition between PARP1 and Ku protein is the finding that in ligase IV-deficient cells, the efficiency of the PARP1-dependent end-joining could be significantly increased by knocking-down Ku70 (Wang, Wu et al. 2006). In ligase IV-deficient cells, Ku protein is still able to bind to the DSB ends, hindering the access of PARP1. However, upon knocking

Discussion

down Ku70, the ends are free for PARP1 binding which enhances the PARP1-dependent end-joining.

A possible mechanism for the PARP1 involvement could be that the progressive end resection eventually exposes longer sequence homologies at the DNA ends, which may provide sufficient stability to complete end-joining even without Xrcc4/ligIV. It is tempting to speculate that DNA ligase III rejoins these ends. In the absence of Ku-proteins the cells used more frequent microhomologies (see Figure 11). The use of such microhomologies increases the stability of the junction producing one gap in each strand flanking these microhomologies. These gaps may be then recognized as individual SSBs, which are better substrates for ligase III than genuine DSBs (Taylor, Whitehouse et al. 2000).

4.3. Gene conversion can replace Nonhomologous end-joining for repairing the DSB but the reverse is not an option

Here we reported a 6-fold increase in GC in Ku80-deficient cells (Figure 18) which is in line with previous studies which showed that loss of Ku70, Xrcc4, DNA-PKcs increased the rate of GC (Clikeman, Khalsa et al. 2001; Pierce, Hu et al. 2001; Delacote, Han et al. 2002; Allen, Halbrook et al. 2003; Stark, Pierce et al. 2004). Couedel et al., reported that GC deficiency augments the IR sensitivity of Ku80 mutant mice (Couedel, Mills et al. 2004), as it does with DNA-PKcs mutant mice (Essers, van Steeg et al. 2000). On light of our findings, the observations of the two aforementioned studies can be explained. In the NHEJ mutant animals, GC efficiency is increased which partially compensated for the deficiency in NHEJ. In the double mutant animals, however, GC is not an option and that is why the IR-sensitivity is increased. In consistency, a synergistic increase in IR sensitivity was reported for *Rad54^{-/-}/Ku70^{-/-}* Drosophila larvae and chicken cells (DT40) (Takata, Sasaki et al. 1998; Kooistra, Pastink et al. 1999). Altogether, these data properly reflect that NHEJ and GC can compete with each other for the repair of a DSB in some circumstances. Our data indicate that Ku protein may regulate this competition. Possibly, when Ku binds to DNA ends, on one hand it inhibits the access of Rad52 which helps loading Rad51 onto the DSB ends. On the other hand, it may protect the ends for resection step which is needed for the GC. Hence in the absence of Ku protein, GC can compensate for NHEJ in DSB repair.

The ability of Rad51 to form foci and initiate GC in G1 even at a low efficiency may lead to a recombination between homologous chromosomes or pseudo genes in G1 (Kim, Krasieva et al. 2005; Al-Minawi, Saleh-Gohari et al. 2008). Such recombination might cause LOH and translocations and eventually tumorigenesis. So, it is necessary for the cells to exhibit regulatory mechanisms that can suppress GC in G1. Here, we speculate that Ku protein plays an important role in the regulatory network that may inhibit GC from acting in

Discussion

G1. In accordance, lymphoma frequency is higher in Ku80 knockout mice compared with in Rad54^{-/-}/Ku80^{-/-} double mutant mice (Couedel, Mills et al. 2004). The increased level in lymphoma observed in Ku80^{-/-} cells can be a result of miss-regulation on GC in G1 due to the absence of functional Ku protein, leading to a high rate of translocations between chromosomes in these animals. However, in double mutant mice, the recombination Rad54 gene is missing and hence GC is not available.

The exact effect of GC deficiency on NHEJ has not been clearly tested until now. In the current study, we reported no change in NHEJ efficiency after GC-deficient background upon Rad51-knockdown (Figure 19). This is consistent with the thoughts that the 3'-ssDNA ends generated as substrates for GC can no longer be channelled towards NHEJ. During every round of DNA replication, moving replication forks encounter countless obstacles and lesions on the DNA template. This can result in prolonged stalling of the fork and, for example after collision with unrepaired SSBs (single strand breaks), fork collapse and the generation of DNA DSBs (Jeggo 1998; Morgan, Corcoran et al. 1998; Olive 1998). Such replication associated DSBs are repaired by GC. The finding that NHEJ can not be an option for the cells to afford DSBs gives a proper mechanism to avoid the employment of NHEJ to repair the replication associated DSBs that may lead to misjoining between different loci resulting in many translocations and hence tumorigenesis (Takata, Sasaki et al. 1998; Kooistra, Pastink et al. 1999).

4.4. Switch to single strand annealing

We have reported that the frequency of SSA is increased 8-fold in Ku80-deficient cells compared to their wild type counterparts. This indicates that in the absence of Ku proteins the repair is guided towards SSA (Figure 20). This conclusion is supported by the observation of Stark et al., who reported a shift towards SSA in Ku70-knockout mouse cells (Stark, Pierce et al. 2004). A similar switch from the end-joining mode to SSA has been described in a cell-free system if the length of homologies extended beyond 25 nt (Kuhfittig-Kulle, Feldmann et al. 2007).

The fact that the repair is guided to SSA in Ku-deficient cells can be explained by two ways; (1) the absence of Ku protein allows Rad52 to freely bind to the DSB ends and hence guides the repair to SSA. This explanation can be supported by the end binding competition between Rad52 and Ku proteins. Rad52 has been shown biochemically to bind to and mediate ligation of blunt and cohesive ends similar to Ku (Van Dyck, Stasiak et al. 1999). Under identical conditions, however, Ku preferably bound to ends with short protrusions while Rad52 strongly favoured long single-stranded overhangs (Ristic, Modesti et al. 2003). The absence of Ku might significantly facilitate access of Rad52 to DSB ends. (2) The

Discussion

absence of Ku protein as an end protective factor enhances end degradation which initiates SSA. SSA requires long 3' single-strands for homology search and strand-annealing, and the initial resection of DSB ends has been suggested to guide the choice between these pathways (Frank-Vaillant and Marcand 2002; Aylon, Liefshitz et al. 2004; Ira, Pellicioli et al. 2004). However, the Ku protein 'hides' DNA ends, protects them from degradation (Mimori and Hardin 1986; Liang, Romanienko et al. 1996) and hence prevents channelling repair towards recombination.

In Ku80-deficient cells a long mean deletion length (45 bp) was reported on the one hand with the pure NHEJ substrate pEJ (Figure 12). This is in agreement with previous studies using Ku-deficient MEFs or hamster cells showing extensive bases loss in pure end-joining substrates (Schulte-Uentrop, El-Awady et al. 2008). On the other hand, using pEJSSA substrate a mean deletion length of only 5 bp was reported in Ku80-deficient cells. The end degradation during NHEJ has never reached into any of the homologous repeat sequences. However, in these cells we reported an enhanced rate of SSA (Figure 20) which means that the end resection reaches beyond the two homologous sequences during SSA. Collectively, this suggests that the end resection in pEJSSA is under regulation to somehow direct the repair to SSA. Although it was suggested that the end resection has a decisive role in choosing the repair pathways, it is not clear till now for mammalian cells whether this is true. However, here and for the first time we suggest that the end resection does not decide the choice between NHEJ and SSA in mammalian cells. The two nearby repetitive sequences are recognized, properly by a helicase and/or Rad52, and actively guide the repair towards SSA before the end resection starts. In addition Rad52 binding to the ends might control this resection step to initiate SSA.

In addition, our study shows another branch of regulation on SSA mediated by GC. We reported that Rad51-knockdown, i.e. GC is not an option, increases the use of SSA (Figure 20B), indicating a competition between GC and SSA that goes in favour of GC in the presence of Rad51. In line with this model of competition, several studies have reported a decrease in GC and an increase in SSA rate in cells lack functional recombination proteins such as Rad51 (Stark, Pierce et al. 2004), Rad54 (Dronkert, Beverloo et al. 2000), BARD or BRCA2 (Tutt, Bertwistle et al. 2001; Stark, Pierce et al. 2004). Many cancers are promoted by deficiencies in GC due to Rad51 overexpression (Richardson, Stark et al. 2004), Rad54 mutations (Matsuda, Miyagawa et al. 1999), loss of functions of Brca1 or Brca2 (Moynahan, Pierce et al. 2001; Tutt, Bertwistle et al. 2001). The link between GC deficiencies and cancer promotion can be explained by our finding that in GC deficiency, the repair is switched to SSA mutagenic pathway which may offer a way for a tumour cell not only to possibly survive but also to accumulate genetic instability. A good example is the deficiency in Brca2 which in turn causes GC deficiency and enhanced rate of SSA (Stark, Pierce et al. 2004) results in

Discussion

the accumulation of chromosome aberrations (Patel, Yu et al. 1998), which is quite similar to what has been observed in cells depleted of Rad51 (Lim and Hasty 1996).

Using pEJSSA substrate, we reported that knockdown of Rad51 increases the usage of SSA; surprisingly at the expense of NHEJ even in Ku80-proficient cells (Figure 20B). This indicates a novel function for Rad51 in maintaining the genomic integrity by controlling the balance between NHEJ and the mutagenic SSA pathways in favour of the former. Currently, we present thoughts to explain this interesting finding. After DNA damage Rad51 interacts physically with Rad52 (Chen, Yuan et al. 1999) promoting strand exchange during GC (Benson, Baumann et al. 1998). This binding, however, inhibits Rad52-mediated strand annealing which is the critical function of Rad52 during SSA (Wu, Kantake et al. 2008) (Stark, Pierce et al. 2004). Rad52 not bound to Rad51 is still able to compete with Ku proteins for the DSB ends mediating SSA. After Rad51-knockdown, more Rad52 is freely available to compete with Ku for end binding and may promote SSA as it retains its Rad51-independent strand-annealing function (Krejci, Song et al. 2002). Accordingly, in double deficient background (Ku80-deficiency and Rad51-knockdown), the repair is shuttled from both NHEJ and GC to SSA, presumably through enhancing end binding of Rad52. Together, our current model predicts that the most mutagenic pathway, the SSA pathway, is under dual control by both Ku and Rad51 proteins. Additionally, this model suggests that SSA is the least desirable option for the cell. Together, these data suggest a critical role for both NHEJ and GC pathways in maintaining genomic stability not only by faithfully repairing the DSBs but also by inhibition of the mutagenic SSA pathway.

4.5. A hierarchy for DSB repair

Based on the findings from this study, we reported here that NHEJ, GC and SSA repair pathways have a complex interrelationship which determines whether or not the repair occurs faithfully. We present here a model for DSB repair (Figure 23) which is dominated by the Ku protein. Due to its abundance and high affinity (Lieber, Ma et al. 2003), (a) Ku occupies all DNA ends suppressing the PARP1-dependent end-joining, GC and SSA from acting on such ends and initiating the conservative classical NHEJ. (b) In the absence of Ku, the control on these pathways is relaxed and the ends are free for the accessibility of their players namely; PARP1 and Rad52/Rad51. The repair is guided to the PARP1-dependent nonconservative end-joining. In addition, both GC and SSA can partly substitute for NHEJ and rescue repair proficiency. Furthermore, Rad51 controls SSA by engaging Rad52 to the strand exchange and inhibits the strand annealing function of Rad52 (Wu, Kantake et al. 2008). (c) If Rad51 is lacking, more Rad52 is available to promote SSA at the expense of NHEJ. (d) When neither NHEJ (due to Ku-deficiency) nor GC (due to Rad51 knockdown) is an option, the repair will be channelled to the most mutagenic SSA pathway (if available)

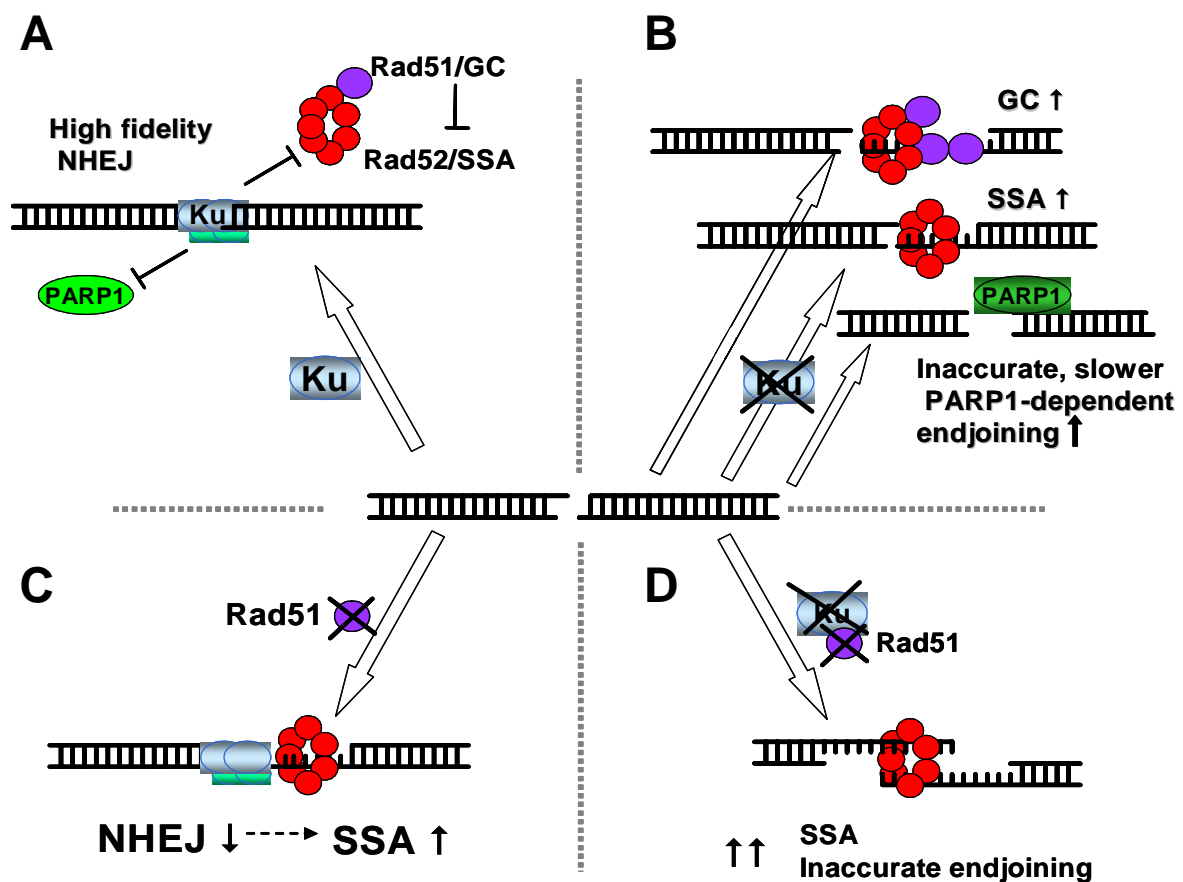


Figure 23. Presumptive fate for repairing of I-SceI-induced DSB. A model for DSB repair dominated by the Ku protein. (a) In wild type cells, Ku occupies all DNA ends suppressing the PARP1-dependent end-joining, GC and SSA and initiating the conservative classical NHEJ. (b) In Ku-deficient cells, the control on these pathways is relaxed due to absence of functional Ku protein. The ends are free for the accessibility of PARP, Rad51 and Rad52. The repair is guided to the PARP1-dependent end-joining, GC and SSA. (c) After Rad51-knockdown, the cells promote SSA at the expense of NHEJ. (d) When neither NHEJ (due to Ku-deficiency) nor GC (due to Rad51 knockdown) is an option, the repair will be channelled to the most mutagenic SSA pathway.

which may provide a rescue mechanism to prevent cell death. In summary, this model describes a crosstalk between the above mentioned repair pathways that follows a functional hierarchy with NHEJ as the dominant pathway. Its active compound Ku, and may be others too, suppress both GC and SSA. GC as represented by Rad51 is also dominant over SSA not only directly but as shown here by keeping the balance between NHEJ and SSA in favour of the former and hence SSA is the last option to repair the DSB. The cells reasonably avoid SSA pathway because of the mutagenic potentiality.

4.6. Clinical relevance and perspectives

We like to emphasize that the proposed hierarchy here is explained by the constitutive properties of the proteins involved, such as high or low abundance, affinity to the studied DNA structures and the formation of protein-protein interactions. It remains to be addressed in the future studies whether and how upstream signals, such as phosphorylation, Poly(ADP-ribose)ylation, ubiquitylation or SUMOylation, would additionally modify or fine-tune this crosstalk between NHEJ, GC, and SSA. In addition to the current indicated regulators, the discovery of other regulators for the crosstalk and hence the choice between the repair pathways is indeed important for the future studies for clinical application. These regulators may be useful as biomarkers of genomic instability to improve the ability to understand the early stages of cancer and hence to detect it in its earliest stages when the treatment is more effective. On the other hand, these regulators can be targets to discover powerful inhibitors of DNA repair that function as chemo-sensitizers.

The use of inhibitors for DNA damage response or for a specific repair pathway have been demonstrated to work as mono-therapy or therapy-sensitizers in tumour cells with defects in another DNA repair mechanism. The most notable example so far is the use of PARP inhibitors to treat breast and ovarian cancer cells that harbour BRCA1 or BRCA2 deficiency (Bryant, Schultz et al. 2005; Farmer, McCabe et al. 2005). These cells are defective in the repair by gene conversion (Moynahan, Chiu et al. 1999; Moynahan, Pierce et al. 2001). Recently, it has been found that BRCA1 or BRCA2 deficiency leads to a dramatic hypersensitivity to PARP inhibitors alone or in combination with other chemotherapeutic drugs such as temozolomide (DNA alkylator that cause replication fork collapse), raising hopes for developing a powerful, targeted therapy for these tumours (Bryant, Schultz et al. 2005; Farmer, McCabe et al. 2005). This can be explained by the role of PARP enzymes in sensing DNA damage and signalling the repair. When PARP activity is impaired, the cells may fail to detect and repair the damage. Moreover, PARP inhibitors induce single-strand breaks that can result in DSBs as a result of stalled replication forks. Such lesions would normally be repaired by GC, but this is prohibited in BRCA1- or BRCA2-deficient cancer cells (Schultz, Lopez et al. 2003; Helleday, Bryant et al. 2005; Fisher, Hochegger et al. 2007). Translation of these observations has led to phase II clinical trials of monotherapy using the PARP inhibitor AZD2281 (AstraZeneca) on patients with breast and ovarian cancer who harbour mutations in BRCA1 or BRCA2 genes. Cells that are defective in recombination-related proteins other than BRCA1 or BRCA2, such as RAD51, RAD54, XRCC2, XRCC3, replication protein A1 (RPA1), ATM, ATR, CHK1, CHK2, NBS1 (also known as NBN) and components of the Fanconi anaemia repair pathway, also show increased sensitivity to PARP inhibition (Bryant, Schultz et al. 2005; Bryant and Helleday 2006; McCabe, Turner et

Discussion

al. 2006). This suggests that PARP inhibitors might also be suitable in treating several types of tumours with defects in GC.

The complex network of DSB repair proteins and the hierarchy between the repair pathways represent a rich field to exploit in the improvement of both chemo- and radiotherapeutic strategies in cancer therapy. Some tumours are treated with a drug that cripples their ability to repair the DSBs in order to sensitize these tumours to a specific therapy. While, it may improve the treatment of some tumours, this strategy may have no effect or even increase the resistance to the same therapy in other types of tumours. Many mechanisms of therapy resistance have been proposed including drug uptake and efflux, detoxification of the drug or inhibition of apoptosis. However, these mechanisms can not fully explain why many tumour patients relapse with resistance towards this therapy. This resistance could be explained by the presence in these tumours of a different hierarchy between the repair pathways which leads to enhancement of the repair of the lesions induced by this drug. The unveiling of the crosstalk and the hierarchy between the repair pathways in each tumour will enable us to predict a resistance of tumour patients to specific therapy before the beginning of treatment. Moreover, if a hierarchy or crosstalk between the DSB repair pathways is discovered in tumour cells which is different from that in normal cells. This difference can be used to specifically attack the cancer cells avoiding normal ones or at least minimizing the side effects on them.

Furthermore, the aforementioned crosstalk may enable us to improve the efficiency of the targeted gene therapy. Targeted gene therapy has been used as a cornerstone treatment of many genetic diseases, including accurate gene replacement and transgene insertion into low-risk regions of the genome. The improvement strategy depends mainly on suppressing NHEJ-mediated random integration and enhancing GC-mediated integration into the desired loci. Proteins that regulate the choice between NHEJ and GC are excellent targets for such strategy. A possible method to improve targeted gene therapy is to use a drug that specifically inhibits NHEJ, such as DNA-PK inhibitors. The inhibition of NHEJ will in turn stimulate GC efficiency and hence enhances gene targeting and unleash the full potential of targeted gene therapy with minimum risk of unfavourable side effects.

4.7. Features of the chromosomal repair substrates

The use of I-SceI-based repair assays has greatly advanced our understanding of the molecular mechanisms and genetic determinants of homologous recombination (Moynahan and Jasin 1997; Richardson, Moynahan et al. 1998; Allen, Halbrook et al. 2003; Golding, Rosenberg et al. 2004; Saleh-Gohari and Helleday 2004; Saleh-Gohari and Helleday 2004; Stark, Pierce et al. 2004; Schildkraut, Miller et al. 2005), and more recently, several

Discussion

investigators have begun to successfully employ NHEJ substrates (Lin, Waldman et al. 2003; Ma, Kim et al. 2003; Guirouilh-Barbat, Huck et al. 2004; van Heemst, Brugmans et al. 2004; Dahm-Daphi, Hubbe et al. 2005; Xie, Hartlerode et al. 2007). However, several caveats need to be recognized. For example, studying the impact of a genetic manipulation on the functional repair readout may only produce evidence of an indirect relationship. It also remains to be defined to which extent I-SceI-type ends are models for the DSBs which are generated during normal DNA metabolism or after exposure to DNA damaging agents. By their nature, I-SceI assays select for DSB induction and processing events that trigger the reporter/selection signal. As a result, repair efficiency and pathway utilization may be to a certain degree assay specific. With regard to the NHEJ assays employed here, recombination events require a pop-out of the sequence between the two tandem I-SceI sites. Thus, factors that influence simultaneous I-SceI cleavage and synapsis of the cleaved ends can principally affect the repair readout.

Of note, however, our and Lopez labs have recently reported a strikingly different phenotype of XRCC4- and Ku80-deficient cells with regard to the repair of I-SceI-induced DSBs, which mirrored the embryonic lethality of XRCC4 knock-out mice as opposed to the viability of the Ku80 knock-out (Guirouilh-Barbat, Huck et al. 2004; Schulte-Uentrop, El-Awady et al. 2008). These findings suggest that I-SceI ends may be representative of DSB generated during normal cell development.

5. REFERENCES

- Al-Minawi, A. Z., N. Saleh-Gohari, et al. (2008). "The ERCC1/XPF endonuclease is required for efficient single-strand annealing and gene conversion in mammalian cells." Nucleic Acids Res **36**(1): 1-9.
- Allen, C., J. Halbrook, et al. (2003). "Interactive competition between homologous recombination and non-homologous end-joining." Mol Cancer Res **1**(12): 913-20.
- Ariumi, Y., M. Masutani, et al. (1999). "Suppression of the poly(ADP-ribose) polymerase activity by DNA-dependent protein kinase in vitro." Oncogene **18**(32): 4616-25.
- Audebert, M., B. Salles, et al. (2004). "Involvement of poly(ADP-ribose) polymerase-1 and XRCC1/DNA ligase III in an alternative route for DNA double-strand breaks rejoining." J Biol Chem **279**(53): 55117-26.
- Aylon, Y., B. Liefshitz, et al. (2004). "The CDK regulates repair of double-strand breaks by homologous recombination during the cell cycle." Embo J **23**(24): 4868-75.
- Bakkenist, C. J. and M. B. Kastan (2003). "DNA damage activates ATM through intermolecular autophosphorylation and dimer dissociation." Nature **421**(6922): 499-506.
- Barnes, D. E., G. Stamp, et al. (1998). "Targeted disruption of the gene encoding DNA ligase IV leads to lethality in embryonic mice." Curr Biol **8**(25): 1395-8.
- Baskaran, R., L. D. Wood, et al. (1997). "Ataxia telangiectasia mutant protein activates c-Abl tyrosine kinase in response to ionizing radiation." Nature **387**(6632): 516-9.
- Batty, D. P. and R. D. Wood (2000). "Damage recognition in nucleotide excision repair of DNA." Gene **241**(2): 193-204.
- Batzer, M. A. and P. L. Deininger (2002). "Alu repeats and human genomic diversity." Nat Rev Genet **3**(5): 370-9.
- Baumann, P. and S. C. West (1998). "Role of the human RAD51 protein in homologous recombination and double-stranded-break repair." Trends Biochem Sci **23**(7): 247-51.
- Benjamin, R. C. and D. M. Gill (1980). "Poly(ADP-ribose) synthesis in vitro programmed by damaged DNA. A comparison of DNA molecules containing different types of strand breaks." J Biol Chem **255**(21): 10502-8.
- Benson, F. E., P. Baumann, et al. (1998). "Synergistic actions of Rad51 and Rad52 in recombination and DNA repair." Nature **391**(6665): 401-4.
- Bentley, J., C. P. Diggle, et al. (2004). "DNA double strand break repair in human bladder cancer is error prone and involves microhomology-associated end-joining." Nucleic Acids Res **32**(17): 5249-59.
- Bochar, D. A., L. Wang, et al. (2000). "BRCA1 is associated with a human SWI/SNF-related complex: linking chromatin remodeling to breast cancer." Cell **102**(2): 257-65.
- Bouchard, V. J., M. Rouleau, et al. (2003). "PARP-1, a determinant of cell survival in response to DNA damage." Exp Hematol **31**(6): 446-54.
- Brown, M. L., D. Franco, et al. (2002). "Role of poly(ADP-ribosyl)ation in DNA-PKcs-independent V(D)J recombination." Proc Natl Acad Sci U S A **99**(7): 4532-7.
- Bryans, M., M. C. Valenzano, et al. (1999). "Absence of DNA ligase IV protein in XR-1 cells: evidence for stabilization by XRCC4." Mutat Res **433**(1): 53-8.
- Bryant, H. E. and T. Helleday (2006). "Inhibition of poly (ADP-ribose) polymerase activates ATM which is required for subsequent homologous recombination repair." Nucleic Acids Res **34**(6): 1685-91.

References

- Bryant, H. E., N. Schultz, et al. (2005). "Specific killing of BRCA2-deficient tumours with inhibitors of poly(ADP-ribose) polymerase." *Nature* **434**(7035): 913-7.
- Bugreev, D. V., O. M. Mazina, et al. (2006). "Rad54 protein promotes branch migration of Holliday junctions." *Nature* **442**(7102): 590-3.
- Burma, S., B. P. Chen, et al. (2001). "ATM phosphorylates histone H2AX in response to DNA double-strand breaks." *J Biol Chem* **276**(45): 42462-7.
- Cao, L., E. Alani, et al. (1990). "A pathway for generation and processing of double-strand breaks during meiotic recombination in *S. cerevisiae*." *Cell* **61**(6): 1089-101.
- Caspari, T. (2000). "How to activate p53." *Curr Biol* **10**(8): R315-7.
- Celeste, A., S. Petersen, et al. (2002). "Genomic instability in mice lacking histone H2AX." *Science* **296**(5569): 922-7.
- Chaganti, R. S., S. Schonberg, et al. (1974). "A manifold increase in sister chromatid exchanges in Bloom's syndrome lymphocytes." *Proc Natl Acad Sci U S A* **71**(11): 4508-12.
- Chan, D. W., B. P. Chen, et al. (2002). "Autophosphorylation of the DNA-dependent protein kinase catalytic subunit is required for rejoining of DNA double-strand breaks." *Genes Dev* **16**(18): 2333-8.
- Chao, C., S. Saito, et al. (2000). "p53 transcriptional activity is essential for p53-dependent apoptosis following DNA damage." *Embo J* **19**(18): 4967-75.
- Chaudhuri, J., U. Basu, et al. (2007). "Evolution of the immunoglobulin heavy chain class switch recombination mechanism." *Adv Immunol* **94**: 157-214.
- Chen, B. P., D. W. Chan, et al. (2005). "Cell cycle dependence of DNA-dependent protein kinase phosphorylation in response to DNA double strand breaks." *J Biol Chem* **280**(15): 14709-15.
- Chen, F., A. Nastasi, et al. (1997). "Cell cycle-dependent protein expression of mammalian homologs of yeast DNA double-strand break repair genes Rad51 and Rad52." *Mutat Res* **384**(3): 205-11.
- Chen, G., S. S. Yuan, et al. (1999). "Radiation-induced assembly of Rad51 and Rad52 recombination complex requires ATM and c-Abl." *J Biol Chem* **274**(18): 12748-52.
- Chen, J., D. P. Silver, et al. (1998). "Stable interaction between the products of the BRCA1 and BRCA2 tumour suppressor genes in mitotic and meiotic cells." *Mol Cell* **2**(3): 317-28.
- Chen, J. J., D. Silver, et al. (1999). "BRCA1, BRCA2, and Rad51 operate in a common DNA damage response pathway." *Cancer Res* **59**(7 Suppl): 1752s-1756s.
- Chen, L., K. Trujillo, et al. (2000). "Interactions of the DNA ligase IV-XRCC4 complex with DNA ends and the DNA-dependent protein kinase." *J Biol Chem* **275**(34): 26196-205.
- Chiu, C. Y., R. B. Cary, et al. (1998). "Cryo-EM imaging of the catalytic subunit of the DNA-dependent protein kinase." *J Mol Biol* **284**(4): 1075-81.
- Chu, G. (1997). "Double strand break repair." *J Biol Chem* **272**(39): 24097-100.
- Clikeman, J. A., G. J. Khalsa, et al. (2001). "Homologous recombinational repair of double-strand breaks in yeast is enhanced by MAT heterozygosity through yKU-dependent and -independent mechanisms." *Genetics* **157**(2): 579-89.
- Corneo, B., R. L. Wendland, et al. (2007). "Rag mutations reveal robust alternative end-joining." *Nature* **449**(7161): 483-6.

References

- Couedel, C., K. D. Mills, et al. (2004). "Collaboration of homologous recombination and nonhomologous end-joining factors for the survival and integrity of mice and cells." Genes Dev **18**(11): 1293-304.
- Cox, M. M. (2001). "Recombinational DNA repair of damaged replication forks in *Escherichia coli*: questions." Annu Rev Genet **35**: 53-82.
- d'Adda di Fagagna F, H. M., Tong WM, Roth D, Lansdorp PM, Wang ZQ, Jackson SP (2001). "Effects of DNA nonhomologous end-joining factors on telomere length and chromosomal stability in mammalian cells " Current Biology **11**(15): 1192-1196.
- D'Silva, I., J. D. Pelletier, et al. (1999). "Relative affinities of poly(ADP-ribose) polymerase and DNA-dependent protein kinase for DNA strand interruptions." Biochim Biophys Acta **1430**(1): 119-26.
- Dahm-Daphi, J., P. Hubbe, et al. (2005). "Nonhomologous end-joining of site-specific but not of radiation-induced DNA double-strand breaks is reduced in the presence of wild-type p53." Oncogene **24**(10): 1663-72.
- Davies, A. A., J. Y. Masson, et al. (2001). "Role of BRCA2 in control of the RAD51 recombination and DNA repair protein." Mol Cell **7**(2): 273-82.
- de Klein, A., A. G. van Kessel, et al. (1982). "A cellular oncogene is translocated to the Philadelphia chromosome in chronic myelocytic leukaemia." Nature **300**(5894): 765-7.
- Delacote, F., M. Han, et al. (2002). "An *xrcc4* defect or Wortmannin stimulates homologous recombination specifically induced by double-strand breaks in mammalian cells." Nucleic Acids Res **30**(15): 3454-63.
- DiBiase, S. J., Z. C. Zeng, et al. (2000). "DNA-dependent protein kinase stimulates an independently active, nonhomologous, end-joining apparatus." Cancer Res **60**(5): 1245-53.
- Difilippantonio, M. J., S. Petersen, et al. (2002). "Evidence for replicative repair of DNA double-strand breaks leading to oncogenic translocation and gene amplification." J Exp Med **196**(4): 469-80.
- Difilippantonio, M. J., J. Zhu, et al. (2000). "DNA repair protein Ku80 suppresses chromosomal aberrations and malignant transformation." Nature **404**(6777): 510-4.
- Ding, Q., Y. V. Reddy, et al. (2003). "Autophosphorylation of the catalytic subunit of the DNA-dependent protein kinase is required for efficient end processing during DNA double-strand break repair." Mol Cell Biol **23**(16): 5836-48.
- Dronkert, M. L., H. B. Beverloo, et al. (2000). "Mouse RAD54 affects DNA double-strand break repair and sister chromatid exchange." Mol Cell Biol **20**(9): 3147-56.
- Drouet, J., C. Delteil, et al. (2005). "DNA-dependent protein kinase and XRCC4-DNA ligase IV mobilization in the cell in response to DNA double strand breaks." J Biol Chem **280**(8): 7060-9.
- Durant, S. T. and J. A. Nickoloff (2005). "Good timing in the cell cycle for precise DNA repair by BRCA1." Cell Cycle **4**(9): 1216-22.
- Elliott, B., C. Richardson, et al. (2005). "Chromosomal translocation mechanisms at intronic *al*u elements in mammalian cells." Mol Cell **17**(6): 885-94.
- Esashi, F., N. Christ, et al. (2005). "CDK-dependent phosphorylation of BRCA2 as a regulatory mechanism for recombinational repair." Nature **434**(7033): 598-604.
- Essers, J., R. W. Hendriks, et al. (1997). "Disruption of mouse RAD54 reduces ionizing radiation resistance and homologous recombination." Cell **89**(2): 195-204.

References

- Essers, J., H. van Steeg, et al. (2000). "Homologous and non-homologous recombination differentially affect DNA damage repair in mice." Embo J **19**(7): 1703-10.
- Fan, W. and X. Wu (2004). "DNA polymerase lambda can elongate on DNA substrates mimicking non-homologous end-joining and interact with XRCC4-ligase IV complex." Biochem Biophys Res Commun **323**(4): 1328-33.
- Farmer, H., N. McCabe, et al. (2005). "Targeting the DNA repair defect in BRCA mutant cells as a therapeutic strategy." Nature **434**(7035): 917-21.
- Feldmann, E., V. Schmiemann, et al. (2000). "DNA double-strand break repair in cell-free extracts from Ku80-deficient cells: implications for Ku serving as an alignment factor in non-homologous DNA end-joining." Nucleic Acids Res **28**(13): 2585-96.
- Ferguson, D. O. and F. W. Alt (2001). "DNA double strand break repair and chromosomal translocation: lessons from animal models." Oncogene **20**(40): 5572-9.
- Ferguson, D. O., J. M. Sekiguchi, et al. (2000). "The nonhomologous end-joining pathway of DNA repair is required for genomic stability and the suppression of translocations." Proc Natl Acad Sci U S A **97**(12): 6630-3.
- Finnie, N. J., T. M. Gottlieb, et al. (1995). "DNA-dependent protein kinase activity is absent in xrs-6 cells: implications for site-specific recombination and DNA double-strand break repair." Proc Natl Acad Sci U S A **92**(1): 320-4.
- Fisher, A. E., H. Hohegger, et al. (2007). "Poly(ADP-ribose) polymerase 1 accelerates single-strand break repair in concert with poly(ADP-ribose) glycohydrolase." Mol Cell Biol **27**(15): 5597-605.
- Franco, S., F. W. Alt, et al. (2006). "Pathways that suppress programmed DNA breaks from progressing to chromosomal breaks and translocations." DNA Repair (Amst) **5**(9-10): 1030-41.
- Frank-Vaillant, M. and S. Marcand (2002). "Transient stability of DNA ends allows nonhomologous end-joining to precede homologous recombination." Mol Cell **10**(5): 1189-99.
- Frank, K. M., J. M. Sekiguchi, et al. (1998). "Late embryonic lethality and impaired V(D)J recombination in mice lacking DNA ligase IV." Nature **396**(6707): 173-7.
- Galande, S. and T. Kohwi-Shigematsu (1999). "Poly(ADP-ribose) polymerase and Ku autoantigen form a complex and synergistically bind to matrix attachment sequences." J Biol Chem **274**(29): 20521-8.
- Gao, Y., Y. Sun, et al. (1998). "A critical role for DNA end-joining proteins in both lymphogenesis and neurogenesis." Cell **95**(7): 891-902.
- Gatei, M., D. Young, et al. (2000). "ATM-dependent phosphorylation of nibrin in response to radiation exposure." Nat Genet **25**(1): 115-9.
- Golding, S. E., E. Rosenberg, et al. (2004). "Double strand break repair by homologous recombination is regulated by cell cycle-independent signalling via ATM in human glioma cells." J Biol Chem **279**(15): 15402-10.
- Gong, C., P. Bongiorno, et al. (2005). "Mechanism of nonhomologous end-joining in mycobacteria: a low-fidelity repair system driven by Ku, ligase D and ligase C." Nat Struct Mol Biol **12**(4): 304-12.
- Grawunder, U., M. Wilm, et al. (1997). "Activity of DNA ligase IV stimulated by complex formation with XRCC4 protein in mammalian cells." Nature **388**(6641): 492-5.
- Gu, H., I. Forster, et al. (1990). "Sequence homologies, N sequence insertion and JH gene utilization in VHDJH joining: implications for the joining mechanism and the ontogenetic timing of Ly1 B cell and B-CLL progenitor generation." Embo J **9**(7): 2133-40.

References

- Gudmundsdottir, K. and A. Ashworth (2006). "The roles of BRCA1 and BRCA2 and associated proteins in the maintenance of genomic stability." Oncogene **25**(43): 5864-74.
- Guirouilh-Barbat, J., S. Huck, et al. (2004). "Impact of the KU80 pathway on NHEJ-induced genome rearrangements in mammalian cells." Mol Cell **14**(5): 611-23.
- Haber, J. E. (2000). "Partners and pathways repairing a double-strand break." Trends Genet **16**(6): 259-64.
- Haber, J. E. (2000). "Recombination: a frank view of exchanges and vice versa." Curr Opin Cell Biol **12**(3): 286-92.
- Haber, J. E. and W. Y. Leung (1996). "Lack of chromosome territoriality in yeast: promiscuous rejoining of broken chromosome ends." Proc Natl Acad Sci U S A **93**(24): 13949-54.
- Hall, E. and P. D. (1994). "Radiobiology for the radiobiologist." JB Lippincott company, Philadelphia, Pennsylvania, 4th ed.: 478.
- Helleday, T. (2003). "Pathways for mitotic homologous recombination in mammalian cells." Mutat Res **532**(1-2): 103-15.
- Helleday, T., H. E. Bryant, et al. (2005). "Poly(ADP-ribose) polymerase (PARP-1) in homologous recombination and as a target for cancer therapy." Cell Cycle **4**(9): 1176-8.
- Helleday, T., J. Lo, et al. (2007). "DNA double-strand break repair: from mechanistic understanding to cancer treatment." DNA Repair (Amst) **6**(7): 923-35.
- Hess, M. T., U. Schwitter, et al. (1997). "Bipartite substrate discrimination by human nucleotide excision repair." Proc Natl Acad Sci U S A **94**(13): 6664-9.
- Ira, G., A. Pellicioli, et al. (2004). "DNA end resection, homologous recombination and DNA damage checkpoint activation require CDK1." Nature **431**(7011): 1011-7.
- Ivanov, E. L., N. Sugawara, et al. (1996). "Genetic requirements for the single-strand annealing pathway of double-strand break repair in *Saccharomyces cerevisiae*." Genetics **142**(3): 693-704.
- Jankovic, M., A. Nussenzweig, et al. (2007). "Antigen receptor diversification and chromosome translocations." Nat Immunol **8**(8): 801-8.
- Jeggo, P. A. (1998). "DNA breakage and repair." Adv Genet **38**: 185-218.
- Jeggo, P. A. and L. M. Kemp (1983). "X-ray-sensitive mutants of Chinese hamster ovary cell line. Isolation and cross-sensitivity to other DNA-damaging agents." Mutat Res **112**(6): 313-27.
- Jeggo, P. A., L. M. Kemp, et al. (1982). "The application of the microbial "tooth-pick" technique to somatic cell genetics, and its use in the isolation of X-ray sensitive mutants of Chinese hamster ovary cells." Biochimie **64**(8-9): 713-5.
- Johnson, R. D. and M. Jasin (2000). "Sister chromatid gene conversion is a prominent double-strand break repair pathway in mammalian cells." Embo J **19**(13): 3398-407.
- Kabotyanski, E. B., L. Gomelsky, et al. (1998). "Double-strand break repair in Ku86- and XRCC4-deficient cells." Nucleic Acids Res **26**(23): 5333-42.
- Karanjawala, Z. E., U. Grawunder, et al. (1999). "The nonhomologous DNA end-joining pathway is important for chromosome stability in primary fibroblasts." Curr Biol **9**(24): 1501-4.
- Kawamoto, T., K. Araki, et al. (2005). "Dual roles for DNA polymerase eta in homologous DNA recombination and translesion DNA synthesis." Mol Cell **20**(5): 793-9.

References

- Keeney, S. and M. J. Neale (2006). "Initiation of meiotic recombination by formation of DNA double-strand breaks: mechanism and regulation." *Biochem Soc Trans* **34**(Pt 4): 523-5.
- Khanna, K. K. and S. P. Jackson (2001). "DNA double-strand breaks: signalling, repair and the cancer connection." *Nat Genet* **27**(3): 247-54.
- Kim, J. S., T. B. Krasieva, et al. (2005). "Independent and sequential recruitment of NHEJ and HR factors to DNA damage sites in mammalian cells." *J Cell Biol* **170**(3): 341-7.
- Koch, C. A., R. Agyei, et al. (2004). "Xrcc4 physically links DNA end processing by polynucleotide kinase to DNA ligation by DNA ligase IV." *Embo J* **23**(19): 3874-85.
- Kooistra, R., A. Pastink, et al. (1999). "The *Drosophila melanogaster* DmRAD54 gene plays a crucial role in double-strand break repair after P-element excision and acts synergistically with Ku70 in the repair of X-ray damage." *Mol Cell Biol* **19**(9): 6269-75.
- Kraus, E., W. Y. Leung, et al. (2001). "Break-induced replication: a review and an example in budding yeast." *Proc Natl Acad Sci U S A* **98**(15): 8255-62.
- Krejci, L., B. Song, et al. (2002). "Interaction with Rad51 is indispensable for recombination mediator function of Rad52." *J Biol Chem* **277**(42): 40132-41.
- Kuhfittig-Kulle, S., E. Feldmann, et al. (2007). "The mutagenic potential of non-homologous end-joining in the absence of the NHEJ core factors Ku70/80, DNA-PKcs and XRCC4-LigIV." *Mutagenesis* **22**(3): 217-33.
- Kurimasa, A., S. Kumano, et al. (1999). "Requirement for the kinase activity of human DNA-dependent protein kinase catalytic subunit in DNA strand break rejoining." *Mol Cell Biol* **19**(5): 3877-84.
- Lander, E. S., L. M. Linton, et al. (2001). "Initial sequencing and analysis of the human genome." *Nature* **409**(6822): 860-921.
- Lasko, D., W. Cavenee, et al. (1991). "Loss of constitutional heterozygosity in human cancer." *Annu Rev Genet* **25**: 281-314.
- Lee, J. H. and T. T. Paull (2005). "ATM activation by DNA double-strand breaks through the Mre11-Rad50-Nbs1 complex." *Science* **308**(5721): 551-4.
- Lee, J. W., L. Blanco, et al. (2004). "Implication of DNA polymerase lambda in alignment-based gap filling for nonhomologous DNA end-joining in human nuclear extracts." *J Biol Chem* **279**(1): 805-11.
- Lee, S., L. Cavallo, et al. (1997). "Human p53 binds Holliday junctions strongly and facilitates their cleavage." *J Biol Chem* **272**(11): 7532-9.
- Lengauer, C., K. W. Kinzler, et al. (1998). "Genetic instabilities in human cancers." *Nature* **396**(6712): 643-9.
- Leuther, K. K., O. Hammarsten, et al. (1999). "Structure of DNA-dependent protein kinase: implications for its regulation by DNA." *Embo J* **18**(5): 1114-23.
- Li, B., S. Navarro, et al. (2004). "Identification and biochemical characterization of a Werner's syndrome protein complex with Ku70/80 and poly(ADP-ribose) polymerase-1." *J Biol Chem* **279**(14): 13659-67.
- Li, G., C. Nelsen, et al. (2002). "Ku86 is essential in human somatic cells." *Proc Natl Acad Sci U S A* **99**(2): 832-7.
- Liang, F., P. J. Romanienko, et al. (1996). "Chromosomal double-strand break repair in Ku80-deficient cells." *Proc Natl Acad Sci U S A* **93**(17): 8929-33.
- Lieber, M. R., Y. Ma, et al. (2003). "Mechanism and regulation of human non-homologous DNA end-joining." *Nat Rev Mol Cell Biol* **4**(9): 712-20.

References

- Lim, D. S. and P. Hasty (1996). "A mutation in mouse rad51 results in an early embryonic lethal that is suppressed by a mutation in p53." Mol Cell Biol **16**(12): 7133-43.
- Lim, D. S., S. T. Kim, et al. (2000). "ATM phosphorylates p95/nbs1 in an S-phase checkpoint pathway." Nature **404**(6778): 613-7.
- Lin, Y., B. C. Waldman, et al. (2003). "Suppression of high-fidelity double-strand break repair in mammalian chromosomes by pifithrin-alpha, a chemical inhibitor of p53." DNA Repair (Amst) **2**(1): 1-11.
- Lodish, H., A. Berk, et al. (2004). "Molecular biology of the cell" WH Freeman: New York, NY. 5th ed.: 963.
- Lundin, C., K. Erixon, et al. (2002). "Different roles for nonhomologous end-joining and homologous recombination following replication arrest in mammalian cells." Mol Cell Biol **22**(16): 5869-78.
- Luo, G., I. M. Santoro, et al. (2000). "Cancer predisposition caused by elevated mitotic recombination in Bloom mice." Nat Genet **26**(4): 424-9.
- Ma, J. L., E. M. Kim, et al. (2003). "Yeast Mre11 and Rad1 proteins define a Ku-independent mechanism to repair double-strand breaks lacking overlapping end sequences." Mol Cell Biol **23**(23): 8820-8.
- Ma, Y., U. Pannicke, et al. (2005). "The DNA-dependent protein kinase catalytic subunit phosphorylation sites in human Artemis." J Biol Chem **280**(40): 33839-46.
- Ma, Y., K. Schwarz, et al. (2005). "The Artemis:DNA-PKcs endonuclease cleaves DNA loops, flaps, and gaps." DNA Repair (Amst) **4**(7): 845-51.
- Mahajan, K. N., S. A. Nick McElhinny, et al. (2002). "Association of DNA polymerase mu (pol mu) with Ku and ligase IV: role for pol mu in end-joining double-strand break repair." Mol Cell Biol **22**(14): 5194-202.
- Mari, P. O., B. I. Florea, et al. (2006). "Dynamic assembly of end-joining complexes requires interaction between Ku70/80 and XRCC4." Proc Natl Acad Sci U S A **103**(49): 18597-602.
- Marti, T. M., C. Kunz, et al. (2002). "DNA mismatch repair and mutation avoidance pathways." J Cell Physiol **191**(1): 28-41.
- Matsuda, M., K. Miyagawa, et al. (1999). "Mutations in the RAD54 recombination gene in primary cancers." Oncogene **18**(22): 3427-30.
- McCabe, N., N. C. Turner, et al. (2006). "Deficiency in the repair of DNA damage by homologous recombination and sensitivity to poly(ADP-ribose) polymerase inhibition." Cancer Res **66**(16): 8109-15.
- McIlwraith, M. J., A. Vaisman, et al. (2005). "Human DNA polymerase eta promotes DNA synthesis from strand invasion intermediates of homologous recombination." Mol Cell **20**(5): 783-92.
- Meek, K., P. Douglas, et al. (2007). "trans Autophosphorylation at DNA-dependent protein kinase's two major autophosphorylation site clusters facilitates end processing but not end-joining." Mol Cell Biol **27**(10): 3881-90.
- Michel, B., M. J. Flores, et al. (2001). "Rescue of arrested replication forks by homologous recombination." Proc Natl Acad Sci U S A **98**(15): 8181-8.
- Mimori, T. and J. A. Hardin (1986). "Mechanism of interaction between Ku protein and DNA." J Biol Chem **261**(22): 10375-9.
- Mohaghegh, P., J. K. Karow, et al. (2001). "The Bloom's and Werner's syndrome proteins are DNA structure-specific helicases." Nucleic Acids Res **29**(13): 2843-9.

References

- Morgan, W. F., J. Corcoran, et al. (1998). "DNA double-strand breaks, chromosomal rearrangements, and genomic instability." Mutat Res **404**(1-2): 125-8.
- Morris, T. and J. Thacker (1993). "Formation of large deletions by illegitimate recombination in the HPRT gene of primary human fibroblasts." Proc Natl Acad Sci U S A **90**(4): 1392-6.
- Mortensen, U. H., C. Bendixen, et al. (1996). "DNA strand annealing is promoted by the yeast Rad52 protein." Proc Natl Acad Sci U S A **93**(20): 10729-34.
- Moshous, D., C. Pannetier, et al. (2003). "Partial T and B lymphocyte immunodeficiency and predisposition to lymphoma in patients with hypomorphic mutations in Artemis." J Clin Invest **111**(3): 381-7.
- Motycka, T. A., T. Bessho, et al. (2004). "Physical and functional interaction between the XPF/ERCC1 endonuclease and hRad52." J Biol Chem **279**(14): 13634-9.
- Moynahan, M. E., J. W. Chiu, et al. (1999). "Brca1 controls homology-directed DNA repair." Mol Cell **4**(4): 511-8.
- Moynahan, M. E. and M. Jasin (1997). "Loss of heterozygosity induced by a chromosomal double-strand break." Proc Natl Acad Sci U S A **94**(17): 8988-93.
- Moynahan, M. E., A. J. Pierce, et al. (2001). "BRCA2 is required for homology-directed repair of chromosomal breaks." Mol Cell **7**(2): 263-72.
- Nick McElhinny, S. A., J. M. Havener, et al. (2005). "A gradient of template dependence defines distinct biological roles for family X polymerases in nonhomologous end-joining." Mol Cell **19**(3): 357-66.
- Nickoloff, J. (2002). "Recombination:mechanisms and roles in tumourigenesis." In:Bertino JR, ed. Encyclopedia of cancer. 2nd edition. San Diego, USA: Elsevier Science 2002: 49-59.
- Nimonkar, A. V., A. Z. Ozsoy, et al. (2008). "Human exonuclease 1 and BLM helicase interact to resect DNA and initiate DNA repair." Proc Natl Acad Sci U S A **105**(44): 16906-11.
- Noordzij, J. G., N. S. Verkaik, et al. (2003). "Radiosensitive SCID patients with Artemis gene mutations show a complete B-cell differentiation arrest at the pre-B-cell receptor checkpoint in bone marrow." Blood **101**(4): 1446-52.
- Ogawa, T., X. Yu, et al. (1993). "Similarity of the yeast RAD51 filament to the bacterial RecA filament." Science **259**(5103): 1896-9.
- Olive, P. L. (1998). "The role of DNA single- and double-strand breaks in cell killing by ionizing radiation." Radiat Res **150**(5 Suppl): S42-51.
- Pannicke, U., Y. Ma, et al. (2004). "Functional and biochemical dissection of the structure-specific nuclease ARTEMIS." Embo J **23**(9): 1987-97.
- Paques, F. and J. E. Haber (1999). "Multiple pathways of recombination induced by double-strand breaks in *Saccharomyces cerevisiae*." Microbiol Mol Biol Rev **63**(2): 349-404.
- Patel, K. J., V. P. Yu, et al. (1998). "Involvement of Brca2 in DNA repair." Mol Cell **1**(3): 347-57.
- Paull, T. T., D. Cortez, et al. (2001). "Direct DNA binding by Brca1." Proc Natl Acad Sci U S A **98**(11): 6086-91.
- Paull, T. T. and M. Gellert (1998). "The 3' to 5' exonuclease activity of Mre 11 facilitates repair of DNA double-strand breaks." Mol Cell **1**(7): 969-79.
- Pfeiffer, P., S. Thode, et al. (1994). "Mechanisms of overlap formation in nonhomologous DNA end-joining." Mol Cell Biol **14**(2): 888-95.

References

- Pfeiffer, P. and W. Vielmetter (1988). "Joining of nonhomologous DNA double strand breaks in vitro." Nucleic Acids Res **16**(3): 907-24.
- Pierce, A. J., P. Hu, et al. (2001). "Ku DNA end-binding protein modulates homologous repair of double-strand breaks in mammalian cells." Genes Dev **15**(24): 3237-42.
- Powell, S. N., H. Willers, et al. (2002). "BRCA2 keeps Rad51 in line. High-fidelity homologous recombination prevents breast and ovarian cancer?" Mol Cell **10**(6): 1262-3.
- Puck, T. T. and P. I. Marcus (1956). "Action of x-rays on mammalian cells." J Exp Med **103**(5): 653-66.
- Ramsden, D. A. and M. Gellert (1998). "Ku protein stimulates DNA end-joining by mammalian DNA ligases: a direct role for Ku in repair of DNA double-strand breaks." Embo J **17**(2): 609-14.
- Raynard, S., W. Bussen, et al. (2006). "A double Holliday junction dissolvasome comprising BLM, topoisomerase IIIalpha, and BLAP75." J Biol Chem **281**(20): 13861-4.
- Reddy, G., E. I. Golub, et al. (1997). "Human Rad52 protein promotes single-strand DNA annealing followed by branch migration." Mutat Res **377**(1): 53-9.
- Riballo, E., S. E. Critchlow, et al. (1999). "Identification of a defect in DNA ligase IV in a radiosensitive leukaemia patient." Curr Biol **9**(13): 699-702.
- Richardson, C., M. E. Moynahan, et al. (1998). "Double-strand break repair by interchromosomal recombination: suppression of chromosomal translocations." Genes Dev **12**(24): 3831-42.
- Richardson, C., J. M. Stark, et al. (2004). "Rad51 overexpression promotes alternative double-strand break repair pathways and genome instability." Oncogene **23**(2): 546-53.
- Ristic, D., M. Modesti, et al. (2003). "Rad52 and Ku bind to different DNA structures produced early in double-strand break repair." Nucleic Acids Res **31**(18): 5229-37.
- Rogakou, E. P., C. Boon, et al. (1999). "Megabase chromatin domains involved in DNA double-strand breaks in vivo." J Cell Biol **146**(5): 905-16.
- Roth, D. B., T. N. Porter, et al. (1985). "Mechanisms of nonhomologous recombination in mammalian cells." Mol Cell Biol **5**(10): 2599-607.
- Rothkamm, K., I. Kruger, et al. (2003). "Pathways of DNA double-strand break repair during the mammalian cell cycle." Mol Cell Biol **23**(16): 5706-15.
- Rothkamm, K., M. Kuhne, et al. (2001). "Radiation-induced genomic rearrangements formed by nonhomologous end-joining of DNA double-strand breaks." Cancer Res **61**(10): 3886-93.
- Ruscetti, T., B. E. Lehnert, et al. (1998). "Stimulation of the DNA-dependent protein kinase by poly(ADP-ribose) polymerase." J Biol Chem **273**(23): 14461-7.
- Saleh-Gohari, N. and T. Helleday (2004). "Conservative homologous recombination preferentially repairs DNA double-strand breaks in the S phase of the cell cycle in human cells." Nucleic Acids Res **32**(12): 3683-8.
- Saleh-Gohari, N. and T. Helleday (2004). "Strand invasion involving short tract gene conversion is specifically suppressed in BRCA2-deficient hamster cells." Oncogene **23**(56): 9136-41.
- Sargent, R. G., M. A. Brennehan, et al. (1997). "Repair of site-specific double-strand breaks in a mammalian chromosome by homologous and illegitimate recombination." Mol Cell Biol **17**(1): 267-77.

References

- Sargent, R. G., J. L. Meservy, et al. (2000). "Role of the nucleotide excision repair gene ERCC1 in formation of recombination-dependent rearrangements in mammalian cells." Nucleic Acids Res **28**(19): 3771-8.
- Sargent, R. G., R. L. Rolig, et al. (1997). "Recombination-dependent deletion formation in mammalian cells deficient in the nucleotide excision repair gene ERCC1." Proc Natl Acad Sci U S A **94**(24): 13122-7.
- Schildkraut, E., C. A. Miller, et al. (2005). "Gene conversion and deletion frequencies during double-strand break repair in human cells are controlled by the distance between direct repeats." Nucleic Acids Res **33**(5): 1574-80.
- Schmid, C. W. (1996). "Alu: structure, origin, evolution, significance and function of one-tenth of human DNA." Prog Nucleic Acid Res Mol Biol **53**: 283-319.
- Schulte-Uentrop, L., R. A. El-Awady, et al. (2008). "Distinct roles of XRCC4 and Ku80 in non-homologous end-joining of endonuclease- and ionizing radiation-induced DNA double-strand breaks." Nucleic Acids Res **36**(8): 2561-9.
- Schultz, N., E. Lopez, et al. (2003). "Poly(ADP-ribose) polymerase (PARP-1) has a controlling role in homologous recombination." Nucleic Acids Res **31**(17): 4959-64.
- Sharpless, N. E., D. O. Ferguson, et al. (2001). "Impaired nonhomologous end-joining provokes soft tissue sarcomas harbouring chromosomal translocations, amplifications, and deletions." Mol Cell **8**(6): 1187-96.
- Shinohara, A., M. Shinohara, et al. (1998). "Rad52 forms ring structures and co-operates with RPA in single-strand DNA annealing." Genes Cells **3**(3): 145-56.
- Shrivastav, M., L. P. De Haro, et al. (2008). "Regulation of DNA double-strand break repair pathway choice." Cell Res **18**(1): 134-47.
- Shuman, S. (1994). "Novel approach to molecular cloning and polynucleotide synthesis using vaccinia DNA topoisomerase." J Biol Chem **269**(51): 32678-84.
- Sigurdsson, S., S. Van Komen, et al. (2001). "Mediator function of the human Rad51B-Rad51C complex in Rad51/RPA-catalyzed DNA strand exchange." Genes Dev **15**(24): 3308-18.
- Singleton, M. R., L. M. Wentzell, et al. (2002). "Structure of the single-strand annealing domain of human RAD52 protein." Proc Natl Acad Sci U S A **99**(21): 13492-7.
- Smit, A. F. (1996). "The origin of interspersed repeats in the human genome." Curr Opin Genet Dev **6**(6): 743-8.
- Smith, G. C. and S. P. Jackson (1999). "The DNA-dependent protein kinase." Genes Dev **13**(8): 916-34.
- Smith, P. K., R. I. Krohn, et al. (1985). "Measurement of protein using bicinchoninic acid." Anal Biochem **150**(1): 76-85.
- Sonoda, E., M. S. Sasaki, et al. (1998). "Rad51-deficient vertebrate cells accumulate chromosomal breaks prior to cell death." Embo J **17**(2): 598-608.
- Soulas-Sprauel, P., G. Le Guyader, et al. (2007). "Role for DNA repair factor XRCC4 in immunoglobulin class switch recombination." J Exp Med **204**(7): 1717-27.
- Soutoglou, E., J. F. Dorn, et al. (2007). "Positional stability of single double-strand breaks in mammalian cells." Nat Cell Biol **9**(6): 675-82.
- Stark, J. M., A. J. Pierce, et al. (2004). "Genetic steps of mammalian homologous repair with distinct mutagenic consequences." Mol Cell Biol **24**(21): 9305-16.
- Strout, M. P., G. Marcucci, et al. (1998). "The partial tandem duplication of ALL1 (MLL) is consistently generated by Alu-mediated homologous recombination in acute myeloid leukemia." Proc Natl Acad Sci U S A **95**(5): 2390-5.

References

- Subramanian, D. and J. D. Griffith (2002). "Interactions between p53, hMSH2-hMSH6 and HMG I(Y) on Holliday junctions and bulged bases." *Nucleic Acids Res* **30**(11): 2427-34.
- Sugawara, N., G. Ira, et al. (2000). "DNA length dependence of the single-strand annealing pathway and the role of *Saccharomyces cerevisiae* RAD59 in double-strand break repair." *Mol Cell Biol* **20**(14): 5300-9.
- Sugiyama, T., J. H. New, et al. (1998). "DNA annealing by RAD52 protein is stimulated by specific interaction with the complex of replication protein A and single-stranded DNA." *Proc Natl Acad Sci U S A* **95**(11): 6049-54.
- Symington, L. S. (2002). "Role of RAD52 epistasis group genes in homologous recombination and double-strand break repair." *Microbiol Mol Biol Rev* **66**(4): 630-70, table of contents.
- Takata, M., M. S. Sasaki, et al. (1998). "Homologous recombination and non-homologous end-joining pathways of DNA double-strand break repair have overlapping roles in the maintenance of chromosomal integrity in vertebrate cells." *Embo J* **17**(18): 5497-508.
- Takeda, S., K. Nakamura, et al. (2007). "Ctp1/CtIP and the MRN complex collaborate in the initial steps of homologous recombination." *Mol Cell* **28**(3): 351-2.
- Tan, T. L., J. Essers, et al. (1999). "Mouse Rad54 affects DNA conformation and DNA-damage-induced Rad51 foci formation." *Curr Biol* **9**(6): 325-8.
- Tauchi, H., J. Kobayashi, et al. (2002). "Nbs1 is essential for DNA repair by homologous recombination in higher vertebrate cells." *Nature* **420**(6911): 93-8.
- Taylor, R. M., C. J. Whitehouse, et al. (2000). "The DNA ligase III zinc finger stimulates binding to DNA secondary structure and promotes end-joining." *Nucleic Acids Res* **28**(18): 3558-63.
- Thompson, L. H. and D. Schild (2002). "Recombinational DNA repair and human disease." *Mutat Res* **509**(1-2): 49-78.
- Tong, W. M., U. Cortes, et al. (2002). "Synergistic role of Ku80 and poly(ADP-ribose) polymerase in suppressing chromosomal aberrations and liver cancer formation." *Cancer Res* **62**(23): 6990-6.
- Tutt, A., D. Bertwistle, et al. (2001). "Mutation in Brca2 stimulates error-prone homology-directed repair of DNA double-strand breaks occurring between repeated sequences." *Embo J* **20**(17): 4704-16.
- van den Bosch, M., R. T. Bree, et al. (2003). "The MRN complex: coordinating and mediating the response to broken chromosomes." *EMBO Rep* **4**(9): 844-9.
- Van Dyck, E., A. Z. Stasiak, et al. (1999). "Binding of double-strand breaks in DNA by human Rad52 protein." *Nature* **401**(6751): 403.
- Van Dyck, E., A. Z. Stasiak, et al. (2001). "Visualization of recombination intermediates produced by RAD52-mediated single-strand annealing." *EMBO Rep* **2**(10): 905-9.
- van Heemst, D., L. Brugmans, et al. (2004). "End-joining of blunt DNA double-strand breaks in mammalian fibroblasts is precise and requires DNA-PK and XRCC4." *DNA Repair (Amst)* **3**(1): 43-50.
- Vanasse, G. J., P. Concannon, et al. (1999). "Regulated genomic instability and neoplasia in the lymphoid lineage." *Blood* **94**(12): 3997-4010.
- Walker, J. R., R. A. Corpina, et al. (2001). "Structure of the Ku heterodimer bound to DNA and its implications for double-strand break repair." *Nature* **412**(6847): 607-14.

References

- Wang, H., A. R. Perrault, et al. (2003). "Biochemical evidence for Ku-independent backup pathways of NHEJ." Nucleic Acids Res **31**(18): 5377-88.
- Wang, H., B. Rosidi, et al. (2005). "DNA ligase III as a candidate component of backup pathways of nonhomologous end-joining." Cancer Res **65**(10): 4020-30.
- Wang, M., W. Wu, et al. (2006). "PARP-1 and Ku compete for repair of DNA double strand breaks by distinct NHEJ pathways." Nucleic Acids Res **34**(21): 6170-82.
- Wang, Y., D. Cortez, et al. (2000). "BASC, a super complex of BRCA1-associated proteins involved in the recognition and repair of aberrant DNA structures." Genes Dev **14**(8): 927-39.
- Ward, I. M. and J. Chen (2001). "Histone H2AX is phosphorylated in an ATR-dependent manner in response to replicational stress." J Biol Chem **276**(51): 47759-62.
- Weaver, D. T. (1996). "Regulation and repair of double-strand DNA breaks." Crit Rev Eukaryot Gene Expr **6**(4): 345-75.
- Weinfeld, M., M. A. Chaudhry, et al. (1997). "Interaction of DNA-dependent protein kinase and poly(ADP-ribose) polymerase with radiation-induced DNA strand breaks." Radiat Res **148**(1): 22-8.
- Weinstock, D. M., B. Elliott, et al. (2006). "A model of oncogenic rearrangements: differences between chromosomal translocation mechanisms and simple double-strand break repair." Blood **107**(2): 777-80.
- West, S. C. (2003). "Molecular views of recombination proteins and their control." Nat Rev Mol Cell Biol **4**(6): 435-45.
- Weterings, E. and D. J. Chen (2008). "The endless tale of non-homologous end-joining." Cell Res **18**(1): 114-24.
- Weterings, E. and D. C. van Gent (2004). "The mechanism of non-homologous end-joining: a synopsis of synapsis." DNA Repair (Amst) **3**(11): 1425-35.
- Whitmore, S. E., C. S. Potten, et al. (2001). "Effect of photoreactivating light on UV radiation-induced alterations in human skin." Photodermatol Photoimmunol Photomed **17**(5): 213-7.
- Willers, H., J. Husson, et al. (2006). "Distinct mechanisms of nonhomologous end-joining in the repair of site-directed chromosomal breaks with noncomplementary and complementary ends." Radiat Res **166**(4): 567-74.
- Wu, L. and I. D. Hickson (2003). "The Bloom's syndrome helicase suppresses crossing over during homologous recombination." Nature **426**(6968): 870-4.
- Wu, Y., N. Kantake, et al. (2008). "Rad51 protein controls Rad52-mediated DNA annealing." J Biol Chem **283**(21): 14883-92.
- Xie, A., A. Hartlerode, et al. (2007). "Distinct roles of chromatin-associated proteins MDC1 and 53BP1 in mammalian double-strand break repair." Mol Cell **28**(6): 1045-57.
- Yan, C. T., C. Boboila, et al. (2007). "IgH class switching and translocations use a robust non-classical end-joining pathway." Nature **449**(7161): 478-82.
- Yano, K., K. Morotomi-Yano, et al. (2008). "Ku recruits XLF to DNA double-strand breaks." EMBO Rep **9**(1): 91-6.
- Yoo, S., A. Kimzey, et al. (1999). "Photocross-linking of an oriented DNA repair complex. Ku bound at a single DNA end." J Biol Chem **274**(28): 20034-9.
- Yuan, S. S., H. L. Chang, et al. (2003). "Ionizing radiation-induced Rad51 nuclear focus formation is cell cycle-regulated and defective in both ATM(-/-) and c-Abl(-/-) cells." Mutat Res **525**(1-2): 85-92.

References

- Yuan, Z. M., Y. Huang, et al. (1998). "Regulation of Rad51 function by c-Abl in response to DNA damage." J Biol Chem **273**(7): 3799-802.
- Zha, S., F. W. Alt, et al. (2007). "Defective DNA repair and increased genomic instability in Cernunnos-XLF-deficient murine ES cells." Proc Natl Acad Sci U S A **104**(11): 4518-23.
- Zhang, Y. and J. D. Rowley (2006). "Chromatin structural elements and chromosomal translocations in leukemia." DNA Repair (Amst) **5**(9-10): 1282-97.
- Zhu, C., K. D. Mills, et al. (2002). "Unrepaired DNA breaks in p53-deficient cells lead to oncogenic gene amplification subsequent to translocations." Cell **109**(7): 811-21.
- Zhuang, J., J. Zhang, et al. (2006). "Checkpoint kinase 2-mediated phosphorylation of BRCA1 regulates the fidelity of nonhomologous end-joining." Cancer Res **66**(3): 1401-8.

Risk and safety statements for the compound used in the study

| Name of the reagent | Risk phrases | Safety Phrases |
|--|-------------------|-------------------|
| 2-Propanol | 11-36-67 | 7-16-24/25-26 |
| Acetic acid | 10-35 | 23-26-45 |
| Ampicillin | 42/43 | 23-36/37-45 |
| Aprotinin | | 22 |
| BCA protein assay kit | 25/42/43 | 22/36/37/45 |
| Bestatin | | 22-24/25 |
| Bromophenol blue | | 22-24/25 |
| Calcium chloride | 36 | 22-24 |
| Canamycin-sulphate | | 22-24/25 |
| Coomassie brilliant blue | | 22-24/25 |
| Crystal violet | 45-22-41-50/53 | 53-26-39-45-60-61 |
| Disodium hydrogen phosphate | | 22-24/25 |
| Dithiotheratol (DTT) | 22-36/37/38 | 26-36 |
| DMSO | 36/37/38 | 23-26-36 |
| EDTA | 36-52/53 | 61 |
| Enhanced chemiluminescence (ECL) detection kit | 22753 | 60761 |
| Ethanol | 11 | 7-16 |
| Ethidium bromide | 22-26-36/37/38-68 | 26-28-36/37-45 |
| HEPES | 36, 37, 38 | 26, 36 |

| | | |
|---------------------------------|-------------------------------|-------------------|
| Hydrochloric acid | 34-37 | 26-36/37/39-45 |
| Leupeptin | | 22-24/25 |
| Magnesium chloride | | 22-24/25 |
| Methanol | 11-23/24/25-39/23-24/25 | 7-16-36/37-45 |
| Paraformaldehyde | 23/24/25-34-39/23/24/25-40-43 | 26-36/37/39-45-51 |
| Penicillin | 42/43 | 22-36/37 |
| Pepstatin | | 22-24/25 |
| PMSF | 26-36/37/39-45 | 25-34 |
| Postassium chloride | | 22-24/25 |
| Postassium dihydrogen phosphate | 34 | 26-45 |
| Qiagen plasmid mini kit | 10-35/36/38/11-36-67/42/43 | 13/26/26/46 |
| Quiagen plasmid Maxi kit | 10-35/36/38/11-36-67/42/43 | 13/26/26/46 |
| SDS | 11-21/22-36/37/38 | 26-36/37 |
| Sodium fluoride | 25-32-36/38 | 22-36-45 |
| Sodium hydroxide | 35 | 26-37/39-45 |
| Streptomycin | 61-22 | 53-36/37/39-45 |
| Trizma base | 36/37/38 | 26-36 |
| Trypsin | 36/37/38-42 | 22-24-26-36/37 |
| Xylene cyanol | 36/37/38 | 26-36 |
| β -mercaptoethanol | 20/22-24-34-51/53 | 26-36/37/39-45-61 |

Acknowledgements

First of all I kneel to Allah truly thankful for supporting me to continue my research and compile this thesis.

I send all my respect and gratitude to DAAD for financially supporting the first two years of my Ph.D. program.

I'd like to dedicate this work to my family and all my friends. They are pleased, I hope that they are a bit proud of me too, and I guess I owe them a lot. My Mom and Dad have to be thanked for always being enthusiastic about everything. They're brilliant to talk a problem through with, and I've appreciated their help and advice on loads of things. Thanks to my brother Ossama and my sisters Inas and Bossy for being my closest friends. Thanks to my lovely wife Maha, and my beautiful kids Islam and Iman for cheering me up when necessary and making me feel the warm during what I have been doing. Also, thanks for my wife's family specially her Mom and Dad for supporting me a lot during my work here and in Egypt. Also I am deeply thankful to my colleague Abeer who also belong to my family. She actually pushed me to apply for the DAAD scholarship at a time I was really depressed to do that. Without her help I could not reach to what I have reached right now.

I'd like to thank all the people in the laboratory of Radiobiology and Experimental Radio-oncology for the open and collaborative atmosphere throughout my Ph.D.

I would like to express my deepest appreciation to Prof. Dr. E. Dikomey. It would have been very difficult to continue my life in Germany without his support. More importantly, his kindness and scientific guidance were major factors that helped me to continue in this thesis. I thank him for introducing me into the field of "Radio-oncology", for his non-pressing guidance and pushing me to think more and more.

I am deeply indebted to PD. Dr. J. Dahm-Daphi, my research advisor; for a lot of helpful conversations, sharing ideas and personal experience, pushing me to think more about biological meaning of phenomena than about the technical questions. His brilliant discussions and comments have made me enjoy working with him during my Ph.D. Without his help, it would have been impossible to continue my stay in Germany and get my Ph.D. degree. Also thanks for putting up with my stressedness during my writing over the past few months, and has been lovely all the time, even when his attempts to get me to relax have been thwarted.

I deeply thank my colleagues Sabine Schumacher, Raphael Rosskopf, Tim Rhein for supporting me in a big part of the experiments performed in this thesis. I wish them a great success in their careers.

I also really appreciate the help I got at the biochemistry and molecular biology dept. Hamburg University, from Prof. Dr. C. Betzel and all his students

I send my greetings to the whole staff in Tumour Biology Department in National Cancer Institute in Egypt for facilitating my stay here in Germany. Also I send special greetings and appreciation to both Prof. Dr. Abdel Hady Abdel Wahab and Dr. Rafaat El- Awady for being my support in many stages in my life.

Thanks for everyone else who's been in the lab at any stage in the past four years for providing me with help, support and other fun.

Curriculum Vitae

Personal Data

Family Name : Mansour
First name : Wael Yassin
Address : Klaus-Groth straÙe 29, 20535-Hamburg
Date of Birth : 25th of January 1974
Birthplace : El-Behira, Egypt
Nationality : Egyptian

Graduation

1990 : High secondary school, Elbehira, Egypt
1991-1995 : B. Sc. In biochemistry, Faculty of Science, Alexandria University, Egypt
1997-2001 : M. Sc. in biochemistry and molecular biology, Faculty of Science, Ain Shams University, Egypt
Since 2004 : Ph. D. in biochemistry and molecular biology, Biochemistry dept, Hamburg University, Germany

Work experience

1996 – 2000 : Demonstrator of biochemistry in Cancer Biology department, National Cancer Institute, Cairo University. During this period I pursued my Master degree.

Topic: Detection of mutations in solid tumours.

2001 – 2004 : Assistant lecturer of biochemistry and molecular biology in Cancer biology department, National Cancer Institute, Cairo University. During this period I successfully passed more focused courses in cancer biology and epidemiology in National Cancer Institute, Cairo University, Egypt. At the same time, I have joined a running project.

Topic: Detection of micro-metastasis in Egyptian breast cancer patients.

2004 – 2006 : A two years DAAD scholarship for Ph.D. degree in a channel program between Cairo University and Hamburg University.

Since 2006 : A Ph.D. scholarship from University Hospital Hamburg-Eppendorf (UKE) in the laboratory of radiobiology and experimental radio-oncology, Hamburg University (Head of the lab: Prof. Dr. Ekkehard Dikomey).

Topic: Regulation of double strand break repair pathways

List of publications

Papers:

- Mansour W. Y., Schumacher S., Rosskopf R., Rhein T., Schmidt-Petersen F., Gatzemeier G., Haag F., Borgmann K., Willers H., and Dahm-Daphi J. (2008). "Hierarchy of nonhomologous end-joining, single-strand annealing and gene conversion at site-directed DNA double-strand breaks." *Nucleic Acids Res* 36(12): 4088-98.
- Ulla Kasten-Pisula, Apostolos Menegakis, Ingo Brammer, Kerstin Borgmann, Wael Y. Mansour, Sarah Degenhardt, Mechthild Krause, Andreas Schreiber, Jochen Dahm-Daphi, Cordula Petersen, Ekkehard Dikomey, Michael Baumann. (2009). "The extreme radiosensitivity of the squamous cell carcinoma SKX is due to a defect in double-strand break repair" *Radiotherapy and Oncology* 90 (2009) 257–264.
- Mansour W. Y., Rhein T., and Dahm-Daphi J. "Involvement of PARP1 in DSB repair in Ku-deficient mammalian cells" in processing.

Conference proceedings:

- Mansour W. Y., Borgmann K., and Dahm-Daphi J. Creation of a single strand specific construct competition of non-homologous end-joining and single-strand annealing. 2nd Workshop "Recombination and Repair", Hamburg, Germany, 2005. (Oral presentation)
- Mansour W. Y., Schmidt-Petersen F., Borgmann K., and Dahm-Daphi J. Ku80 has little impact on non-homologous end-joining but suppresses homologous recombination and single-strand annealing. 9th Biennial Meeting of the DGDR, Hamburg, Germany, 2006. (Oral presentation)
- Mansour W. Y., Schmidt-Petersen F., Borgmann K., Haag F., Willers H., and Dahm-Daphi J. Impact of single strand annealing as a DSB repair pathway: a cross-talk with both NHEJ and HR. DEGRO (13. Jahreskongress der Deutschen Gesellschaft für Radioonkologie e.V.), Hannover, Germany, 2007. (Poster presentation).
- Mansour W. Y., Schmidt-Petersen F., Borgmann K., Haag F., Willers H., and Dahm-Daphi J. Ku80 has a little impact on nonhomologous end-joining but suppresses both single strand annealing and gene conversion. 10th International Wolfsberg Meeting on Molecular Radiation Biology/Oncology. Wolfsberg, Switzerland, 2007. (Poster presentation).
- Mansour W. Y., Schumacher S., Rosskopf R., Rhein T., Haag F., Willers H., and Dahm-Daphi J. Cross-talk of nonhomologous end-joining, single strand annealing and gene conversion for repairing chromosomal DSB in mammalian cells. 1st German-French DNA repair meeting, Toulouse, France, 2007. (Oral presentation).
- Rieckmann T., Kocken S., Köcher S., Rhein T., Dahm-Daphi J., and Mansour W. Y. Ku-dependent and -independent end-joining of I-SceI-induced DSB differ in their velocity and fidelity but are equally efficient. 10th Biennial Meeting of DGDR, Berlin, Germany, 2008. (Poster presentation).
- Mansour W. Y., Schumacher S., Rosskopf R., Rhein T., Schmidt-Petersen F., Gatzemeier G., Haag F., Borgmann K., Willers H., and Dahm-Daphi J. Hierarchy of nonhomologous end-joining, single-strand annealing and gene conversion at site-directed

DNA double-strand breaks. Biochemical Society Annual Symposium, DNA damage: from causes to cures, Robinson college, Cambridge, UK, 2008. (Oral presentation).

Selbständigkeitserklärung

Hiermit versichere ich, dass ich die vorliegende Arbeit selbständig und ohne unerlaubte fremde Hilfe angefertigt habe. Ich habe keine anderen als die im Literaturverzeichnis angeführten Quellen benutzt und sämtliche Textstellen, die wörtlich oder sinngemäß aus veröffentlichten oder unveröffentlichten Schriften entnommen wurden und alle Angaben, die auf mündlichen Auskünften beruhen, als solche kenntlich gemacht. Zusammenarbeiten sind im Text genannt.

Die Arbeit wurde zuvor keiner Prüfungsbehörde in gleicher oder ähnlicher Form vorgelegt.

Wael Yassin Mansour

Hamburg, 5. Februar 2009